UNIVERSITEIT VAN PRETORIA
UNIVERSITY OF PRETORIA
YUNIBESITHI YA PRETORIA

Finite element analysis of vibrating elastic structures

by

Sonja du Toit

Submitted in partial fulfilment of the requirements for the degree

Philosophiae Doctor

in the Department of Mathematics and Applied Mathematics
in the Faculty of Natural and Agricultural Sciences

University of Pretoria
Pretoria

April 2020

The financial assistance of the National Research Foundation (NRF) towards this research is hereby acknowledged. Opinions expressed and conclusions arrived at, are those of the author and are not necessarily to be attributed to the NRF.

© University of Pretoria

UNIVERSITEIT VAN PRETORIA
UNIVERSITY OF PRETORIA
YUNIBESITHI YA PRETORIA

DECLARATION

I, the undersigned, hereby declare that the dissertation submitted herewith for the degree Philosophiae Doctor to the University of Pretoria contains my own, independent work and has not been submitted for any degree at any other university.

Name: Sonja du Toit

Date: April 2020

© University of Pretoria

UNIVERSITEIT VAN PRETORIA
UNIVERSITY OF PRETORIA
YUNIBESITHI YA PRETORIA

Title	Finite element analysis of vibrating elastic structures
Name	Sonja du Toit
Supervisor	Prof N F Janse van Rensburg
Co-supervisor	Dr M Labuschagne
Department	Mathematics and Applied Mathematics
Degree	Philosophiae Doctor

In this thesis mathematical models for vibrating elastic structures are derived and analysed using finite element approximations where necessary.

The most important contribution in this thesis is the development of the Local Linear Timoshenko (LLT) model and its applications. Using the well-known equations of motion for a one-dimensional solid or rod, these equations are rigorously simplified for planar motion. To complete the model, the constitutive equations for shear and bending is adapted from the linear Timoshenko theory.

A significant property of the model is that existing linear and nonlinear models can be derived from it. This promotes insight into the LLT model itself as well as existing models. In particular, by making the appropriate assumptions for small vibrations, a number of models published by other authors, were derived. Of importance is an adapted version of the linear Timoshenko model which allows for longitudinal vibration and a special case for transverse vibration of a Timoshenko beam with an axial force.

The variational equations of motion for the LLT model was easy to derive but the constitutive equations could not simply be substituted into them. Nevertheless, in the thesis a well defined variational form for the Local Linear Timoshenko model is derived. Using the variational form, finite element approximations of problems can be formulated. A rigorously defined algorithm was developed which is a substantial contribution. Through numerical experiments, convergence was demonstrated. While solutions of LLT and linear models compared well for small vibrations, it was shown that the LLT model can be applied to cases where the solutions of linear beam models are not realistic.

A model for earthquake induced oscillations in vertical structures, based on the Timoshenko model, was derived. The model was transformed to that for a cantilever beam with homogeneous boundary conditions. This made

© University of Pretoria

it possible to compare beam models using modal analysis. This adapted Timoshenko model was compared to the Twin-beam model of E Miranda. The models compared poorly and both predicted the measured fundamental period completely wrong. This is due to the lack of reliable information on additional mass not contributing to stiffness.

As an alternative, a building was modelled as a series of beams connected by rigid bodies to represent floors. Correct modelling of interface conditions made it possible to derive the variational form, which is a significant contribution. An adapted Mixed Finite Element approximation was thus possible and a system of ordinary differential equations was derived which can be used for simulations.

Finally, new interface and boundary conditions for a hybrid Timoshenko beam model with a tip body were derived. This model is an improvement on previous versions since elasticity at the interfaces is taken into account. The derivation of the estimates required to apply the general theory for existence needed to be done with care and the proofs were by no means trivial. The new model can also be used to evaluate cases where "rigid" boundary and interface conditions may not be realistic.

The numerical experiments in this thesis had limited scope. It was mainly used to complement the theory, for convergence experiments (e.g. LLT model) or to examine the feasibility of a model (e.g. vertical structure and Hybrid model).

© University of Pretoria

Contents

1 Vibrating elastic solids and structures **6**

1.1 Introduction 6

1.2 Classical linear beam models 8

1.2.1 Timoshenko model 9

1.2.2 Simplified models 11

1.2.3 Comparison of natural frequencies and modes 12

1.3 Variational forms and existence of solutions for the Timoshenko model 14

1.3.1 Variational form 15

1.3.2 Weak variational form 16

1.3.3 Existence of solutions for general second order hyperbolic problems 18

1.3.4 Existence of solutions for the Timoshenko beam problem 20

2 Local linear Timoshenko beam **21**

2.1 Introduction 21

2.2 Dynamics of a rod 24

2.2.1 Conservation laws 24

© University of Pretoria

2.2.2 Momentum, angular momentum and body force 25
2.2.3 Forces and couples due to traction 26
2.2.4 Equations of motion for a one-dimensional model 27
2.3 Planar motion 28
2.4 Local linear approximation 29
2.4.1 Constitutive equations 29
2.4.2 Local linear Timoshenko beam model 32
2.5 Simplified models 34
2.6 Small vibrations 36
2.6.1 Linear and possible nonlinear models 37
2.6.2 Adapted linear Timoshenko model 38
2.6.3 Nonlinear Timoshenko model of Sapir and Reiss 39
2.6.4 Beam models without shear 40
2.7 Variational forms and existence of solutions 41
2.7.1 Local linear Timoshenko model 42
2.7.2 Linear approximation of the Local linear model 43
2.7.3 Adapted Timoshenko model 43
2.8 Weak variational form and existence for the adapted Timoshenko model 44
2.9 Connection between the constitutive equations and three-dimensional elasticity 46
2.9.1 Equilibrium problem 46
2.9.2 Trial solution 48
2.9.3 Warping of a cross-section 51

© University of Pretoria

3 Finite element analysis of the Local Linear Timoshenko beam model 53

3.1 Scope of the study 53

3.2 Finite element approximation 54

3.2.1 Formulation of the semi-discrete problem 54

3.2.2 Piecewise linear basis functions 56

3.2.3 System of Ordinary differential equations 57

3.3 Numerical experiments for convergence 61

3.3.1 Small vibrations 61

3.3.2 Forced vibration 66

3.4 Applicability of the Local Linear Timoshenko model 70

3.4.1 Comparison to classical linear Timoshenko model . . . 70

3.4.2 Nonlinear oscillations of the Local Linear Timoshenko beam model 74

3.4.3 Conclusion 76

4 Wind and earthquake induced oscillations of vertical structures 77

4.1 Introduction 77

4.2 Two beam models for high-rise structures 79

4.2.1 Adapted Timoshenko model 79

4.2.2 Twin-beam model of Miranda and Taghavi 81

4.2.3 Damping 83

4.2.4 Wind-induced oscillations 84

4.3 Modal analysis and parameters 84

4.3.1 Natural frequencies of the Twin-beam model 85

© University of Pretoria

UNIVERSITEIT VAN PRETORIA
UNIVERSITY OF PRETORIA
YUNIBESITHI YA PRETORIA

4.3.2 Stiffness parameters 86
4.3.3 Natural frequencies and the fundamental period 87
4.3.4 Comparison of two buildings 87
4.3.5 Remarks on modal analysis 88
4.4 Semi-discrete finite element approximation 89
4.5 Finite element simulations 91
4.6 Conclusion 94

5 Multiple beam model 96
5.1 Introduction 96
5.2 Model problem 97
5.3 Variational form 98
5.4 Semi-discrete approximation 101
5.4.1 Variational form in a finite dimensional subspace . . . 101
5.4.2 Basis functions 104
5.4.3 Matrices and systems of ordinary differential equations 107
5.5 Conclusion 109

6 Cantilever Timoshenko beam and tip body with elastic behaviour at the interfaces 111
6.1 Introduction 111
6.2 The model problems 113
6.2.1 Equations of motion 113
6.2.2 Boundary and interface conditions 114
6.2.3 Proposed new model 116

© University of Pretoria

6.3 Variational form 119
6.4 Weak variational form 122
6.5 Equivalent norms and inequalities 125
6.6 Existence 128
6.7 Semi-discrete finite element approximation 128
6.7.1 Semi-discrete problem 128
6.7.2 Convergence and error estimates 129
6.8 System of ordinary differential equations 130
6.9 Numerical results and conclusion 131

7 Conclusion **134**
7.1 Overview 134
7.2 Results 137
7.3 Ongoing and future research 139
7.3.1 Adapted Timoshenko beam model 140
7.3.2 Finite element analysis of the Local Linear Timoshenko model 143
7.3.3 Other possibilities for future work 143

A Sobolev Spaces **151**

© University of Pretoria

Chapter 1

Vibrating elastic solids and structures

1.1 Introduction

The research for this doctoral degree is part of an ongoing project on vibration analysis. Although wide ranging, the research thus far was restricted to linear problems. For the present study the idea was to continue on linear problems, including structures consisting of beams and plates, but also to venture into nonlinear beam theory. It soon became clear that the identified research problems on beams alone were already too ambitious. Therefore the focus of this thesis is on beam models.

There is a vast literature on beams and their applications. For example, beams can be part of an elastic multi-structure (as in [CDKP87]), used to manipulate an object (as in [LM88]), model a slender vertical structure (as in [LVV05]) or even nanotubes (as in [ASD16]). It is noticeable that authors are often rather vague about assumptions such as "thick", "thin", "small vibrations", "large motion", etc. when considering various linear and nonlinear beam models. The choice between linear and nonlinear models, and in the linear case, between Timoshenko and Euler-Bernoulli theory is rarely motivated in precise terms. There are countless examples where mathematical models are simplified by making additional assumptions, e.g. neglecting terms which are considered to be small. However, there are few examples where solutions are compared to see if the additional assumptions are actually justified.

© University of Pretoria

The research for the doctoral degree started with linear problems involving beams. From previous publications we concluded that the Timoshenko theory is the best linear theory for small planar transverse vibrations of beams. (More detail is provided in Section 1.2.)

Concerning linear vibration models involving beams, three research problems were identified where the Timoshenko theory can be employed:

> *A vertical structure, e.g. a high rise building or industrial chimney which is modelled as a beam.* In the initial searches we found it curious that beam models for vertical structures did not include a Timoshenko or other shear models. In Chapter 4 wind and earthquake induced oscillations in vertical structures are investigated.
>
> *A structure modelled as a series of connected beams with rigid bodies between the beams.* Such a model with Timoshenko beams to model a high-rise structure is considered. The feasibility of this model is investigated in Chapter 5.
>
> *A hybrid model where a rigid body is fixed to one end of the beam.* The validity of the interface (and boundary conditions) considered in previous articles can be questioned. In Chapter 6 new interface and boundary conditions which model elastic interfaces are derived.

In the three applications mentioned above the focus is on the modelling. For a mathematical model to be useful, it must be well posed. This will be the case for the linear model problems above if it can be proved that they are special cases of the general linear vibration problem in [VV02]. An example is provided in Section 1.3. To evaluate models and investigate properties of solutions it is desirable that representations of solutions are available. If not, one has to rely on numerical approximations. In this thesis the Finite Element Method is used and wherever possible and relevant convergence results and error estimates are presented or at least references provided.

As mentioned, Timoshenko's theory is realistic, but it is linear and may only be used for small vibrations. The question may well be asked whether a nonlinear Euler-Bernoulli model may not be better if the deflection is not sufficiently small. It is therefore necessary to consider the motion of beams where displacements are too large for the linear theory. In the ongoing project on vibration analysis the idea came up to consider a nonlinear Timoshenko beam. This idea lead to the unpublished technical report [Van15]. The next

© University of Pretoria

year an improved technical report [VDB16] was written but not published. (The new model was named the *Local Linear Timoshenko beam*.) Further improvement was necessary and it became part of the research for the doctoral degree.

Chapter 2 of the thesis is the improvement on [VDB16], see Section 2.1 for a detailed account of the changes. As mentioned, we consider it important that a mathematical model be well posed. But existence theory for nonlinear vibration problems is a research field in its own right and we considered even a literature study as beyond the scope of the thesis. An obvious strategy is to assume that a solution for a model problem exists and compute approximations.

It was decided to develop an algorithm based on a finite element approximation. It proved to be quite a challenge. Preliminary calculations were carried out by me for the report [VDB16] to see if the model would yield acceptable results, which it did. For the doctoral study, the algorithm was formulated rigorously (and presented in Chapter 3) so that it could be analyzed at some stage. More numerical experiments were done to test for convergence of approximations and to compare the new model to the linear Timoshenko beam. The results are presented in Chapter 3.

In the rest of this chapter the classical linear beam models are revisited and used as an introduction to the more complex models discussed in the following chapters.

Note As stated in the declaration, this thesis is my own work. I will however use the pronoun 'we' in the thesis due to the valuable advice and guidance provided by my supervisors.

1.2 Classical linear beam models

As mentioned, the research started with the application of linear beam models. To facilitate the discussion on beams in this thesis, it was decided to revisit the classical models.

In this section the Timoshenko and other simplified beam models are presented in dimensionless form. The merits of the Timoshenko model are discussed and the other beam models are evaluated using natural frequencies. In Subsection 1.2.2 it is briefly explained how the Euler-Bernoulli theory can

© University of Pretoria

be derived from the Timoshenko theory by making additional assumptions.

1.2.1 Timoshenko model

A convincing derivation is found in [Cow66] and solutions compare well to solutions of multi-dimensional models, see e.g. [SP06] and [LVV09]. On the other hand, the Euler-Bernoulli model does not always compare well to the Timoshenko model as shown in [VV06] and [LVV09].

In [Tim21] and [Tim22] Timoshenko made an improvement to beam theory by introducing shear deformation into the model. The rigorous derivation of the Timoshenko theory in [Cow66] provides a convincing argument in favour of this theory. In the articles [SP06] and [LVV09] it is demonstrated how the Timoshenko theory captures multi-dimensional effects with surprising accuracy. In particular, in [LVV09] the authors showed that the Timoshenko model adequately accounts for the warping of a cross-section. (The angle of rotation ϕ of a cross-section matches the average rotation of a cross-section of a two-dimensional model.)

Remark In Chapter 2 it is shown how the linear Timoshenko theory can be derived from the nonlinear theory.

It is advantageous to consider the equations of motion and constitutive equations separately. Equations of motion:

$$\rho A\partial_t^2 w = \partial_x V + Q, \tag{1.2.1}$$
$$\rho I\partial_t^2 \phi = V + \partial_x M, \tag{1.2.2}$$

where w is the deflection, ϕ is the angle of rotation of the cross-section, V is the shear force, M is the bending moment and Q is an external force density (load). Also, ρ is the density, A the cross-sectional area and I the area moment of inertia of the beam. The constitutive equations for the moment M and the shear force V are

$$M = EI\partial_x\phi, \tag{1.2.3}$$
$$V = AG\kappa^2\big(\partial_x w - \phi\big). \tag{1.2.4}$$

In these equations, E and G are elastic constants and κ^2 the shear coefficient or shear correction factor. The reader is referred to [Tim37, p 337-338], [Fun65, p 323-324], [Cow66] and [Inm94, p 337-338] for standard derivations.

© University of Pretoria

Next, the equations of motion and constitutive equations are written in dimensionless form. Set

$$\tau = \frac{t}{t_0}\,, \quad \xi = \frac{x}{\ell}\,, \quad w^*(\xi,\tau) = \frac{w(x,t)}{\ell} \quad \text{and} \quad \phi^*(\xi,\tau) = \phi(x,t).$$

The forces and moments in dimensionless form are

$$Q^*(\xi,\tau) = \frac{\ell Q(x,t)}{G\kappa^2 A}, \quad V^*(\xi,\tau) = \frac{V(x,t)}{G\kappa^2 A} \quad \text{and} \quad M^*(\xi,\tau) = \frac{M(x,t)}{\ell G\kappa^2 A}\,.$$

The following dimensionless parameters are introduced

$$\alpha = \frac{A\ell^2}{I}\,, \quad \beta = \frac{AG\kappa^2\ell^2}{EI} \quad \text{and} \quad \gamma = \frac{\beta}{\alpha} = \frac{G\kappa^2}{E}\,.$$

The parameters α and β are subject to huge variations but γ range between $\frac{1}{6}$ and $\frac{1}{2}$, see e.g. [VV06], [LVV09] and the references there in.

A convenient choice for t_0 is

$$t_0 = \ell\sqrt{\frac{\rho}{G\kappa^2}}\,.$$

Returning to the original notation, the dimensionless form of the **Timoshenko model** is presented:

$$\partial_t^2 w = \partial_x V + Q, \tag{1.2.5}$$

$$\frac{1}{\alpha}\,\partial_t^2\phi = V + \partial_x M, \tag{1.2.6}$$

$$M = \frac{1}{\beta}\,\partial_x\phi, \tag{1.2.7}$$

$$V = \partial_x w - \phi. \tag{1.2.8}$$

Boundary conditions for a cantilever beam

The boundary conditions are

$$w(0,t) = \phi(0,t) = 0$$

at the clamped end and

$$M(1,t) = 0 \quad \text{and} \quad V(1,t) = 0$$

© University of Pretoria

at the free end.

Boundary conditions for a pinned-pinned beam

The boundary conditions are

$$w(0,t) = w(1,t) = 0$$

and

$$M(0,t) = M(1,t) = 0$$

1.2.2 Simplified models

Rayleigh model

For the Rayleigh model it is assumed that the cross section remains perpendicular to the neutral plane. This implies that $\partial_x w = \phi$. The model can be derived from the Timoshenko theory. First eliminate V from (1.2.5) and (1.2.6) to obtain

$$\partial_t^2 w = \frac{1}{\alpha}\,\partial_t^2 \partial_x \phi - \partial_x^2 M + Q. \tag{1.2.9}$$

Now substitute ϕ by $\partial_x w$ to obtain the model:

$$\partial_t^2 w = \frac{1}{\alpha}\,\partial_t^2 \partial_x^2 w - \partial_x^2 M + Q, \tag{1.2.10}$$

$$M = \frac{1}{\beta}\,\partial_x^2 w. \tag{1.2.11}$$

The constitutive equation for the shear force V is now redundant.

The **boundary conditions** are the same as for the Timoshenko beam except that $\partial_x w = 0$ replaces $\phi = 0$ at a clamped end.

Euler-Bernoulli model

The rotary inertia term $\frac{1}{\alpha}\partial_t^2 \partial_x^2 w$ is omitted from the Rayleigh model to obtain the Euler-Bernoulli model. The boundary conditions are the same.

Shear model

© University of Pretoria

In the Rayleigh theory, shear is not taken into account. However, it is well known that the correction to the Euler-Bernoulli model by including rotary inertia is not sufficient, see e.g. [Inm94], [SP06] and [LVV09].

In [HBW99] the authors consider four linear beam theories: the three models presented above and one where shear is taken into account but not rotary inertia. To obtain this last mentioned model, simply omit the rotary inertia term in the Timoshenko beam model. From a mathematical point of view it means that α is extremely large but β not. This does not agree with the fact that $\gamma > \frac{1}{6}$, but the model yields better results than the Rayleigh model in some applications. We do have our reservations about the model but results can be obtained using separation of variables.

The shear model consists of Equations (1.2.5), (1.2.7), (1.2.8) and instead of (1.2.6), the equation

$$V + \partial_x M = 0.$$

1.2.3 Comparison of natural frequencies and modes

In this subsection the natural frequencies of vibration are considered in order to compare the beam models. Using this approach, the Timoshenko theory is compared to a multi-dimensional model in [SP06] and [LVV09] where as the Timoshenko, Rayleigh and Euler-Bernoulli models are compared in [VV06] and [LVV09].

The results in [VV06] and [LVV09] are acceptable where it is assumed that $\alpha = 4\beta$. The authors conclude that the Rayleigh and Euler-Bernoulli models are useful for large β. For β approximately 300 the fundamental frequency for these models is acceptable but not the higher frequencies. Consequently it is risky to use these models for $\beta < 300$.

The shear model was not considered in [VV06] or [LVV09] and I considered it necessary to compare.

Timoshenko model

For the modal analysis of the system in Subsection 1.2.1, [VV06] is followed. A pair of functions $w(x,t) = T(t)u(x)$ and $\phi(x,t) = T(t)\psi(x)$ is considered as a possible solution. This requires consideration of the corresponding

© University of Pretoria

eigenvalue problem.

$$-u'' + \psi' = \lambda u, \tag{1.2.12}$$

$$-\frac{1}{\beta}\psi'' - u' + \psi = \frac{\lambda}{\alpha}\psi, \tag{1.2.13}$$

with the boundary conditions for a **cantilever** beam given by

$$u(0) = \psi(0) = u'(1) - \psi(1) = \psi'(1) = 0. \tag{1.2.14}$$

For a **pinned-pinned** beam the boundary conditions are

$$u(0) = \psi'(0) = u(1) = \psi'(1) = 0.$$

Note that the eigenfunctions are vector valued. The function T satisfies $T'' = -\lambda T$ and hence the natural angular frequencies are equal to $\sqrt{\lambda}$.

To calculate the eigenvalues for a cantilever beam, use [VV06, Equation (25)]

$$\left(\frac{\lambda+\mu^2}{\lambda-\omega^2} + \frac{\lambda-\omega^2}{\lambda+\mu^2}\right)\cosh\mu\cos\omega + \left(\frac{\omega}{\mu} - \frac{\mu}{\omega}\right)\sinh\mu\sin\omega = 2, \tag{1.2.15}$$

with

$$\Delta = \frac{4\gamma}{(1+\gamma)^2}\frac{\alpha}{\lambda} + \frac{(1-\gamma)^2}{(1+\gamma)^2}, \tag{1.2.16}$$

$$\omega^2 = \frac{\lambda}{2}(1+\gamma)\left(\sqrt{\Delta}+1\right) \text{ and} \tag{1.2.17}$$

$$\mu^2 = \frac{\lambda}{2}(1+\gamma)\left(\sqrt{\Delta}-1\right). \tag{1.2.18}$$

By making use of interval division the values of λ can be obtained from Equation (1.2.15).

Shear model

The method in [VV06] can be adapted for the new problem. To calculate eigenvalues, use the eigenvalue problem for Timoshenko with $\lambda = 0$ in equation (1.2.13) but not in (1.2.12). To justify this, replace $\frac{1}{\alpha}$ by $\frac{\gamma}{\beta}$ and let $\gamma = 0$. (It is clear that λ depends continuously on γ.) Using this substitution the work in [VV06, Section 4] can be adapted to show that the frequency Equation (1.2.15) is still valid. To calculate the eigenvalues let $\gamma = 0$ in Equations (1.2.17) and (1.2.18) and $\gamma\alpha = \beta$ in (1.2.16) to obtain

$$\omega^2 = \frac{\lambda}{2}\left(\sqrt{1+\frac{4\beta}{\lambda}}+1\right) \text{ and } \mu^2 = \frac{\lambda}{2}\left(\sqrt{1+\frac{4\beta}{\lambda}}-1\right).$$

© University of Pretoria

The Shear model approximates the Timoshenko model more accurately than the Rayleigh model for $\beta < 300$.

Example Cantilever

Consider $\beta = 75$ (β may be small for some applications) and $\beta = 300$.

	$\beta = 75$		$\beta = 300$	
	Timoshenko	Shear	Timoshenko	Shear
k	λ_k	λ_k	λ_k	λ_k
1	0.1530	0.1551	1.4266	1.4602
2	4.2191	4.5131	9.6570	10.0936
3	23.057	25.295	31.0573	33.0646
4	61.802	68.757	70.5052	75.9940

Table 1.1: Eigenvalues for Timoshenko and Shear models

Even though these compare reasonably well, the procedure for obtaining the eigenvalues are identical, so there is no gain in using the Shear model.

In conclusion, from this comparison of standard or classical beam models it is clear that the Timoshenko model is the best option.

1.3 Variational forms and existence of solutions for the Timoshenko model

As mentioned, it is desirable that mathematical models should be well posed. For linear vibration problems, the theory in [VV02] or [VS19] can be applied. To illustrate, consider the Timoshenko model problem for a cantilever beam presented in Section 1.2. First the problem is written in variational form (in Subsection 1.3.1). In Subsection 1.3.2 the weak variational form of the problem is presented while in Subsection 1.3.3 the existence theory of solutions for general second order hyperbolic problems is discussed. The general theory is applied to the present problem in Subsection 1.3.4.

New problems are introduced in later chapters.

The variational form of the different model problems can also be used for finite element approximations. The formulation of the problem and the prop-

© University of Pretoria

erties of the relevant spaces are also useful to prove convergence of the finite element approximations and for the derivation of error estimates. General results such as those in [BV13] and [BSV17] can then be applied.

1.3.1 Variational form

The variational form for the Cantilever beam is derived below. It is derived in the usual way starting with the equations of motion (1.2.5) and (1.2.6). These equations are multiplied by test functions v and ψ respectively and integrated. The forced boundary conditions for the test functions are $v(0) = \psi(0) = 0$ and therefore a space of test functions is defined as

$$T[0,1] = \{g \in C^1[0,1] \mid g(0) = 0\}.$$

Performing integration by parts and using the boundary conditions, yields the variational form.

Model problem in variational form

Find the functions w and ϕ such that $w(\cdot,t)$ and $\phi(\cdot,t)$ are in $T[0,1]$ for all $t > 0$ and the following hold

$$\int_0^1 \partial_t^2 w(\cdot,t)v = -\int_0^1 V(\cdot,t)v' + \int_0^1 Q(\cdot,t)v, \tag{1.3.1}$$

$$\int_0^1 \frac{1}{\alpha}\partial_t^2 \phi(\cdot,t)\psi = \int_0^1 V(\cdot,t)\psi - \int_0^1 M(\cdot,t)\psi' \tag{1.3.2}$$

for all $\langle v, \psi\rangle \in T[0,1] \times T[0,1]$.

Equations (1.3.1) and (1.3.2) are the **variational equations of motion**. This together with Equations (1.2.7) and (1.2.8), produces the system in variational form. For the model problem one must prescribe initial values for w, ϕ, $\partial_t w$ and $\partial_t \phi$. Denote these by w_0, ϕ_0, w_d and ϕ_d respectively.

Remark For other problems, e.g. a pinned-pinned beam, it is only necessary to change the space of test functions.

© University of Pretoria

1.3.2 Weak variational form

The weak variational form is used to establish the existence of weak solutions. It is also used to prove convergence of the finite element approximation.

Adding Equations (1.3.1) and (1.3.2) yields

$$\int_0^1 \partial_t^2 w(\cdot,t)v + \frac{1}{\alpha}\int_0^1 \partial_t^2\phi(\cdot,t)\psi = \int_0^1 V(\cdot,t)(\psi - v') - \int_0^1 M(\cdot,t)\psi' + \int_0^1 Q(\cdot,t)v. \tag{1.3.3}$$

Using new notation, the variational form can be written in a compact form. Let u denote the pair $\langle w, \phi\rangle$.

The following bilinear forms are introduced.

For u_i and v_i in $\mathcal{L}^2(0,1)$,

$$c(u,v) = \int_0^1 u_1 v_1 + \int_0^1 \frac{1}{\alpha}\, u_2 v_2.$$

For u_i and v_i in $T[0,1]$,

$$b(u,v) = \int_0^1 \frac{1}{\beta} u_2' v_2' + \int_0^1 (u_1' - u_2)(v_1' - v_2), \tag{1.3.4}$$

Using the bilinear forms the variational form (1.3.3) can be written as

$$c(\partial_t^2 u(\cdot,t), v) + b(u(\cdot,t), v) = (Q(\cdot,t), v_1), \tag{1.3.5}$$

where (f,g) denote $\int_0^1 fg$.

Let J be any interval. Instead of considering functions w and ϕ defined on $[0,1]\times J$, consider functions $u_i : J \to \mathcal{L}^2(0,1)$. (If the problem has a classical solution, then $u_1(t)(x) = w(x,t)$ and $u_2(t)(x) = \phi(x,t)$).

Definition Derivative of a function with values in Banach space Y

Let t be any interior point of J. Suppose there exists a $v \in Y$ such that

$$\lim_{h\to 0} \left\| h^{-1}\big(u(t+h) - u(t)\big) - v \right\|_Y = 0,$$

then v is the derivative of u at t. Write $u'(t)$ for the derivative and $u'(t) \in Y$ to show that the derivative exists with respect to the norm of Y. The derivative

© University of Pretoria

(function) u' is defined in the usual way as $u'(t)$ for every $t \in J$, with u'' defined by $(u')'$.

Instead of the problem in (1.3.5), consider a problem of the form

$$c(u''(t), v) + b(u(t), v) = (Q(\cdot, t), v_1). \tag{1.3.6}$$

Care should be taken to ensure that the function u has the necessary differentiability and continuity properties for the above problem to make sense. To write the model problem in weak variational form, suitable function spaces are needed.

The Hilbert space $\mathcal{L}^2(\Omega)$ and Sobolev space $H^m(\Omega)$ are defined in Appendix A. The necessary product spaces are now defined:

$X = \mathcal{L}^2(0,1) \times \mathcal{L}^2(0,1)$,

$H^1 = H^1(0,1) \times H^1(0,1)$.

An element $y \in X$ is written as $y = \langle y_1, y_2 \rangle$.

The inner product for $\mathcal{L}^2(0,1)$ is denoted by $(\cdot, \cdot)$.

A natural inner product for X is

$$(x, y)_X = (x_1, y_1) + (x_2, y_2),$$

and the corresponding norm is denoted by $\| \cdot \|_X$.

The natural inner product for the product space H^1 is

$$(x, y)_{H^1} = (x_1, y_1)_1 + (x_2, y_2)_1$$

and the corresponding norm is denoted by $\| \cdot \|_{H^1}$.

The following propositions can be proved for the Timoshenko beam problem but proofs for similar problems appear in various publications and will therefore not be repeated here. (See also Chapter 6.)

Proposition 1.3.1. *The bilinear form c is an inner product for X.*

Definition Inertia space W

The vector space X equipped with the inner product c is referred to as the space W. The norm $\| \cdot \|_W$ is defined by $\|u\|_W = \sqrt{c(u,u)}$.

© University of Pretoria

Proposition 1.3.2. *The norms* $\|\cdot\|_W$ *and* $\|\cdot\|_X$ *are equivalent.*

Let $V(0,1)$ be the closure of $T[0,1]$ in $H^1(0,1)$ and define the product space V as

$$V = V(0,1) \times V(0,1).$$

Proposition 1.3.3. *The bilinear form* b *is an inner product for* V*.*

Definition Energy space V

The space V equipped with the inner product b is referred to as the energy space. The norm $\|\cdot\|_V$ is defined by $\|u\|_V = \sqrt{b(u,u)}$.

Proposition 1.3.4. V *is a dense subset of* W*.*

Proposition 1.3.5. *The norms* $\|\cdot\|_V$ *and* $\|\cdot\|_{H^1}$ *are equivalent on* V*.*

Notation Let q_X be the mapping $t \to \langle Q(\cdot,t), 0\rangle$.

From the definition of the bilinear form b it is now possible to define the weak variational form for the Timoshenko beam problem.

Problem in weak variational form Find u such that for each $t > 0$, $u(t) \in V$, $u'(t) \in V$, $u''(t) \in W$ and

$$c(u''(t), v) + b(u(t), v) = (q_X(t), v)_X \quad \text{for each} \quad v \in V, \tag{1.3.7}$$

with $u(0) = u_0 = \langle w_0, \phi_0\rangle$ and $u'(0) = u_d = \langle w_d, \phi_d\rangle$.

1.3.3 Existence of solutions for general second order hyperbolic problems

The weak variational form of the Timoshenko model problem in Subsection 1.3.2 is a special case of the problem in [VV02]. The general theory from that article includes damping which is represented by the bilinear form a below:

$$c(u''(t), v) + a(u'(t), v) + b(u(t), v) = (q_X(t), v)_X.$$

The following assumptions are made in the article: V, W and X are real Hilbert spaces with $V \subset W \subset X$ and $b(\cdot,\cdot)$, $c(\cdot,\cdot)$ and $(\cdot,\cdot)_X$ are the inner

© University of Pretoria

products for V, W and X respectively. The corresponding norms are $\|\cdot\|_V$, $\|\cdot\|_W$ and $\|\cdot\|_X$.

Assumptions

The following assumptions are made for the theory in [VV02].

E1 V is dense in W and W is dense in X.

E2 There exist a positive constant κ_1 such that $\|v\|_W \leq \kappa_1\|v\|_V$ for each $v \in V$.

E3 There exist a positive constant κ_2 such that $\|w\|_X \leq \kappa_2\|w\|_W$ for each $w \in W$.

E4 The bilinear form a is non-negative, symmetric and bounded on V.

For the case of weak damping, Assumption E4 is replaced by the next assumption.

Assumption E4W The bilinear form a is non-negative, symmetric and bounded on W, i.e.

$$|a(u,v)| \leq K_a\|u\|_W\|v\|_W.$$

Definition The space E_b

$E_b = \{x \in V \mid \text{there exists a } y \in W \text{ such that } c(y,v) = b(x,v) \text{ for all } v \in V\}$.

Theorem 1.3.1. *[VV02, Theorem 1] Suppose Assumptions E1 to E4 hold. If, for $u_0 \in V$ and $u_1 \in V$, there exists some $y \in W$ such that*

$$b\big(u_0,v\big) + a\big(u_1,v\big) = c\big(y,v\big) \quad \textit{for all } v \in V, \tag{1.3.8}$$

then, for each $f \in C^1\big([0,\infty);X\big)$, there exists a unique solution

$$u \in C^1\big([0,\infty);V\big) \cap C^2\big([0,\infty);W\big)$$

for the general linear vibration problem.

Note that there is a typing error in [VV02, Theorem 1], where the condition in the theorem states that $u_1 \in W$. An inspection of the proof reveals that it should be $u_1 \in V$ as it is corrected above. (This was also noted in [VS19].) The result is obtained from semigroup theory and it is proved in [VV02] that

© University of Pretoria

condition (1.3.8) is equivalent to the statement that the pair $\langle u_0, u_1 \rangle$ is in the domain of the infinitesimal generator. Condition (1.3.8) is therefore also necessary for existence.

In the case of **weak damping** the next theorem from the same article should be used.

Theorem 1.3.2. *[VV02, Theorem 2] If a is bounded with respect to the norm in W, then there exists a unique solution $u \in C^1((-\infty, \infty); V) \cap C^2((-\infty, \infty); W)$ for the general linear vibration problem for each $u_0 \in E_b$, each $u_1 \in V$ and each $f \in C^1((-\infty, \infty); X)$.*

Remark Other existence results are available in the literature, e.g. [Sho77] and [LM72]. The result from [VV02] is convenient for our problem, since it is given in terms of bilinear forms.

1.3.4 Existence of solutions for the Timoshenko beam problem

It is not difficult to apply the theory in the previous subsection to establish the existence of a unique solution for the Timoshenko beam problem in Subsection 1.3.2. It is a special case of the general problem. In our case damping is neglected, hence the bilinear form $a = 0$. From the results in Subsection 1.3.2, it is clear that Assumptions E1 to E3 and E4W hold. Using the existence result for weak damping in [VV02] with $a = 0$ a solution exists with the properties as stated in the following theorem.

Theorem 1.3.3. *Let J be an open interval containing zero. If $q_X \in C^1(J, X)$, then there exists a unique solution*

$$u \in C^1(J, V) \cap C^2(J, W)$$

for the Timoshenko beam problem for each $u_0 \in E_b$ and $u_1 \in V$. If $q_X = 0$ then $u \in C^1((-\infty, \infty), V) \cap ((-\infty, \infty), W)$.

The theory is applied to a more complex problem in Chapter 6. It is also shown in Chapter 6 how the general theory on convergence can be applied to a model problem.

© University of Pretoria

Chapter 2

Local linear Timoshenko beam

2.1 Introduction

As explained in Section 1.1, the technical reports [Van15] and [VDB16] preceded the research for the doctoral degree regarding nonlinear beam theory. As preparation for the work in [VDB16] the articles [SVQ86], [SVQ87], [Ant76] and [Ant96] were consulted.

J C Simo and L Vu-Quoc published a number of articles on large motion of beams and plates. In the paper [SVQ87] they treat the role of nonlinear theories in the analysis. They mention that large motion of beams and plates has been studied since 1958. They proceed to report on 12 other publications up to 1986, discussing shortcomings and even wrong results. They conclude that: "Fully nonlinear (geometrically exact) structural theories, such as in [SVQ86] exactly account for all inertial effects; ...". (Of course all the other relevant effects are also accounted for.) The one-dimensional theory is developed for a three-dimensional beam considering "Fully nonlinear strain measures ....". The article includes numerical aspects and the results are directly applicable.

It is clear from [Ant76] that Antman is a researcher specializing in rigorous mathematical theories where the emphasis is on deriving properties from precisely formulated definitions and assumptions. In 1996 Antman published a survey article [Ant96] concerning "..... recent results and open problems for the equations of motion for geometrically exact theories on nonlinearly viscoelastic and elastic rods." (The term *rod* here refers to a one-dimensional

© University of Pretoria

continuum and it includes beams, bars and columns.) He states that "....only recently have the equations of rods attained a form readily accessible to analysis." He referred to six papers published between 1985 and 1991, all by J C Simo and L Vu-Quoc.

While the articles in the "two streams" mentioned above contain impressive results, the main objective of this study must not be forgotten: comparison of different models for the same real world situation. And, even in the case of planar motion, there is already a lot of uncertainty. A logical first step is to consider the planar motion of a beam where the material is linearly elastic. Since the Timoshenko theory provides an excellent approximation for three-dimensional elastic behaviour with plane stress, it was decided to adapt the constitutive equations of the Timoshenko theory for large displacements (in [VDB16]). The model was named the *Local Linear Timoshenko beam* model (from now on referred to as LLT model).

For this doctoral research the aim was to improve and extend the work in [VDB16]. The improved version is Chapter 2 of the thesis. Every section was rewritten and new sections created. Changes vary from slight to significant. Some duplication was unavoidable.

First, we had another look at the relevant articles, especially [SVQ87]. The nonlinear model in [SVQ87] was compared to the LLT model in [VDB16].

In [SVQ86] and [SVQ87] a model is derived for the planar motion of a non-linear elastic beam. The authors used Hamilton's principle and derived the so called inertia operator in the inertial frame. The inertia terms are rather involved but in this approach the stiffness operator takes a simple form.

In our approach no use is made of a moving reference system. The model derived in this chapter appears completely different from the one in [SVQ86] and [SVQ87]. The inertia terms are simple but the constitutive equations appear complex. No use is made of sketches to define displacements or angles. Instead, the use of elementary differential geometry enables one to give unambiguous definitions and absolute clarity. The model appears more complicated but is not really, as explained in Subsection 2.4.2.

The article [LA12] is interesting for more than one reason. The authors motivate their work by mentioning "numerous applications in engineering". Regarding the mathematical models for large motion the authors also refer to articles by Antman and Simo and Vu-Quoc and state that modelling is still a challenging problem. According to them, obtaining "efficient numerical

© University of Pretoria

solution(s)" is another challenge.

First, in the next section, equations of motion for a one-dimensional model are derived from the conservation laws for momentum and angular momentum. The result is also in [VDB16] and is not new. It was however necessary to include the derivation to explain the assumptions for the model. The equations of motion for planar motion follows easily.

To obtain the LLT model, we adapt the constitutive equations of the Timoshenko theory.

In Section 2.6 approximations of the LLT model for small vibrations are investigated. Linear and nonlinear models are derived. The derivation of the models in [SR79] and [LL91], from the LLT model, is new. Two adapted versions of the linear Timoshenko model, with axial force, are also derived from the LLT model instead of merely inserting the force in the linear model.

It is also shown in this section that the so called "nonlinear Timoshenko" models in [SR79] and [Aro01] are almost linear. These models can be derived from the linearized equations of motion of the LLT model using the constitutive equations for shear and bending but a nonlinear constitutive equation for the axial force.

Section 2.6 is a significant improvement on the corresponding part of [VDB16].

In Section 2.8 the variational form for the linear and nonlinear Timoshenko models are derived and existence of a solution for the Adapted Timoshenko model is discussed.

Possible "derivation" of the constitutive equations is considered in Section 2.9. It must be emphasized that the use of the constitutive equations adapted from the Timoshenko theory, is an assumption and any attempt to derive them will involve additional assumptions. However, it is instructive to investigate the connection between the constitutive equations for the shear force and bending moment and three-dimensional elasticity. It shows why warping of a cross-section is inevitable. Although Section 2.9 differs from the derivation of the linear Timoshenko theory in [Cow66] there are interesting similarities.

© University of Pretoria

2.2 Dynamics of a rod

2.2.1 Conservation laws

Using the material description of motion, consider a solid with reference configuration the region $\mathcal{B}$ and any point X in $\mathcal{B}$. Suppose the position of the point at time t is $\bar{R}(X,t)$. The velocity of the point at time t is then $\bar{v}(X,t) = \partial_t \bar{R}(X,t)$. One may consult for example [Ant76] and [Fun65].

The conservation laws for momentum and angular momentum act as the basic assumptions of the theory. Suppose $\mathcal{R}$ is an arbitrary part of $\mathcal{B}$ with boundary Σ. Let ρ denote the density, and $\bar{b}$ the body force (density).

Conservation of momentum

$$\frac{d}{dt}\int_{\mathcal{R}} \rho\bar{v}\; dV = F_\Sigma + \int_{\mathcal{R}} \bar{b}\; dV, \tag{2.2.1}$$

where F_Σ denotes the resultant force due to traction on Σ.

Conservation of angular momentum

$$\frac{d}{dt}\int_{\mathcal{R}} (\bar{R}-\bar{p})\times\rho\bar{v}\; dV = M_\Sigma + \int_{\mathcal{R}} (\bar{R}-\bar{p})\times\bar{b}\; dV, \tag{2.2.2}$$

where $\bar{p}$ is any fixed point. The contribution to the moment due to traction is denoted by M_Σ.

The term rod in this section is used in the sense of [Ant76] and [Ant96]. A rigorous (and general) description can be found in these publications. In this chapter the solid $\mathcal{B}$ is a special case of a rod and it is assumed that it has the following property in the undeformed state: there exists a straight line segment in $\mathcal{B}$ such that every cross-section perpendicular to this line has its centroid on the line. (This straight line is referred to as the axis.) Use the undeformed state as reference configuration and choose coordinates for the reference configuration in such a way that the axis is the line $y = z = 0$.

Initially it is assumed that every cross-section executes a rigid motion (as is commonly done, see e.g. [SVQ87], [LL91] and [LA12]). To be specific, assume that the position of a point $X = (x,y,z)$ in $\mathcal{B}$ at time t is given by

$$\bar{R}(X,t) = \bar{r}_0(x,t) + y\bar{e}_y(x,t) + z\bar{e}_z(x,t), \tag{2.2.3}$$

where $\bar{e}_y$ and $\bar{e}_z$ are mutually orthogonal unit vectors. This implies that $\bar{e}_y$ and $\bar{e}_z$ "move with the cross-section" and a cross-section remains plane

© University of Pretoria

during the motion. Clearly $\bar{r}_0(x,t)$ is the position of the centroid $(x,0,0)$ of a cross section at time t and the position of X relative to the centroid is $\bar{r}(X,t) = y\bar{e}_y(x,t) + z\bar{e}_z(x,t)$. The normal vector $\bar{e}_y \times \bar{e}_z$ is denoted by $\bar{e}_x$.

Remark The warping of cross-sections is discussed in Section 2.9.

2.2.2 Momentum, angular momentum and body force

In the conservation laws formulated above, $\mathcal{R} \subset \mathcal{B}$ may be arbitrary. Now, consider a special case where $\mathcal{R}$ is the part of the solid between $x = a$ and $x = b$, i.e.

$$\mathcal{R} = \left\{ X \in \mathcal{B} \;\middle|\; a \leq x \leq b \right\}.$$

The velocity of the point (x,y,z) at time t is

$$\bar{v} = \partial_t \bar{r}_0 + \partial_t \bar{r} = \partial_t \bar{r}_0 + y\partial_t \bar{e}_y + z\partial_t \bar{e}_z.$$

Due to the constraints on the motion, the expressions for momentum and angular momentum simplify.

Momentum If the density ρ is constant, then the momentum of $\mathcal{R}$ is

$$\int_{\mathcal{R}} \rho\bar{v}(\cdot,t)\; dV = \rho \int_a^b A(x)\partial_t \bar{r}_0(x,t)\; dx, \tag{2.2.4}$$

where $A(x)$ is the area of the cross-section.

Angular momentum If the density ρ is constant, then the angular momentum of $\mathcal{R}$ about $\bar{0}$ is

$$\begin{aligned} \int_{\mathcal{R}} \bar{R} \times \rho\bar{v} dV &= \rho \int_a^b A(x)\bar{r}_0(x,t) \times \partial_t \bar{r}_0(x,t)\; dx \\ &+ \rho \int_a^b \int_{\mathcal{D}} \bar{r}(X,t) \times \partial_t \bar{r}(X,t)\; dA dx, \end{aligned} \tag{2.2.5}$$

where $\mathcal{D} = \mathcal{D}(x)$ denotes the relevant cross-section. The derivation is easy if one first show that

$$\int_{\mathcal{D}} \bar{r}(X,t)\; dA = 0 \quad \text{and} \quad \int_{\mathcal{D}} \partial_t \bar{r}(X,t)\; dA = 0.$$

© University of Pretoria

Body force For many applications (e.g. gravity or magnetism) it is realistic to assume that

$$\int_{\mathcal{R}} \bar{b}\, dV = \int_a^b \bar{b}_1(x,t)\; A(x)\; dx. \tag{2.2.6}$$

Assuming that $\bar{b}$ is approximately constant over a cross-section it may be replaced by the force density $\bar{b}_1$ without an additional couple. To consider the possibility of a distributed moment density is beyond the scope of this thesis.

2.2.3 Forces and couples due to traction

The boundary Σ of $\mathcal{R}$ consists of three parts: the cross-sections $\mathcal{D}(a)$ and $\mathcal{D}(b)$ and part of the outer surface of the solid between the cross-sections.

The traction on a cross-section $\mathcal{D}(x_c)$ is equivalent to a force $\bar{F}(x_c,t)$ acting at the centroid $\bar{r}_0(x_c,t)$ and a couple $\bar{M}(x_c,t)$. The following **function convention** is used: $\bar{F}(x_c,t)$ and $\bar{M}(x_c,t)$ are the force and couple acting on the part of the solid where $x \leq x_c$. Consequently the forces exerted **on** $\mathcal{R}$ are $\bar{F}(b,t)$ and $-\bar{F}(a,t)$ and the couples are $\bar{M}(b,t)$ and $-\bar{M}(a,t)$. Justification for this is discussed in Section 2.9.

For a slender solid it is assumed that the traction on the outer surface results in a distributed load $\bar{t}_S$ so that the force on $\mathcal{R}$ is

$$\int_a^b \bar{t}_S(x,t)\; dx. \tag{2.2.7}$$

(An example of this is viscous damping.)

The formulas for the forces and couples on $\mathcal{R}$ are

$$F_\Sigma = \bar{F}(b,t) - \bar{F}(a,t) + \int_a^b \bar{t}_S(x,t)\; dx \tag{2.2.8}$$

and

$$M_\Sigma = \bar{r}_0(b,t) \times \bar{F}(b,t) - \bar{r}_0(a,t) \times \bar{F}(a,t) + \bar{M}(b,t) - \bar{M}(a,t). \tag{2.2.9}$$

© University of Pretoria

2.2.4 Equations of motion for a one-dimensional model

From a mathematical point of view we now have a one-dimensional model for a slender solid, often referred to as a rod (or Cosserat rod). The reference configuration is $[0, \ell]$ where ℓ is the length of the axis.

Due to Equations (2.2.1), (2.2.4), (2.2.6), and (2.2.8), the *conservation law* for momentum may be reformulated for a one-dimensional model.

Conservation of momentum

$$\frac{d}{dt}\int_a^b \rho A \partial_t \bar{r}_0(x,t)\, dx = \bar{F}(b,t) - \bar{F}(a,t) + \int_a^b (b(x,t) + \bar{t}_s(x,t))dx.$$

Adding $\bar{b}_1$ and $\bar{t}_S$ the resultant load density is $\bar{P} = \bar{b}_1 + \bar{t}_S$.

It is useful to introduce the following notation (recalling that ρ is constant)

$$\bar{H}(x,t) = \rho \int_{\mathcal{D}} \bar{r} \times \partial_t \bar{r} dA.$$

The quantity $\bar{H}(x,t)$ is referred to as the angular momentum density (about the centroid).

Combining Equations (2.2.2) (2.2.5) and (2.2.9) yields the *conservation law* for angular momentum for a one-dimensional model.

Conservation of angular momentum

$$\begin{aligned}&\frac{d}{dt}\int_a^b \rho A \bar{r}_0(x,t) \times \partial_t \bar{r}_0(x,t) dx + \frac{d}{dt}\int_a^b \bar{H}(x,t)\, dx \\ &= \bar{r}_0(b,t) \times \bar{F}(b,t) - \bar{r}_0(a,t) \times \bar{F}(a,t) + \bar{M}(b,t) - \bar{M}(a,t) \\ &+ \int_a^b \bar{r}_0(x,t) \times \bar{P}(x,t)\, dx.\end{aligned}$$

The equations of motion follow from the conservation laws. From the conservation law for momentum:

$$\int_a^b \rho A \partial_t^2 \bar{r}_0(x,t)\, dx = \int_a^b \partial_x \bar{F}(x,t)\, dx + \int_a^b \bar{P}(x,t)\, dx.$$

The first equation of motion follows from the fact that $[a, b]$ is arbitrary.

© University of Pretoria

Equations of motion

$$\rho A \partial_t^2 \bar{r}_0 = \partial_x \bar{F} + \bar{P}, \tag{2.2.10}$$
$$\partial_t \bar{H} = \partial_x \bar{r}_0 \times \bar{F} + \partial_x \bar{M}. \tag{2.2.11}$$

To derive the second equation of motion first prove, using the standard argument above, that

$$\rho A \bar{r}_0 \times \partial_t^2 \bar{r}_0 + \partial_t \bar{H} = \partial_x (\bar{r}_0 \times \bar{F}) + \partial_x \bar{M} + \bar{r}_0 \times \bar{P}.$$

Now, $\partial_x(\bar{r}_0 \times \bar{F}) = \partial_x \bar{r}_0 \times \bar{F} + \bar{r}_0 \times \partial_x \bar{F}$ and hence the result follows by combining this result with Equation (2.2.10).

Equations (2.2.10) and (2.2.11) correspond to Equations (2.11) and (2.12) in [Ant96] where they are referred to as the classical forms of the equations of motion. The system is given by Equations (8) in [LA12], where references are provided regarding the derivation.

More detail on the angular momentum density is provided in [Ant96] and [LA12] but it is not required for the rest of this chapter.

2.3 Planar motion

Recall (from Equation (2.2.3)) that the position of a point (x, y, z) at time t is given by

$$\bar{R}(x, y, z, t) = \bar{r}_0(x, t) + y\bar{e}_y(x, t) + z\bar{e}_z(x, t),$$

where $\bar{e}_x$, $\bar{e}_y$ and $\bar{e}_z$ "move with the cross-section". Let $\{\bar{e}_1, \bar{e}_2, \bar{e}_3\}$ denote an orthonormal set "fixed" in space forming a right-handed triad. For planar motion assume that

$$\bar{r}_0(x, t) = u(x, t)\bar{e}_1 + w(x, t)\bar{e}_2$$

and $\bar{e}_z(t) = \bar{e}_3$ for each t. Note that the motion of each point is in a plane perpendicular to $\bar{e}_3$.

Since the tangent vector is

$$\partial_x \bar{r}_0(x, t) = \partial_x u(x, t)\bar{e}_1 + \partial_x w(x, t)\bar{e}_2,$$

it follows that the angle $\theta(x, t)$ of the tangent vector with the direction of $\bar{e}_1$ satisfies

$$\cos\theta = \|\partial_x \bar{r}_0\|^{-1} \partial_x u, \tag{2.3.1}$$
$$\sin\theta = \|\partial_x \bar{r}_0\|^{-1} \partial_x w. \tag{2.3.2}$$

© University of Pretoria

The unit tangent vector is given by

$$\bar{e}_T(x,t) \quad = \quad \cos\theta(x,t)\bar{e}_1 + \sin\theta(x,t)\bar{e}_2.$$

It is clear that cross-sections rotate about the $z-$axis. The angle of rotation ϕ is defined by

$$\cos\phi = \bar{e}_x \cdot \bar{e}_1 \quad \text{and} \quad \sin\phi = \bar{e}_y \cdot \bar{e}_2.$$

Consequently,

$$\begin{aligned} \bar{e}_y(x,t) &= -\sin\phi(x,t)\bar{e}_1 + \cos\phi(x,t)\bar{e}_2, \\ \bar{e}_x(x,t) &= \cos\phi(x,t)\bar{e}_1 + \sin\phi(x,t)\bar{e}_2. \end{aligned}$$

Since $\bar{e}_y \times \bar{e}_x = -\bar{e}_3 = -\bar{e}_z$, it follows that $\bar{e}_y \times \bar{e}_z = \bar{e}_x$, the unit normal to the cross-section, as required. Also, ϕ is equal to the angle between a cross section and $\bar{e}_2$ and the angle between the normal vector and $\bar{e}_1$. It follows from elementary trigonometry that $\theta - \phi$ is the angle between the normal vector to the cross-section and tangent vector.

For planar motion it is necessary that the angular momentum density $\bar{H} = H\bar{e}_z$. If $\mathcal{D}$ is symmetric with respect to the $y-$axis, then an elementary calculation shows that the angular momentum density is

$$\bar{H}(x,t) = \rho I \ \partial_t\phi(x,t)\bar{e}_3, \tag{2.3.3}$$

where I is the area moment of inertia about the $z-$axis.

To derive the equations of motion for planar motion, use Equations (2.2.10) and (2.2.11) together with

$$\partial_t^2\bar{r}_0 = \partial_t^2 u\bar{e}_1 + \partial_t^2 w\bar{e}_2 \quad \text{and} \quad \partial_t\bar{H} = \rho I \ \partial_t^2\phi\bar{e}_3.$$

Equations of motion for planar motion

$$\begin{aligned} \rho A\partial_t^2 u &= \partial_x F_1 + P_1, & (2.3.4)\\ \rho A\partial_t^2 w &= \partial_x F_2 + P_2, & (2.3.5)\\ \rho I\partial_t^2\phi &= \partial_x u F_2 - \partial_x w F_1 + \partial_x M_3. & (2.3.6) \end{aligned}$$

2.4 Local linear approximation

2.4.1 Constitutive equations

To obtain a mathematical model, the equations of motion (2.3.4), (2.3.5) and (2.3.6), must be supplemented with constitutive equations. If it is assumed

© University of Pretoria

that the motion is locally linear, then a natural choice for shear and bending are the constitutive equations of the Timoshenko theory (see Subsection 1.2.1). For the longitudinal strain Hooke's law in its simplest form is used. However, the axial force is not equal to F_1 and the shear force is not equal to F_2 due to the rotation of the tangent vector. In fact

$$F_1 = S\cos\theta - V\sin\theta, \tag{2.4.1}$$
$$F_2 = S\sin\theta + V\cos\theta, \tag{2.4.2}$$

where S denotes the axial force and V the shear force.

In the Timoshenko theory the angle between the tangent vector and the normal to the cross-section is considered to be the "average" shear strain. If it is assumed that the shear $\theta - \phi$ is small and the product of the thickness and $\partial_x\phi$ is small, then the following constitutive equations may be used.

$$M = M_3 = EI\partial_x\phi, \tag{2.4.3}$$
$$V = \kappa^2 AG(\theta - \phi). \tag{2.4.4}$$

Remark Consider the constitutive equation for the moment M above and let h denote the diameter of the cross-section in the direction of $\bar{e}_y$. For the model to be realistic, $h\partial_x\phi$ must be small. (Note that $h\partial_x\phi$ is dimensionless.)

To define the mean axial strain ϵ_s, note that

$$(\partial_x s)^2 = \|\partial_x r_0\|^2 = (\partial_x u)^2 + (\partial_x w)^2, \tag{2.4.5}$$

where s is the arc length function. The mean axial strain is defined to be

$$\epsilon_s = \partial_x s - 1. \tag{2.4.6}$$

Assume that

$$S = AE\epsilon_s, \tag{2.4.7}$$

the simplest form of Hooke's law. (The actual strain ϵ is discussed at the end of Subsection 2.4.2). If the constitutive equations above are substituted into the equations of motion, (2.3.4), (2.3.5) and (2.3.6), the model problem is in general nonlinear.

Next, we write the problem in dimensionless form. To some extent this is a repetition of work done in Chapter 1 but because of some differences it is repeated for convenience.

© University of Pretoria

Dimensionless form

Set

$$\tau = \frac{t}{t_0},\ \xi = \frac{x}{\ell},\ u^*(\xi,\tau) = \frac{u(x,t)}{\ell} \text{ and } w^*(\xi,\tau) = \frac{w(x,t)}{\ell}$$

where t_0 needs to be specified. Since ϕ is dimensionless, it follows that

$$\phi^*(\xi,\tau) = \phi(x,t).$$

Next, the forces, force densities and moments are scaled by $AG\kappa^2$, $AG\kappa^2\ell^{-1}$ and $AG\kappa^2\ell$ respectively. For example

$$F_i^*(\xi,\tau) = \frac{F_i(x,t)}{AG\kappa^2},\quad P_i^*(\xi,\tau) = \frac{\ell P_i(x,t)}{AG\kappa^2},\ \text{and } M^*(\xi,\tau) = \frac{M(x,t)}{AG\kappa^2\ell}.$$

The dimensionless form of the equations of motion are

$$\begin{aligned}
\frac{\rho\ell^2}{G\kappa^2T^2}\partial_\tau^2 u^* &= \partial_\xi F_1^* + P_1^*,\\
\frac{\rho\ell^2}{G\kappa^2T^2}\partial_\tau^2 w^* &= \partial_\xi F_2^* + P_2^*,\\
\frac{\rho I}{AG\kappa^2T^2}\partial_\tau^2 \phi^* &= \partial_\xi u^* F_2^* - \partial_\xi w^* F_1^* + \partial_\xi M_3^*.
\end{aligned}$$

A convenient choice for the quantity T is

$$t_0 = \ell\sqrt{\frac{\rho}{G\kappa^2}}.$$

With $\alpha = \dfrac{A\ell^2}{I}$, the equations of motion now read

$$\begin{aligned}
\partial_\tau^2 u^* &= \partial_\xi F_1^* + P_1^*,\\
\partial_\tau^2 w^* &= \partial_\xi F_2^* + P_2^*,\\
\frac{1}{\alpha}\partial_\tau^2 \phi^* &= \partial_\xi s^* V^* + \partial_\xi M_3^*.
\end{aligned}$$

The constitutive equations in dimensionless form are

$$\begin{aligned}
AG\kappa^2 V^* &= AG\kappa^2(\theta^* - \phi^*),\\
AG\kappa^2 S^* &= AE\epsilon_s,\\
AG\kappa^2\ell M^* &= \frac{EI}{\ell}\partial_\xi\phi^*.
\end{aligned}$$

© University of Pretoria

$$\begin{aligned} V^* &= \theta^* - \phi^*, \\ S^* &= \frac{E}{G\kappa^2}\epsilon_s, \\ M^* &= \frac{EI}{AG\kappa^2\ell^2}\partial_\xi \phi^*. \end{aligned}$$

Equations (2.4.1) and (2.4.2) converts trivially to dimensionless form and the other equations for the model, (2.3.1) (2.3.2) and (2.4.5), are effectively in dimensionless form.

The complete model problem is presented in Subsection 2.4.2, using the original notation, with dimensionless constants

$$\alpha = \frac{A\ell^2}{I}, \ \beta = \frac{AG\kappa^2\ell^2}{EI} \quad \text{and} \quad \gamma = \frac{\beta}{\alpha} = \frac{G\kappa^2}{E}.$$

2.4.2 Local linear Timoshenko beam model

Equations of motion

$$\partial_t^2 u = \partial_x F_1 + P_1, \tag{2.4.8}$$
$$\partial_t^2 w = \partial_x F_2 + P_2, \tag{2.4.9}$$
$$\frac{1}{\alpha}\partial_t^2 \phi = \partial_x u F_2 - \partial_x w F_1 + \partial_x M, \tag{2.4.10}$$

with

$$F_1 = S\cos\theta - V\sin\theta, \tag{2.4.11}$$
$$F_2 = S\sin\theta + V\cos\theta \tag{2.4.12}$$

and $\partial_x s$ and θ defined by

$$(\partial_x s)^2 = (\partial_x u)^2 + (\partial_x w)^2, \tag{2.4.13}$$
$$\cos\theta = (\partial_x s)^{-1}\partial_x u, \tag{2.4.14}$$
$$\sin\theta = (\partial_x s)^{-1}\partial_x w. \tag{2.4.15}$$

The constitutive equations are

$$M = \frac{1}{\beta}\partial_x \phi, \tag{2.4.16}$$
$$V = \theta - \phi, \tag{2.4.17}$$
$$S = \frac{1}{\gamma}(\partial_x s - 1). \tag{2.4.18}$$

© University of Pretoria

In our opinion, the model above is equivalent to the model in [SVQ87]. The two models differ in appearance due to the fact that Simo and Vu-Quoc use a moving reference frame for the velocity and acceleration terms. For the same reason comparison will be difficult and time consuming. In the mean time, it is interesting that two models derived through completely different methods could possibly be equivalent.

Boundary conditions The modelling assumptions are as follows. The shear force F and the moment M are both zero at a free end. $M = 0$ at a pinned end where u and w are fixed, while at a clamped end, u, w and ϕ are fixed. (Note that $F = 0$ implies that $S = V = 0$.)

Usually constitutive equations are substituted into equations of motion to yield partial differential equations. Following the usual approach, one would attempt to substitute F_1, F_2 and M into Equations (2.4.8), (2.4.9) and (2.4.10). This is not advisable and fortunately not necessary. Inspection of Equations (2.4.11) to (2.4.18) leads to the conclusion that F_1, F_2 and M are well defined in terms of u, w and ϕ. This model is referred to as "well formulated". A Finite element approximation is presented in Chapter 3 where simulations for this model are done and the results presented in Chapter 3. Three configurations are considered for which the boundary conditions are stated below.

Cantilever beam At the clamped end

$$u(0,t) = w(0,t) = \phi(0,t) = 0. \tag{2.4.19}$$

At the free end the boundary conditions are

$$F_1(t) = F_2(t) = M(1,t) = 0. \tag{2.4.20}$$

Pinned-pinned beam At both endpoints u, w and M are zero, i.e.

$$u(0,t) = w(0,t) = u(1,t) = w(1,t) = 0 \tag{2.4.21}$$
$$M(0,t) = M(1,t) = 0. \tag{2.4.22}$$

Pivoted beam The boundary conditions are the same as for the Cantilever beam except that $\phi(0,t) = 0$ is replaced by $M(0,t) = 0$.

For each model problem the initial values for u, w, ϕ, $\partial_t u$, $\partial_t w$ and $\partial_t \phi$ must be prescribed. Denote this by u_0, w_0, ϕ_0, u_d, w_d and ϕ_d respectively.

© University of Pretoria

Small strains

Recall that small strains are required for linear elasticity. In our model, plane stress is assumed and the resultant strains of importance are the axial strain ϵ and the shear strain $\theta - \phi$. The strain ϵ can be split:

$$\epsilon = \epsilon_s + \epsilon_B,$$

where ϵ_s is the mean strain defined in (2.4.6) and ϵ_B the strain due to bending. From the well known formula

$$\frac{\sigma}{y} = \frac{M}{I}$$

and the constitutive equation (2.4.3), the maximum strain is found to be

$$\epsilon_B \;=\; \partial_x\phi \; y_{\max},$$

which is dimensionless regardless of $\partial_x\phi$ and $y_{\max}$. More detail can be found in Section 2.9.

It is important to bear in mind that the strains $\theta - \phi$ and $\partial_x s - 1$ must be small but the rod strain $\partial_x\phi$ may be an order larger if $h/\ell \approx 1/10$. Consider for example a beam where $I = \frac{1}{12}bh^3$, then

$$\left(\frac{h}{\ell}\right)^2 = 12/\alpha = 1/100 \quad \text{for} \quad \alpha = 1200.$$

Since I is determined by the dimensions and shape of the cross-section of a beam, different values of h^* will be obtained for different structures.

Remark Due to the scaling, dimensionless forces larger than 10^{-2} should be considered large.

2.5 Simplified models

Whether the assumptions that are made are realistic, depend on the nature of forcing, the boundary conditions and initial displacements.

Pivoted beam with constant angular velocity

Consider a beam pivoted at **0**. The boundary conditions are

$$\begin{aligned} u(0,t) &= w(0,t) = 0, \\ M(0,t) &= F_1(1,t) = F_2(1,t) = M(1,t) = 0. \end{aligned}$$

© University of Pretoria

Suppose the force P is equal to zero, i.e. $P = 0$, and it is rotating with constant angular velocity ω. Let $\bar{R}(x, y, z, t) = g(x)(\cos(\omega t)\bar{e}_1 + \sin(\omega t)\bar{e}_2)$ with ω constant. Consequently $u(x, t) = g(x)\cos(\omega t)$, $w(x, t) = g(x)\sin(\omega t)$ and $\theta(t) = \omega t$.

Now, suppose the expressions for u, w and θ are substituted into (2.4.8) to (2.4.12). From Equations (2.4.8) and (2.4.9) it follows that $V' = 0$ and both equations reduce to

$$-\omega^2 g(x) = S'(x).$$

The shear force V is equal to zero due to the boundary condition at the free end. This implies that $\theta = \phi$ and since $\partial_x \phi = 0$, it follows that $M = 0$. Substituting the results into (2.4.10) shows that the equation is satisfied. The left hand side of the equation is clearly zero as well as the last term. For the other terms note that

$$\partial_x(g(x)\cos\omega t)S\sin\omega t - \partial_x(g(x)\sin\omega t)S\cos\omega t = 0.$$

It follows from Equation (2.4.13) that $\partial_x s = g'$. Note that Equations (2.4.14) and (2.4.15) are satisfied. It follows from Equation (2.4.18) and the results for s and S above that

$$g'' = \partial_x^2 s = \gamma S' = -\gamma\omega^2 g.$$

From the boundary condition for $u(0, t)$ and since $S(1) = 0$, the boundary conditions for g are $g(0) = 0$ and $g'(1) = 1$.

We then solve for g and a solution for the original problem is obtained.

Nonlinear Euler-Bernoulli models

If shear strain is ignored, a Cosserat beam is referred to as an extensible Kirchoff beam which one may think of as a "nonlinear Euler-Bernoulli beam".

Using Equations (2.4.11) and (2.4.12), a different form of Equation (2.4.10) is obtained; Equation (2.4.10) may be replaced by

$$\frac{1}{\alpha}\partial_t^2\phi = \partial_x sV + \partial_x M. \tag{2.5.1}$$

The equations of motion are now given by Equations (2.4.8), (2.4.9) and (2.5.1), where ϕ must be replaced by θ. The constitutive equation (2.4.17) is

© University of Pretoria

no longer valid. The new model can be seen as a nonlinear Euler-Bernoulli model where ϕ is replaced by θ in (2.5.1) and (2.4.16) becomes

$$M = \frac{1}{\beta}\,\partial_x\theta. \tag{2.5.2}$$

Since (2.4.17) cannot be used, the shear force V is not known. The model is not "well formulated" in the way the LLT model is. In the linear case V was eliminated before ϕ was replaced by $\partial_x w$ but this is not possible here. The shear force is implicitly defined and there is no easy way to deal with it. Since the LLT model is our concern, this model is not considered any further.

Negligible axial force

If the axial force is negligible (for example when the beam rotates slowly), the axial strain is approximately zero and the modelling assumption is $S = 0$ (which implies that $\partial_x s = 1$). As a consequence the model is simplified. For the **Timoshenko model** the equations of motion remain the same but

$$F_1 = -V\sin\theta, \tag{2.5.3}$$
$$F_2 = V\cos\theta, \tag{2.5.4}$$

and θ is now defined by

$$\cos\theta = \partial_x u, \tag{2.5.5}$$
$$\sin\theta = \partial_x w. \tag{2.5.6}$$

The constitutive equations (2.4.16) and (2.4.17) remain the same but (2.4.18) is redundant. The assumption that $S = 0$ does not affect the boundary conditions but note that now $F = 0$ if and only if $V = 0$.

Now consider the inextensible Kirchoff beam where the axial force is neglected. The assumption $S = 0$ does make the model substantially simpler than before but the complication with the shear force V remains.

2.6 Small vibrations

It is convenient when dealing with small displacements to replace $u(x,t)$ by $x+u(x,t)$ with the result that $\partial_x u$ is replaced by $1+\partial_x u$. For small vibrations

© University of Pretoria

it is usually assumed that $\partial_x u$ and $\partial_x w$ are small or θ is small. It is necessary to be careful since such assumptions may lead to contradictions.

First, just assume that θ is sufficiently small to justify the assumptions $\cos\theta \approx 1$ and $\sin\theta \approx \theta$. Then (2.4.14) implies that $\partial_x s = 1 + \partial_x u$. Next, assume that $\partial_x u$ and $\partial_x w$ are sufficiently small for $(\partial_x u)^2$ and $(\partial_x w)^2$ to be neglected. Then,

$$\begin{aligned} \partial_x s &= \sqrt{(1+\partial_x u)^2 + (\partial_x w)^2} \\ &= \sqrt{1 + 2\partial_x u + (\partial_x u)^2 + (\partial_x w)^2} \\ &\approx 1 + \partial_x u + \frac{1}{2}(\partial_x u)^2 + \frac{1}{2}(\partial_x w)^2. \end{aligned}$$

It follows that

$$\partial_x s \approx 1 + \partial_x u \tag{2.6.1}$$

and the result is the same as when the assumption θ small was used.

In many publications (e.g. [LL91] and [WFH01]) it is assumed that the effect of $\partial_x w$ in the elongation of the beam is significant. This leads to the constitutive equation

$$\partial_x s = 1 + \partial_x u + \frac{1}{2}(\partial_x w)^2. \tag{2.6.2}$$

The arguments advanced thus far are not conclusive since a lot depends on a particular application, see e.g. Subsection 2.6.3.

2.6.1 Linear and possible nonlinear models

To proceed, assume then that $\sin\theta$ and $\cos\theta$ may be replaced by θ and 1 respectively. Then Equations (2.4.11) and (2.4.12) reduce to

$$F_1 = S - V\theta, \tag{2.6.3}$$
$$F_2 = S\theta + V. \tag{2.6.4}$$

Only one constitutive equation changes (due to Equation (2.6.1)):

$$S = \frac{1}{\gamma}\partial_x u. \tag{2.6.5}$$

© University of Pretoria

Note that the system is still nonlinear. Even if one makes a further approximation $\theta \approx \tan\theta = \partial_x w$ the system will still be nonlinear.

To obtain a linear model more assumptions must be made. Let $F_1 = S$ and $F_2 = V$ in (2.4.8) to (2.4.10). Two additional models are obtained. To facilitate the discussion, the different models are numbered.

Model 1 The equations of motion are

$$\partial_t^2 u = \partial_x S + P_1, \tag{2.6.6}$$
$$\partial_t^2 w = \partial_x V + P_2, \tag{2.6.7}$$
$$\frac{1}{\alpha}\partial_t^2 \phi = (1 + \partial_x u)V - \partial_x w S + \partial_x M. \tag{2.6.8}$$

The constitutive equations are

$$M = \frac{1}{\beta}\partial_x \phi, \tag{2.6.9}$$
$$V = \partial_x w - \phi, \tag{2.6.10}$$
$$S = \frac{1}{\gamma}\,\partial_x u. \tag{2.6.11}$$

The boundary conditions are the same as for the LLT beam model in Subsection 2.4.2.

It appears as if the system is still nonlinear but if the boundary conditions for u and S does not involve the other variables, the system decouples and (2.6.6) can be solved. For example, if $u(0,t) = \partial_x u(1,t) = 0$ for (2.6.6), we have a well posed problem.

Once u and S are known, Equations (2.6.7) and (2.6.8) constitutes a linear system. We have forced vibrations due to the time dependent coefficients $\partial_x u$ and S.

2.6.2 Adapted linear Timoshenko model

In some realistic applications, $\partial_t P_1 = 0$ and then $\partial_t S = 0$ if there is no boundary forcing. Since S and $\partial_x u$ are then determined by the boundary conditions, (2.6.1) and

$$0 = \partial_x S + P_1, , \tag{2.6.12}$$

Model 1 above becomes a model for transverse vibration.

© University of Pretoria

Model 2 Adapted Timoshenko model

The resulting model is given by (2.6.12) and

$$\partial_t^2 w = \partial_x V + P_2, \tag{2.6.13}$$

$$\frac{1}{\alpha}\partial_t^2 \phi = (1+\partial_x u)V - S\partial_x w + \partial_x M. \tag{2.6.14}$$

It is a variation on the well-known Timoshenko beam model in Section 1.2. The model is used for a vertical structure in Chapters 4 and 5.

Due to the scaling the forces and force densities are small but to neglect the term $\partial_x w(\cdot,t)S$ altogether may not be wise. However $u' = \gamma S \approx \frac{1}{4}S$ is another matter and the approximation

$$(1+\gamma S)V \approx V \tag{2.6.15}$$

may be considered. This approximation is used in Section 4.2.

2.6.3 Nonlinear Timoshenko model of Sapir and Reiss

In [SR79] the authors derive a nonlinear Timoshenko beam model similar to Model 2, however the nonlinearity arises due to the fact that they use (2.6.2) as a constitutive equation.

Their aim was to study the transient motion of a buckled column using nonlinear Timoshenko beam theory. The authors provide a derivation for their model in an appendix. They start with nonlinear plane strain displacement relations and then make simplifying assumptions eventually leading to a nonlinear Timoshenko model.

In terms of the notation of this section they assume that $\partial_t^2 u$ may be neglected and that $\partial_x S = 0$. Then they use the Hamiltonian to derive Equations (A.15b) and (A.15c):

$$\partial_t^2 w = S\partial_x^2 w + \partial_x V, \tag{2.6.16}$$

$$\frac{1}{\alpha}\partial_t^2 \phi = V + \partial_x M. \tag{2.6.17}$$

Note that this model is linear if $\partial_x S = 0$ and (2.6.5) is used. This is to be expected from the way that the shear strain displacements are linearized in the derivation of the model in [SR79]. However, in [SR79] it is assumed that

$$S = \frac{1}{\gamma}(\partial_x s - 1) = \frac{1}{\gamma}\left(\partial_x u + \frac{1}{2}(\partial_x w)^2\right). \tag{2.6.18}$$

© University of Pretoria

Since $\partial_x S = 0$, it follows that

$$S = \frac{1}{\gamma}(u(1) - u(0)) + \frac{1}{2\gamma}\int_0^1 (\partial_x w(\cdot, t))^2. \tag{2.6.19}$$

The boundary conditions for the pinned-pinned case (or hinged ends) are

$$w(0,t) = \partial_x \phi(0,t) = w(1,t) = \partial_x \phi(1,t) = 0.$$

Remark The system of equations (2.6.16) and (2.6.17) follows from the local linear Timoshenko model if the external transverse body force is zero, and $\partial_x S = 0$. The derivation is based on the same assumptions as in Subsections 2.6.1 and 2.6.2 except that F_2 is replaced by $\partial_x S + V$.

Nonlinear fourth order Timoshenko beam equation

In [SR79] the authors preferred a single partial differential equation formulation for the model, which they derived by eliminating V and ϕ. First, eliminating the angular acceleration in (2.6.17) yields

$$\partial_t^4 w - \partial_t^2(S\partial_x^2 w) - \partial_t^2 \partial_x^2 w + \alpha \partial_x V + \alpha \partial_x^2 M = 0.$$

Now $\alpha \partial_x M = \gamma \partial_x^2 \phi = \gamma \partial_x^3 w - \gamma \partial_x^2 V$ so that V and its partial derivatives can be eliminated using (2.6.16)

$$\begin{aligned} \partial_t^4 w - \partial_t^2(S\partial_x^2 w) - \partial_t^2 \partial_x^2 w - \gamma \partial_x^2 \partial_t^2 w + \alpha \partial_t^2 w \\ +\gamma(1+S)\partial_x^4 w - \alpha S \partial_x^2 w = 0. \end{aligned} \tag{2.6.20}$$

A nonlinear fourth order Timoshenko beam equation is also derived in [Aro01]. The author claims that the partial differential equation above is a special case of his model.

Remark The nonlinear Timoshenko system is not equivalent to Equation (2.6.20). If the pair (w, ϕ) is a solution of the system (2.6.16)-(2.6.17) and sufficiently smooth, then w is a solution of (2.6.20). But, having a solution of this partial differential equation does not enable one to compute the shear force V or angle ϕ. The fourth order equation is not considered any further.

2.6.4 Beam models without shear

In this subsection, it is shown how a number of published models for beams can be obtained from Models 1 and 2 by eliminating shear. Consider Model 1

© University of Pretoria

and recall that dimensionless forces are small. Using the approximation (2.6.15) in (2.6.8) yields

$$\frac{1}{\alpha}\partial_t^2\phi \;=\; V + \partial_x M - \partial_x S. \tag{2.6.21}$$

Combining this equation with (2.6.7) to eliminate V yields

$$\partial_t^2 w - \frac{1}{\alpha}\partial_t^2\partial_x\phi \;=\; \partial_x(\partial_x w S) - \partial_x^2 M + P_2. \tag{2.6.22}$$

Now assume that $\phi = \partial_x w$, then $M = \frac{1}{\beta}\partial_x^2 w$ and substitution of both into Equation (2.6.22) yields the nonlinear partial differential equation

$$\partial_t^2 w - \frac{1}{\alpha}\partial_t^2\partial_x^2 w \;=\; \partial_x(\partial_x w S) - \frac{1}{\beta}\partial_x^4 w + P_2, \tag{2.6.23}$$

where the constitutive equation for S is (2.6.18).

This equation together with (2.6.6) (in Model 1) is the same as the system in [LL91] to model longitudinal and transverse vibrations. The authors use the nonlinear constitutive equation (2.6.18) for S.

A special case of the model in [LL91] is when $\partial_t P_1 = 0$ (as in Subsection 2.6.2). This is the case in [WFH01] where the transverse vibration of a vertical structure is modelled and P_1 is due to gravity.

2.7 Variational forms and existence of solutions

As mentioned in the introduction, existence of solutions is considered in a serious light. However, it is unknown whether an initial boundary value problem for the LLT model is well-posed. To investigate the literature on existence theory for nonlinear partial differential equations of hyperbolic type, is a project in its own right and beyond the scope of this thesis. For the linear system existence and uniqueness of solutions of model problems are considered in Section 2.8.

In this section the different model problems presented in Subsection 2.4.1 are written in variational form. The variational form can be used for theory and for finite element approximations.

© University of Pretoria

2.7.1 Local linear Timoshenko model

The variational form for the Local linear Timoshenko model is derived below. It is derived as in Subsection 1.3.1 starting with the equations of motion. There are three cases, formulated in Subsection 2.4.2.

Cantilever beam The forced boundary conditions for the test functions are $v(0) = z(0) = \psi(0) = 0$ and the space of test functions is defined as

$$T_1[0,1] = \{y \in C^1 \mid y(0) = 0\}.$$

The problem is to find the functions u, w and ϕ such that $u(\cdot,t)$, $w(\cdot,t)$ and $\phi(\cdot,t)$ are in $T_1[0,1]$ for all $t > 0$ and the following hold

$$\int_0^1 \partial_t^2 u(\cdot,t)v = -\int_0^1 F_1(\cdot,t)v' + \int_0^1 P_1(\cdot,t)v, \tag{2.7.1}$$

$$\int_0^1 \partial_t^2 w(\cdot,t)z = -\int_0^1 F_2(\cdot,t)z' + \int_0^1 P_2(\cdot,t)z, \tag{2.7.2}$$

$$\begin{aligned}\int_0^1 \frac{1}{\alpha}\partial_t^2\phi(\cdot,t)\psi &= \int_0^1 (1+\partial_x u(\cdot,t))F_2(\cdot,t)\psi - \int_0^1 \partial_x w(\cdot,t)F_1(\cdot,t)\psi \\ &\quad - \int_0^1 M(\cdot,t)\psi'\end{aligned} \tag{2.7.3}$$

for all $\langle v, z, \psi\rangle \in T_1[0,1] \times T_1[0,1] \times T_1[0,1]$.

Equations (2.7.1), (2.7.2) and (2.7.3) are the **variational equations of motion**. This together with Equations (2.4.11) to (2.4.18), produces the system in variational form. For the model problem one must prescribe initial values for u, w, ϕ, $\partial_t u$, $\partial_t w$ and $\partial_t \phi$. Denote these by u_0, w_0, ϕ_0, u_d, w_d and ϕ_d respectively.

Pinned-pinned beam A space of test functions for a pinned-pinned beam is defined as

$$T_2[0,1] = \{y \in C^1 \mid y(0) = y(1) = 0\}.$$

The problem is to find the functions u, w and ϕ such that $u(\cdot,t)$, $w(\cdot,t) \in T_2[0,1]$ and $\phi(\cdot,t) \in C^1[0,1]$ for all $t > 0$ and Equations (2.7.1), (2.7.2) and (2.7.3) hold for all $\langle v, z, \psi\rangle \in T_2[0,1] \times T_2[0,1] \times C^1[0,1]$.

Pivoted beam

The problem is to find the functions u, w and ϕ such that $u(\cdot,t)$, $w(\cdot,t) \in T_1[0,1]$ and $\phi(\cdot,t) \in C^1[0,1]$ for all $t > 0$ and Equations (2.7.1), (2.7.2) and (2.7.3) hold for all $\langle v, z, \psi\rangle \in T_1[0,1] \times T_1[0,1] \times C^1[0,1]$.

© University of Pretoria

2.7.2 Linear approximation of the Local linear model

Again, for Model 1 the variational form for the Cantilever beam is derived. The space of test functions is the same, $T_1[0,1] = \{v \in C^1[0,1] \mid v(0) = 0\}$.

Model problem 1 in variational form

Find the functions u, w and ϕ such that $u(\cdot,t)$, $w(\cdot,t)$ and $\phi(\cdot,t)$ are all in $T_1[0,1]$ for all $t > 0$ and the following hold

$$\int_0^1 \partial_t^2 u(\cdot,t)v = -\int_0^1 S(\cdot,t)v' + \int_0^1 P_1(\cdot,t)v, \tag{2.7.4}$$

$$\int_0^1 \partial_t^2 w(\cdot,t)z = -\int_0^1 V(\cdot,t)z' + \int_0^1 P_2(\cdot,t)z, \tag{2.7.5}$$

$$\int_0^1 \frac{1}{\alpha}\partial_t^2 \phi(\cdot,t)\psi = \int_0^1 (1+\partial_x u(\cdot,t))V(\cdot,t)\psi - \int_0^1 \partial_x w(\cdot,t)S(\cdot,t)\psi - \int_0^1 M(\cdot,t)\psi' \tag{2.7.6}$$

for all $\langle v, z, \psi\rangle \in T_1[0,1] \times T_1[0,1] \times T_1[0,1]$.

Equations (2.7.4), (2.7.5) and (2.7.6) are the variational equations of motion. This together with the constitutive equations (2.4.16), (2.4.17) and (2.6.5) produces the system in variational form.

For the model problem initial states must be prescribed as before.

2.7.3 Adapted Timoshenko model

The force S is uniquely determined by $S' = -P_1$, with $S(1) = 0$. Since $u' = \gamma S$ and $u(0) = 0$, u is also known. This is now a linear model for transverse vibration which is similar to the (standard) Timoshenko model in Section 1.3. The space of test functions $T_1[0,1]$ is the same as before.

Model problem 2 in variational form

Find the functions w and ϕ such that $w(\cdot,t)$ and $\phi(\cdot,t)$ are in $T_1[0,1]$ for all

© University of Pretoria

$t > 0$ and the following hold

$$\int_0^1 \partial_t^2 w(\cdot,t)v = -\int_0^1 V(\cdot,t)v' + \int_0^1 Q(\cdot,t)v, \tag{2.7.7}$$

$$\int_0^1 \frac{1}{\alpha}\partial_t^2\phi(\cdot,t)\psi = \int_0^1 (1+\gamma S)V(\cdot,t)\psi - \int_0^1 \partial_x w(\cdot,t)S\psi - \int_0^1 M(\cdot,t)\psi' \tag{2.7.8}$$

for all $\langle v, \psi\rangle \in T_1[0,1] \times T_1[0,1]$.

Recall that the approximation $(1+\gamma S)V \approx V$ may be considered.

2.8 Weak variational form and existence for the adapted Timoshenko model

The weak variational form for the adapted Timoshenko model is almost the same as for the (standard) Timoshenko model.

Adding Equations (2.7.7) and (2.7.8) and using the approximation (2.6.15) yields

$$\int_0^1 \partial_t^2 w(\cdot,t)v + \frac{1}{\alpha}\int_0^1 \partial_t^2\phi(\cdot,t)\psi = \int_0^1 V(\cdot,t)(\psi - v') - \int_0^1 S\partial_x w(\cdot,t)\psi - \int_0^1 M(\cdot,t)\psi' + \int_0^1 Q(\cdot,t)v. \tag{2.8.1}$$

Note the additional term containing the force S.

As in Subsection 1.3.2, let u denote the pair $\langle w, \phi\rangle$ and define the following bilinear forms.

For u_i and v_i in $\mathcal{L}^2(0,1)$,

$$c(u,v) = \int_0^1 u_1 v_1 + \int_0^1 \frac{1}{\alpha}\, u_2 v_2.$$

© University of Pretoria

For u_i and v_i in $T_1[0,1]$,

$$\begin{aligned} b_1(u,v) &= \int_0^1 \frac{1}{\beta} u_2' v_2' + \int_0^1 (u_1' - u_2)(v_1' - v_2), && (2.8.2) \\ b_2(u,v) &= \int_0^1 S u_2' v_2, && (2.8.3) \\ b &= b_1 + b_2. \end{aligned}$$

Using the bilinear forms the variational Equation (2.8.1) can be written as

$$c(\partial_t^2 u(\cdot,t), v) + b(u(\cdot,t), v) = (Q(\cdot,t), v_1), \tag{2.8.4}$$

where (f,g) denote $\int_0^1 fg$.

To write the model problem in weak variational form, suitable function spaces are needed, defined in Subsection 1.3.2. Recall the spaces X, W and V with their properties.

Note that in this subsection the inner product for the space V is b_1 instead of b. The norm $\|\cdot\|_V$ is defined by $\|u\|_V = \sqrt{b_1(u,u)}$.

Notation Let q_X be the mapping $t \to \langle Q(\cdot,t), 0\rangle$.

Problem in weak variational form Find u such that for each $t > 0$, $u(t) \in V$, $u'(t) \in V$, $u''(t) \in W$ and

$$c(u''(t), v) + b(u(t), v) = (q_X(t), v)_X \quad \text{for each} \quad v \in V, \tag{2.8.5}$$

with $u(0) = u_0 = \langle w_0, \phi_0\rangle$ and $u'(0) = u_d = \langle w_d, \phi_d\rangle$.

Existence of a unique weak solution for the problem

For the adapted Timoshenko beam problem the bilinear form b is not necessarily symmetric. Therefore the theory in [VV02] cannot be applied to the problem. However, it became known recently that the problem is solvable under certain conditions.

An improvement on the work in [VV02] has been accepted for publication in 2018. In this article, [VS19], it is shown that the symmetry of b is not necessary provided that $|b_2(u,v)| \leq k\|u\|_V\|v\|_W$. As an application the authors used a mathematical model that is referred to as the adapted Timoshenko model in this thesis.

© University of Pretoria

2.9 Connection between the constitutive equations and three-dimensional elasticity

The constitutive equations for the LLT model are (2.4.3), (2.4.4) and (2.4.7) in Subsection 2.4.1. Recall that Equation (2.4.7) is Hooke's law in its simplest form. In this section the aim is to provide some justification for (2.4.3) and (2.4.4).

2.9.1 Equilibrium problem

Recall the set $\mathcal{R}$ of arbitrary thickness $b-a$ used to derive the conservation laws for the one-dimensional model in Subsection 2.2.4. Now suppose that the thickness $\delta = b - a$ is extremely small and refer to it as the disc Δ. It will be shown that for δ small and small strain, a solution of the equations of motion satisfies the equilibrium equations.

Recall that F_Σ denotes the resultant force due to traction on Σ, the boundary of Δ. It is easy to show that there exists a positive constant K such that $\|F_\Sigma\| \leq K\delta$. The proof is the same as the proof of the action reaction principle in the theory of Continuum Mechanics. It follows that

$$\left\| \int_{\mathcal{R}} \text{div}T \; dV \right\| \leq K\delta, \tag{2.9.1}$$

where T denotes the stress tensor in the current configuration. Consequently, in the limit

$$\text{div}T = 0. \tag{2.9.2}$$

The constitutive equations can be "derived" by "solving" the Equilibrium problem (2.9.2) with suitable boundary conditions.

Recall that (by assumption) every cross-section executes a rigid rotation where the normal vector $\bar{e}_x$ is rotated through the angle $\phi(x,t)$. The displacement of Δ can be broken up into three stages. First the centroid of Σ_a is moved to $\bar{r}_0(a,t)$, then Δ is rigidly rotated through the angle $\phi(a,t)$ and lastly it is allowed to undergo deformation. Consider bending and shear of the disc Δ where a couple and shear force is applied at the surfaces (cross-sections) Σ_a (where $x = a$) and Σ_b (where $x = b$).

© University of Pretoria

To formulate the equilibrium problem the local reference system determined by the cross-section Σ_a is used. The coordinates are determined by the unit vectors

$$\begin{aligned} \widehat{e}_1 = e_x(a,t) &= \cos\phi(a,t)\bar{e}_1 + \sin\phi(a,t)\bar{e}_2, \\ \widehat{e}_2 = e_y(a,t) &= -\sin\phi(a,t)\bar{e}_1 + \cos\phi(a,t)\bar{e}_2, \\ \widehat{e}_3 = \bar{e}_z &= \bar{e}_3. \end{aligned}$$

The reference configuration Δ is the set of points (x_1, x_2, x_3) where

$$0 \leq x_1 \leq \delta$$

and (x_2, x_3) in the corresponding cross-section. Assume that Δ is prismatic, i.e. the cross-sections through Δ orthogonal to $\widehat{e}_1$ are all the same. Let h denote the diameter of the cross-section in the direction of $\hat{e}_2$.

The assumption is made that the strains are sufficiently small to justify the application of the infinitesimal theory of linear elasticity. As a consequence, the stress tensor T in the current configuration is approximately the same as in the reference configuration Δ.

The equilibrium equations are

$$\begin{aligned} \partial_1\sigma_{11} + \partial_2\sigma_{12} + \partial_3\sigma_{13} &= 0, \\ \partial_1\sigma_{21} + \partial_2\sigma_{22} + \partial_3\sigma_{23} &= 0, \\ \partial_1\sigma_{31} + \partial_2\sigma_{32} + \partial_3\sigma_{33} &= 0. \end{aligned} \tag{2.9.3}$$

By Hooke's law the infinitesimal strain is

$$\mathcal{E} = \frac{1+\nu}{E}\, T - \frac{\nu}{E}\, tr(T)\, I.$$

A displacement field $\bar{u}$ must satisfy in the interior of Δ: the equilibrium equations, Hooke's law and the definition of infinitesimal strain.

Recall that the boundary of Δ is divided into three parts: the cross-sections Σ_a, Σ_b and the outer surface Σ_{ab} where the normal $\bar{n}$ is orthogonal to $\widehat{e}_1$. The boundary conditions are

$$\begin{aligned} \bar{u} &= \bar{0} \quad \text{on } \Sigma_a \\ T\widehat{e}_1 &\neq 0 \quad \text{on } \Sigma_b, \\ T\bar{n} &= 0 \quad \text{on } \Sigma_{ab}. \end{aligned}$$

© University of Pretoria

For a unique solution $T\hat{e}_1$ must be specified at each point of Σ_b. However, there is not enough information. $T\hat{e}_1$ must result in a shear force and a couple with moment $M\hat{e}_3$ to comply with the assumptions made for the one-dimensional model.

2.9.2 Trial solution

Recall that the axial strain is split: $\epsilon = \epsilon_s + \epsilon_B$. In the analysis that follows the only concern is with the bending stress $E\epsilon_B$ which is simply denoted by σ. For a trial solution, assume plane stress

$$T = \begin{bmatrix} \sigma & \tau & 0 \\ \tau & 0 & 0 \\ 0 & 0 & 0 \end{bmatrix}. \tag{2.9.4}$$

Using Hooke's law

$$\mathcal{E} = \frac{1+\nu}{T}\, S - \frac{\nu}{E}\, tr(T)\, I,$$

we obtain the strain components:

$$\begin{aligned} \epsilon_{11} &= \frac{\sigma}{E}, \\ \epsilon_{12} &= \frac{(1+\nu)\tau}{E}, \\ \epsilon_{22} &= -\nu\epsilon_{11}. \end{aligned} \tag{2.9.5}$$

(Note that $\epsilon_{11} = \epsilon_B$.)

Recall the assumption that the cross-sections remain plain. For a trial solution, assume the following displacement in terms of functions d and ψ:

$$\begin{aligned} u_1(\bar{x}) &= -x_2 \sin\psi(x_1), \\ u_2(\bar{x}) &= d(x_1) + x_2\cos\psi(x_1) - x_2, \\ u_3(\bar{x}) &= 0. \end{aligned} \tag{2.9.6}$$

Note that $\bar{u}(\bar{0}) = \bar{0}$ if $d(0) = 0$ and $\psi(0) = 0$ and hence the boundary condition on Σ_a is satisfied.

The linear approximation of the displacement is

$$U = \begin{bmatrix} -x_2(\cos\psi)\ \psi' & -\sin\psi & 0 \\ d' - x_2(\sin\psi)\ \psi' & \cos\psi - 1 & 0 \\ 0 & 0 & 0 \end{bmatrix}.$$

© University of Pretoria

Assume that ψ is sufficiently small so that $\cos\psi \approx 1$ and $\sin\psi \approx \psi$, then

$$U = \begin{bmatrix} -x_2\ \psi' & -\psi & 0 \\ d' - x_2\ \psi\psi' & 0 & 0 \\ 0 & 0 & 0 \end{bmatrix}.$$

Since $h\psi'$ and hence $x_2\psi'$ are small, it may be assumed that

$$U = \begin{bmatrix} -x_2\ \psi' & -\psi & 0 \\ d' & 0 & 0 \\ 0 & 0 & 0 \end{bmatrix}.$$

By the definition of infinitesimal strain

$$\begin{aligned} \mathcal{E} &= \frac{1}{2}(U + U^t), \\ &= \frac{1}{2}\begin{bmatrix} -2x_2\ \psi' & d' - \psi & 0 \\ d' - \psi & 0 & 0 \\ 0 & 0 & 0 \end{bmatrix} \end{aligned} \tag{2.9.7}$$

and consequently

$$\begin{aligned} \epsilon_{11} &= -x_2\ \psi', \\ \epsilon_{12} &= \frac{1}{2}(d' - \psi)). \end{aligned} \tag{2.9.8}$$

A problem is that the trial solution does not satisfy Hooke's law: there is a discrepancy regarding ϵ_{22}. Using the supposed displacement (trial solution), $\epsilon_{22} = 0$ in (2.9.7) contradicting Equation (2.9.5).

A minor change to the trial solution (in (2.9.6)) is made:

$$u_2(\bar{x}) = d(x_1) + x_2\cos\psi(x_1) - x_2 - \frac{\nu}{2}x_2^2\psi'(x_1). \tag{2.9.9}$$

It is **assumed that** $\psi''(x_1) = 0$. The result is that $\epsilon_{22} = -\nu\epsilon_{11}$ (as required) while ϵ_{12} does not change.

Combining Equations (2.9.5) and (2.9.8) yields

$$\sigma(x_1, x_2) = -Ex_2\ \psi'(x_1), \tag{2.9.10}$$

$$\tau(x_1, x_2) = \frac{E}{2(1+\nu)}\ (d'(x_1) - \psi(x_1)) = G(d'(x_1) - \psi(x_1)). \tag{2.9.11}$$

© University of Pretoria

The solution must satisfy the equilibrium equations, i.e. it is necessary to prove that (2.9.3) holds. Now,

$$\partial_1\sigma + \partial_2\tau \;=\; -Ex_2\psi'' \tag{2.9.12}$$

and

$$\partial_1\tau \;=\; G(d'' - \psi'). \tag{2.9.13}$$

Therefore, Δ is in equilibrium if

$$d'' - \psi' = 0 \quad \text{and} \quad \psi'' = 0. \tag{2.9.14}$$

It is now necessary to relate d', ψ and ψ' to θ, ϕ and ϕ'. Recall that (by assumption) the displacement of Δ can be broken up into three stages. First the centroid of Σ_a is moved to $\bar{r}_0(a,t)$, then Δ is rigidly rotated through the angle $\phi(a,t)$. At this stage $\bar{e}_\tau(a,t) = \bar{e}_x(a,t)$, i.e. $\phi(a,t) = \theta(a,t)$.

Now consider the deformation of Δ. It follows from (2.9.14) that $d'(x) - \psi(x)$ and $\psi'(x)$ are constant. The contribution $d'(x)$ to the strain is due to the additional rotation $\theta(b,t) - \theta(a,t)$ of the neutral plane: $d'(x) = \tan(\theta(b,t) - \theta(a,t)) \approx \theta(b,t) - \theta(a,t)$.

The angle $\psi(b)$ is easily seen to be $\phi(b,t) - \phi(a,t)$. It follows that $d'(x) - \psi(x) = \theta(b,t) - \theta(a,t) - \phi(b,t) + \phi(a,t) = \theta(b,t) - \phi(b,t)$. Clearly $\partial_x\phi(x,t) = \psi'(x)$.

As mentioned, the boundary condition on Σ_a is satisfied. On Σ_b it is only required that the traction be equivalent to a couple and a shear force. By (2.9.4) the traction on Σ_b is $\bar{t} = \sigma\hat{e}_1 + \tau\hat{e}_2$. It is the same for every cross-section. Therefore, for any cross-section $\mathcal{D}$ of Δ,

$$\int_{\mathcal{D}} \sigma \; dA = 0$$

and hence it results in a couple:

$$\int_{\mathcal{D}} (x_1\hat{e}_1 + x_2\hat{e}_2) \times \sigma\hat{e}_1 \; dA = E\phi'(x_1) \int_{\mathcal{D}} x_2^2 e_3 \; dA.$$

Consequently, the constitutive equation (2.4.3) becomes:

$$M = M_3 = EI\phi'. \tag{2.9.15}$$

© University of Pretoria

Remark It follows from (2.9.10) and (2.9.15) that

$$\frac{M}{EI} = \phi' = \frac{\sigma}{-Ex_2}.$$

Compare this to the "well known formula" presented in Subsection 2.4.2.

For the shear force $V\hat{e}_2$,

$$V = \int_{\mathcal{D}} \tau \, dA = AG(\theta - \phi).$$

This is constitutive equation (2.4.4) except for the correction factor κ^2. To understand this, it is necessary to reconsider the rotation of the cross-sections. It follows from (2.9.4) that the traction on Σ_{ab} is $\tau n_2 \hat{e}_1$ and $\tau(\bar{x}) = G(d'(x_1) - \psi(x_1))$. This contradicts the prescribed boundary condition on Σ_{ab}, i.e. $T\bar{n} = \bar{0}$. To fix this, it is necessary to allow warping of the cross-sections.

2.9.3 Warping of a cross-section

A correction term must be super-imposed on the displacement $\bar{u}$ (defined in (2.9.6) and (2.9.9)). Recall that

$$\begin{aligned} u_1(\bar{x}) &= -x_2 \sin\psi(x_1), \\ u_2(\bar{x}) &= d(x_1) + x_2 \cos\psi(x_1) - x_2 - \frac{\nu}{2} x_2^2 \psi'(x_1), \\ u_3(\bar{x}) &= 0. \end{aligned}$$

To allow for the warping of a cross-section the displacement $\bar{w}$ is introduced where

$$w_1(\bar{x}) = u_1(\bar{x}) + \chi(x_2, x_3)$$

but $w_2 = u_2$ and $w_3 = u_3$.

As a result the linear approximation U changes to

$$U = \begin{bmatrix} -x_2(\cos\psi)\ \psi' & -\sin\psi + \partial_2\chi & \partial_3\chi \\ d' - x_2(\sin\psi)\ \psi' & \cos\psi - 1 & 0 \\ 0 & 0 & 0 \end{bmatrix}.$$

© University of Pretoria

The strain tensor is now given by

$$\mathcal{E} = \frac{1}{2}\begin{bmatrix} -2x_2\,\psi' & d'-\psi+\partial_2\chi & \partial_3\chi \\ d'-\psi+\partial_2\chi & 0 & 0 \\ \partial_3\chi & 0 & 0 \end{bmatrix} \tag{2.9.16}$$

and the stress tensor changes to

$$T_w = T + T_\chi = \begin{bmatrix} \sigma & \tau & 0 \\ \tau & 0 & 0 \\ 0 & 0 & 0 \end{bmatrix} + \frac{G}{2}\begin{bmatrix} 0 & \partial_2\chi & \partial_3\chi \\ \partial_2\chi & 0 & 0 \\ \partial_3\chi & 0 & 0 \end{bmatrix}. \tag{2.9.17}$$

Since σ and τ satisfy (2.9.12) and (2.9.13), it follows that χ satisfies Laplace's equation,

$$\partial_2^2\chi + \partial_3^2\chi = 0.$$

The boundary condition for χ is $n_2(\tau + \partial_2\chi) + n_3\partial_3\chi = 0$.

Unfortunately the boundary value problem does not have a unique solution (as is well known). Consequently another assumption, maybe more, must be made. The theory in [Cow66] is similar but not the same. He also reduced the problem at hand to a three-dimensional static problem but in a completely different way. (For one, he did not consider an infinitesimally thin disc.) To obtain a solution, more assumptions were introduced. As stated at the end of Section 2.1, the constitutive equations adapted from the Timoshenko theory is the modelling assumption for the LLT model and in Section 2.9 the aim is merely to investigate the connection between this theory and three-dimensional elasticity. Interestingly, it is mentioned in [LA12] that after solving a beam model problem, "three-dimensional displacement, stress and strain distributions can be conveniently carried out in a post processing by the use of 'warping functions'".

© University of Pretoria

Chapter 3

Finite element analysis of the Local Linear Timoshenko beam model

3.1 Scope of the study

In this chapter the aim is to determine the applicability of the Local Linear Timoshenko beam model (LLT model). The equations of motion and the constitutive equations are given in Section 2.4 by equations (2.4.8) to (2.4.10) and (2.4.16) to (2.4.18) respectively. For the model to be useful, it must be possible to formulate the well-posed problems.

Model problems

Using the linear theory as a guide, three "well formulated" problems were posed in Subsection 2.4.2. Recall that the problems were for a cantilever beam, a pinned-pinned beam and a pivoted beam. There is reason to believe that these problems are well-posed.

Existence and uniqueness

As mentioned, we are not aware of any results regarding the well-posedness of the relevant problems or closely related problems. For the present we have to rely on numerical experiments to see if the model yields acceptable results.

© University of Pretoria

Using a finite element approach, a semi-discrete problem is formulated in Section 3.2. To solve this problem an algorithm was developed to simulate oscillations. This was quite challenging since the dynamics is determined by 11 equations and not the usual system of partial differential equations.

The first experiments, in Section 3.3, are to show that the finite element approximations converge. The approximations obtained for small vibrations in the nonlinear model are compared to the exact solution of the linear model when available. Convergence experiments for large oscillations were also conducted.

The experiments thereafter are to compare the approximate solutions for the LLT model to that of the classical Timoshenko model. This is done in Subsection 3.4.1. In Subsection 3.4.2 a model problem is investigated where the linear theory is not applicable but the LLT model is. The beam was set in motion through forcing. A range of situations were found where the strains remained small but the nonlinear model differed significantly from the linear one.

The theory is incomplete at this stage; however, a numerical method based on finite elements has been developed and the results are more than satisfactory.

3.2 Finite element approximation

In this section it is assumed that the initial boundary value problems which originate from the LLT model are well-posed and hence we proceed to derive an algorithm to compute approximate solutions for each of the three model problems. Recall that the problems are presented in variational form in Subsection 2.7.1. The Galerkin approximation is formulated in Subsections 3.2.1 and 3.2.2 and lastly the problem is presented as a system of ordinary differential equations in Subsection 3.2.3.

3.2.1 Formulation of the semi-discrete problem

Equations (2.7.1), (2.7.2) and (2.7.3) are the variational equations of motion. This, together with Equations (2.4.11) to (2.4.18) present the system in variational form.

© University of Pretoria

Let S^h denote a finite dimensional subspace of $H^1(0,1) \cap C[0,1]$. Also, let S_1^h and S_2^h be subspaces of S^h where $f \in S_1^h$ implies $f(0) = 0$ and $f \in S_2^h$ implies $f(0) = f(1) = 0$. Denote the approximations of u, w and ϕ by u_h, w_h and ϕ_h respectively.

Cantilever beam Note that the ranges of the functions u_h, w_h and ϕ_h are in S_1^h, while the ranges of the functions F_1^h, F_2^h and M^h are in S^h.

The Galerkin approximation of the problem is given by

$$\int_0^1 \partial_t^2 u_h v = -\int_0^1 F_1^h v' + \int_0^1 P_1 v, \tag{3.2.1}$$

$$\int_0^1 \partial_t^2 w_h z = -\int_0^1 F_2^h z' + \int_0^1 P_2 z, \tag{3.2.2}$$

$$\begin{aligned}\int_0^1 \frac{1}{\alpha}\partial_t^2 \phi_h \psi &= \int_0^1 (1+\partial_x u_h) F_2^h \psi - \int_0^1 \partial_x w_h F_1^h \psi \\ &\quad - \int_0^1 M^h \psi',\end{aligned} \tag{3.2.3}$$

for arbitrary functions v, z and ψ in S_1^h.

For each of the other cases the variational form of the Cantilever beam model is referred to and the differences due to the boundary conditions are stated.

Pinned-pinned beam The ranges of the functions u_h and w_h are in S_2^h while the range of ϕ_h is in S^h. Equations (3.2.1), (3.2.2) and (3.2.3) hold for arbitrary v and z in S_2^h and ψ in S^h.

Pivoted beam The functions u_h and w_h have their ranges in S_1^h and ϕ_h its range in S^h. In this case Equations (3.2.1), (3.2.2) and (3.2.3) hold for arbitrary v and z in S_1^h and ψ in S^h.

In theory Equations (2.4.11) to (2.4.18) may be used to calculate F_1^h and F_2^h but in actual practice many difficulties arise. Consider for example Equation (2.4.13). For the finite dimensional approximation it becomes

$$(\partial_x s_h)^2 = (1+\partial_x u_h)^2 + (\partial_x w_h)^2. \tag{3.2.4}$$

If S^h consists of piecewise polynomial functions, then $\partial_x s^h$ will not be a piecewise polynomial at all. One possibility is to use the equation only at the nodes. These and other difficulties will be dealt with in the next subsection.

© University of Pretoria

3.2.2 Piecewise linear basis functions

For the rest of this section S^h is assumed to be the space of C_0 piecewise linear functions. The interval $[0,1]$ is divided into n elements of equal length and the nodes are numbered from 0 to n. Let S^h be the span of the continuous piecewise linear basis functions δ_i, for $i = 0, 1, ..., n$. S_1^h denotes the span of the same basis functions but without δ_0 while S_2^h spans the same basis functions but without δ_0 and δ_n. (See e.g. [SF73, Section 1.5] or [OR76, Section 6.5].)

Cantilever

$$\int_0^1 \partial_t^2 u_h \delta_i = -\int_0^1 F_1^h \delta_i' + \int_0^1 P_1 \delta_i \quad \text{for } i = 1 \text{ to } n, \tag{3.2.5}$$

$$\int_0^1 \partial_t^2 w_h \delta_i = -\int_0^1 F_2^h \delta_i' + \int_0^1 P_2 \delta_i, \quad \text{for } i = 1 \text{ to } n, \tag{3.2.6}$$

$$\begin{aligned}\int_0^1 \frac{1}{\alpha}\partial_t^2 \phi_h \delta_i &= \int_0^1 (1+\partial_x u_h) F_2^h \delta_i - \int_0^1 \partial_x w_h F_1^h \delta_i \\ &\quad -\frac{1}{\beta}\int_0^1 \partial_x \phi_h \delta_i', \quad \text{for } i = 1 \text{ to } n.\end{aligned} \tag{3.2.7}$$

The moment M^h was replaced by $\frac{1}{\beta}\partial_x \phi_h$ but a different approach is required for the force F^h as is explained in the next subsection.

A problem with Equation (3.2.4) is that $\partial_x u_h(\cdot,t)$ and $\partial_x w_h(\cdot,t)$ are discontinuous at the nodes. We define functions $g_u^h(t)$ and $g_w^h(t)$ in $C([0,T];S^h)$ to approximate $\partial_x u(\cdot,t)$ and $\partial_x w(\cdot,t)$: for $u_h(\cdot,t)$ and $w_h(\cdot,t)$ in S_1^h

$$\int_0^1 g_u^h(t)\delta_i = \int_0^1 \partial_x u_h(\cdot,t)\delta_i \quad \text{for } i = 0 \text{ to } n, \tag{3.2.8}$$

$$\int_0^1 g_w^h(t)\delta_i = \int_0^1 \partial_x w_h(\cdot,t)\delta_i \quad \text{for } i = 0 \text{ to } n. \tag{3.2.9}$$

Note that $g_u^h(t)$ and $g_w^h(t)$ are C_0 piecewise linear functions for each t. It follows from (3.2.4) that an approximation for the derivative of the arc length function is $d_s^h \in C([0,T];S^h)$ where

$$(d_s^h)^2 = (1+g_u^h)^2 + (g_w^h)^2. \tag{3.2.10}$$

For computational purposes the interpretation is that

$$d_s^h(x_i,t) = \sqrt{(1+g_u^h(x_i,t))^2 + (g_w^h(x_i,t))^2};$$

© University of Pretoria

the equality holds only at the nodes. The same interpretation is made for Equations (3.2.11) to (3.2.14) below.

Next, it is necessary to define θ^h, an approximation for θ. First, define functions s_θ^h and c_θ^h:

$$s_\theta^h(t) = \frac{g_w^h(t)}{d_s^h(t)}, \tag{3.2.11}$$

$$c_\theta^h(t) = \frac{g_u^h(t)}{d_s^h(t)}. \tag{3.2.12}$$

Next, use both the functions s_θ^h and c_θ^h to define θ_h in $C([0,T];S^h)$ uniquely:

$$\sin(\theta_h) = s_\theta^h \text{ and} \tag{3.2.13}$$

$$\cos(\theta_h) = c_\theta^h. \tag{3.2.14}$$

The constitutive equations for V_h and S_h in $\left([0,T],S^h\right)$ are obviously

$$V_h = \theta_h - \phi_h \text{ and} \tag{3.2.15}$$

$$S_h = \frac{1}{\gamma}(d_s^h - 1), \tag{3.2.16}$$

from (2.4.17) and (2.4.18).

Finally, in theory, F_1^h and F_2^h are defined by (using (2.4.11) and (2.4.12))

$$F_1^h = S_h \cos\phi^h - V_h \sin\phi^h \text{ and} \tag{3.2.17}$$

$$F_2^h = S_h \sin\phi^h + V_h \cos\phi^h. \tag{3.2.18}$$

The right hand sides of (3.2.17) and (3.2.18) are substituted into the integrals in (3.2.5) and (3.2.6).

Recall that initial conditions u_0, w_0, ϕ_0, u_d, w_d and ϕ_d are given for the model problem and need not be in the subspace. The initial conditions u_0^h, w_0^h, ϕ_0^h, u_d^h, w_d^h and ϕ_d^h in the subspace must be chosen. For the simulations in this chapter interpolants are used. For example u_0^h is the interpolant of u_0.

3.2.3 System of Ordinary differential equations

It is important to note that u_h may be considered as a mapping from the real line into S_1^h or as a function of two variables.

© University of Pretoria

From the finite element approximation in the previous subsection a system of ordinary differential equations is derived.

As before, consider the cantilever beam first. Recall that S^h is the span of the set of basis functions $\{\delta_0,\ \delta_1, \cdots,\ \delta_n\}$ and S_1^h is the span of the set of basis functions $\{\delta_1,\ \delta_2, \cdots,\ \delta_n\}$. It is convenient to introduce the following transformations. For any $\bar{x} \in R_{n+1}$, let

$$T^h \bar{x} = \sum_{i=0}^{n} x_i \delta_i \in S^h$$

and for any $\bar{x} \in R_n$, let

$$T_1^h \bar{x} = \sum_{i=1}^{n} x_i \delta_i \in S_1^h.$$

The mappings T_h and T_1^h are obviously linear bijections. Consequently, corresponding to a function w with values in S^h, define a function $\bar{w}$ with values in R_{n+1} by

$$\bar{w}(t) = (T^h)^{-1} w(t).$$

Note that w is differentiable if and only if w_j is differentiable for each j and

$$\frac{d}{dt}\left(\sum_{j=0}^{n} w_j(t)\delta_i\right) = \sum_{j=0}^{n} w_j'(t)\delta_i.$$

The same is true for the second order derivative.

Similarly, for a function w with values in S_1^h, define a function $\bar{w}$ with values in R_n by

$$\bar{w}(t) = (T_1^h)^{-1} w(t).$$

Now, consider Equation (3.2.1). Define the function $\bar{u} \in C([0,\tau]; R^n)$ as

$$\bar{u}(t) = (T_1^h)^{-1} u^h(t).$$

An ordinary differential equation for $\bar{u}$ is then derived from Equation (3.2.1). The following matrices will be used. For $i = 0, \cdots, n$ and $j = 0, \cdots, n$:

$$M_{ij} = (\delta_j, \delta_i),\ K_{ij} = (\delta_j', \delta_i') \text{ and } L_{ij} = (\delta_j, \delta_i'), \tag{3.2.19}$$

Let A be a matrix representing M, K or L. The following notation is introduced:

$$\begin{aligned} A &= A_{ij},\ i = 0, \cdots, n \text{ and } j = 0, \cdots, n, \\ A_0 &= A_{ij},\ i = 1, \cdots, n \text{ and } j = 1, \cdots, n, \\ A_r &= A_{ij},\ i = 1, \cdots, n \text{ and } j = 0, \cdots, n, \\ A_c &= A_{ij},\ i = 0, \cdots, n \text{ and } j = 1, \cdots, n. \end{aligned} \tag{3.2.20}$$

© University of Pretoria

Consider for example Equation (3.2.1). It is obvious how to treat the term on the left and the last term. For the first term on the right, one may define a function $\bar{G}_1$ by

$$\left[\bar{G}_1\right]_i(t) = \int_0^1 F_1^h(\cdot, t)\delta_i', \quad i = 1, 2, \cdots, n, \tag{3.2.21}$$

where F_1^h is defined by (3.2.17) (in theory but not in practice). Therefore it is necessary to compute an approximation for F_1^h.

Equation (3.2.2) is treated similarly.

Calculation of approximations for forces

First, g_u^h and g_w^h are defined by (3.2.8) and (3.2.9) respectively. Therefore $\bar{g}_u(t) = (T^h)^{-1}g_u^h(t)$ and $\bar{g}_w(t) = (T^h)^{-1}g_w^h(t)$ are given by

$$M\bar{g}_u(t) = L_c\bar{u}(t), \tag{3.2.22}$$
$$M\bar{g}_w(t) = L_c\bar{w}(t). \tag{3.2.23}$$

Next, the approximation for the derivative of the arc length function d_s^h is defined by (3.2.10). Rather interpolate, using the components of $\bar{d}_s$, $\bar{g}_u$ and $\bar{g}_w$. Bear in mind that the components of $\bar{g}_u$ and $\bar{g}_w$ are the nodal values of g_u^h and g_w^h. Thus $\bar{d}_s$ is defined by

$$d_{s,i}(t) = \sqrt{(1 + g_{u,i}(t))^2 + (g_{w,i}(t))^2}. \tag{3.2.24}$$

Note that $T^h\bar{d}_s(t) \neq d_s^h(t)$ but it will be an approximation.

Next, the functions $\bar{s}_\theta$, $\bar{c}_\theta$ and $\bar{\theta}$ are defined. Recall that the finite element approximations for the composite functions $\cos(\theta_h)$ and $\sin(\theta_h)$ are denoted by c_θ^h and s_θ^h and defined by Equations (3.2.11) and (3.2.12). Again, use interpolation so that: $s_{\theta,i}(t) = \dfrac{g_{w,i}(t)}{d_{s,i}(t)}$ and $c_{\theta,i}(t) = \dfrac{g_{u,i}(t)}{d_{s,i}(t)}$. ($T^h\bar{s}_\theta \neq s_\theta^h$ but it is an approximation.)

To $\theta^h(t)$ corresponds $\bar{\theta}(t)$. Use $\sin(\theta_i(t)) = s_{\theta,i}(t)$ and $\cos(\theta_i(t)) = c_{\theta,i}(t)$ to define $\theta_i(t)$ uniquely.

It is now possible to consider the constitutive equations (3.2.15) and (3.2.16). Instead of calculating V^h and S^h, calculate $\bar{V}$ and $\bar{S}$ with the idea that $T^h\bar{S}$ and $T^h\bar{V}$ can be used. Consequently, the following is used:

$$\bar{V}(t) = \bar{\theta}(t) - \bar{\phi}(t),$$
$$\bar{S}(t) = \frac{1}{\gamma}(\bar{d}_s(t) - 1).$$

© University of Pretoria

Note that $\bar{\phi} \in R^n$ but $\bar{\theta} \in R^{n+1}$ and $\theta^h(0)$ is not necessarily zero. Therefore, add a first component to $\bar{\phi}$ which is zero to ensure that the dimensions of $\bar{\theta}$ and $\bar{\phi}$ correspond.

The approximations

$$F_1^h = (T^h\bar{S})(T^h\bar{c}_\theta) - (T^h\bar{V})(T^h\bar{s}_\theta) \quad \text{and} \tag{3.2.25}$$
$$F_2^h = (T^h\bar{V})(T^h\bar{c}_\theta) + (T^h\bar{S})(T^h\bar{s}_\theta) \tag{3.2.26}$$

are used in (3.2.1), (3.2.2) and (3.2.3) to derive a system of ordinary differential equations for $\bar{u}$, $\bar{w}$ and $\bar{\phi}$. Recall that a function $\bar{G}_1$ is defined by

$$\left[\bar{G}_1\right]_i(t) = \int_0^1 F_1^h(\cdot,t)\delta_i', \quad i = 1, 2, \cdots, n,$$

where F_1^h is defined by (3.2.25). Define a function $\bar{P}_1$ by

$$P_{1,i}(t) = \int_0^1 P_1(\cdot,t)\delta_i, \quad i = 1, 2, \cdots, n.$$

Similarly, the differential equations for $\bar{w}$ and $\bar{\phi}$ may be derived. The following system is to be solved:

$$M_0\bar{u}'' = \bar{G}_1 + \bar{P}_1, \tag{3.2.27}$$
$$M_0\bar{w}'' = \bar{G}_2 + \bar{P}_2, \tag{3.2.28}$$
$$\frac{1}{\alpha}M_0\bar{\phi}'' = \bar{G}_u - \bar{G}_w - \frac{1}{\beta}K\bar{\phi}, \tag{3.2.29}$$

where $\bar{G}_u$ and $\bar{G}_w$ are defined by

$$\left[\bar{G}_u\right]_i(t) = \int_0^1 F_2^h g_u^h \delta_i, \tag{3.2.30}$$
$$\left[\bar{G}_w\right]_i(t) = \int_0^1 F_1^h g_w^h \delta_i, \tag{3.2.31}$$

for $i = 1, 2, \cdots, n$.

Finally, $T^h\bar{u}$, $T^h\bar{w}$ and $T^h\bar{\phi}$ are considered to be the approximations for u, w, and ϕ. To be precise, define $u_h(\cdot,t) = T^h\bar{u}(t)$ and similarly for w_h and ϕ_h.

Finite differences

To solve the system of ordinary differential equations we make use of central difference approximations for Equations (3.2.27), (3.2.28) and (3.2.29). At

© University of Pretoria

each time step the procedure in this section is used. The known values for $\bar{u}_k$ and $\bar{w}_k$ are used in (3.2.22) and (3.2.23) and $\bar{s}_k$, $\bar{c}_k$ and $\bar{\theta}_k$ are computed. Note that $\bar{V}_k = \bar{\theta}_k - \bar{\phi}_k$. The discrete version of (3.2.27) to (3.2.29) is used to compute $\bar{u}_{k+1}, \bar{w}_{k+1}$ and $\bar{\theta}_{k+1}$.

For the first step we use a predictor corrector procedure.

3.3 Numerical experiments for convergence

After some consideration of the algorithm we concluded that it may be a formidable task to derive error estimates and prove convergence of an approximation; certainly beyond the scope of this preliminary investigation.

Due to the absence of convergence theory, numerical experiments are used to show convergence. For a fixed number of elements the finite difference approximations behaved as expected. Care was taken with each experiment to ensure that the number of time steps were sufficient to ensure that the errors generated through finite difference approximations are negligible. The same procedure is followed for all the experiments in this section.

For the convergence experiments the system of differential equations in Subsection 3.2.3 is considered for small and large motions regardless of whether the strains are small.

The algorithm is not compared to other algorithms and there is no numerical theory that we wish to vindicate by these numerical experiments. Inspection of the graphs for deflection and angle of rotation for different number of elements is considered sufficient.

3.3.1 Small vibrations

For small displacements it is possible to compare the approximations obtained by this model to those for the linear Timoshenko model. The focus will be on the transverse motion of the beam. As such, results are mainly shown for w.

Consider the free vibration of a pinned-pinned beam. Note that for free vibration $P_1 = P_2 = 0$. In the first experiment a pinned-pinned beam with an initial displacement is considered. The exact solution of the linear model

© University of Pretoria

is known. It is reasonable to expect that the linear and nonlinear models will compare well if the initial disturbance is sufficiently small. The exact solution is used to establish whether the numerical results obtained for the non-linear model agree with our expectation as well as to show convergence.

In Subsection 1.2.3 the use of separation of variables for the Timoshenko beam is discussed and the eigenvalues and eigenfunctions for a cantilever beam are calculated. Any natural mode of vibration is a classical solution of the model problem with natural angular frequency $\sqrt{\lambda_k} = \omega_k$.

For the pinned-pinned beam the eigenvalues are the solutions of Equations (21) and (22) on page 63 in [VV06]. The system consists of a linear and a quadratic equation which is easy to solve. For each eigenvalue λ_k there is a corresponding real number A_k and the eigenfunctions that correspond to λ_k are $\langle \sin k\pi x, A_k \cos k\pi x \rangle$. An exact solution of the linear model is

$$\begin{aligned} w_E(x,t) &= c\cos(\omega_k t)\sin(k\pi x), \\ \phi_E(x,t) &= c\cos(\omega_k t) A_k \cos(k\pi x). \end{aligned}$$

Experiment 1: Comparison to the exact solution of the linear model

Consider the first mode of the linear Timoshenko beam model. For the case $\alpha = 1200$, the first mode consists of the eigenvalue $\lambda = 0.3119$ (correct to 4 decimals) with corresponding eigenfunction $\langle \sin \pi x, A \cos \pi x \rangle$, where $A = \dfrac{\pi^2 - \lambda}{\pi}$. The period of the solution is $2\pi/\sqrt{\lambda}$ which is approximately 4π. We anticipate that the corresponding solution of the non-linear problem will be approximately periodic with a period close to the linear model.

The initial condition must be chosen appropriately and therefore a multiple of the eigenfunction is used. (Initially the boundary conditions will be satisfied automatically.) The same initial condition is used for the non-linear problem. The beam is started from rest. For the linear model there is no axial displacement u, therefore we choose $u(x,0) = 0$. The initial conditions are

$$\begin{aligned} w(x,0) &= c\sin(\pi x), \\ \phi(x,0) &= cA\cos(\pi x), \\ u(x,0) &= \partial_t w(x,0) = \partial_t \phi(x,0) = \partial_t u(x,0) = 0, \end{aligned}$$

where the constant c has to be specified. Note that c determines the magnitude of the initial displacement. It must be sufficiently small for the strains

© University of Pretoria

to be small, so we choose $c = 0.001$. The strains are calculated in the initial shape of the beam to verify that they are small. (Recall the discussion in Subsection 2.4.2.) Since $\phi'(x) = -\pi c A \sin \pi x$ it follows that

$$\max |\phi'(x)| = |c(\pi^2 - \lambda)| \leq \pi^2 \times 10^{-3}.$$

From the initial condition it follows that $w'(x) = \pi c \cos \pi x$ and $\phi(x) = cA \cos \pi x$ and hence

$$\max |w' - \phi| = |c(\pi - A)| = \frac{c\lambda}{\pi} < 10^{-4}.$$

Finally, since $u' = 0$, it follows that $(s')^2 = (w')^2 + 1$ and

$$\max |s' - 1| = \sqrt{1 + (\pi c)^2} - 1 \leq \frac{1}{2}(\pi \times 10^{-3})^2.$$

From these calculations it is clear that the initial strains are sufficiently small. For the modal solution the stresses cannot be larger at any given time.

The experiment consists of two parts. First, convergence is shown - both the deflection and angle of rotation curves for $8, 16, 32$ and 64 elements were compared. The results obtained for the deflection of the beam are displayed in Figure 3.1.

Relative differences at $x = 0.5$ were calculated and the results are given below. (Take note of the scale on the vertical axis.) The approximations with n elements are denoted by w_n and the following is calculated:

$$\frac{w_{4n}(0.5) - w_{2n}(0.5)}{w_{2n}(0.5) - w_n(0.5)},$$

where $w_k(0.5)$ denotes the value of w at $x = 0.5$ for $T = 2\pi$. The results are

$$\frac{w_{32}(0.5) - w_{16}(0.5)}{w_{16}(0.5) - w_8(0.5)} = 0.25,$$
$$\frac{w_{64}(0.5) - w_{32}(0.5)}{w_{32}(0.5) - w_{16}(0.5)} = 0.333.$$

Note that the ratios of the differences are less than $\frac{1}{2}$. These results are sufficient to suggest convergence for the pinned-pinned model. (One may conjecture that the order of convergence could be better than order h.)

© University of Pretoria

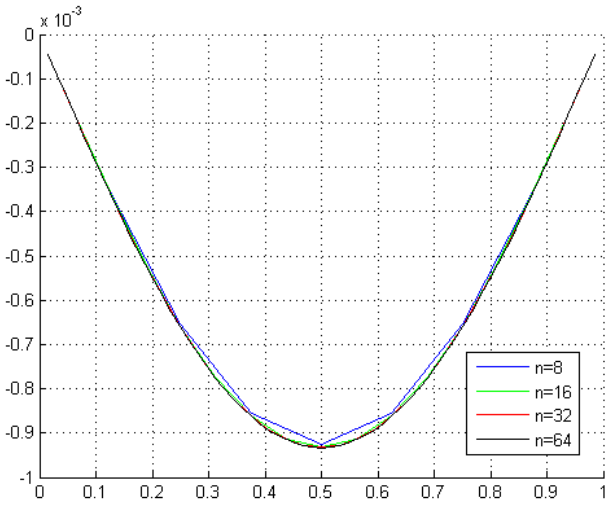

Figure 3.1: Deflection w for $T = 2\pi$, $\alpha = 1200$

Remark Different final times were considered but only $T = 2\pi$ (approximately half a period) is displayed. In Figure 3.2 a part of Figure 3.1 is enlarged to see the results more clearly.

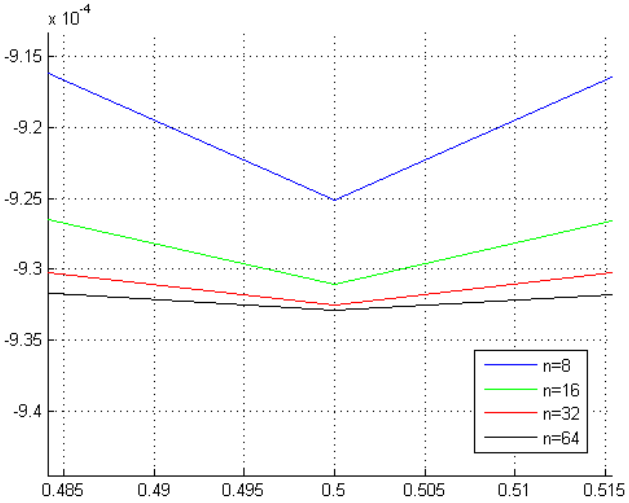

Figure 3.2: Deflection w for $T = 2\pi$, $\alpha = 1200$ (Enlarged)

Next, the approximation of the solution of the nonlinear problem and the *exact solution of the linear model* are compared. The values $\alpha = 1200$,

© University of Pretoria

$T = 2\pi$, $n = 32$ and $c = 0.001$ are used. The results for the deflection of the beam are shown in Figure 3.3.

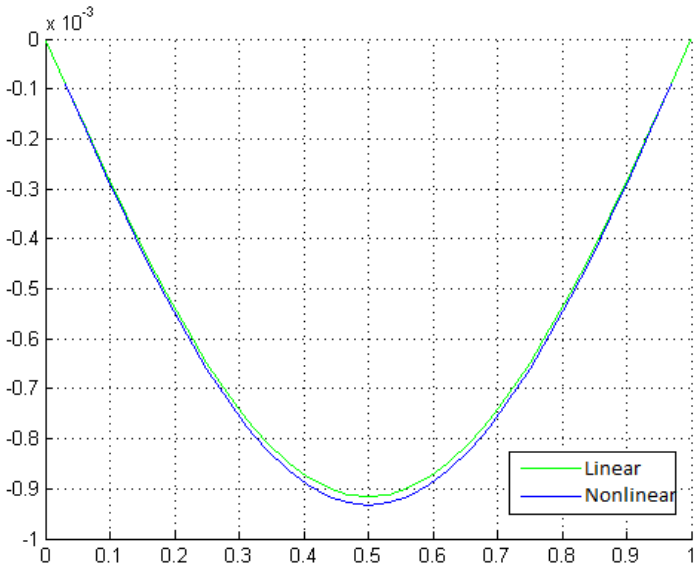

Figure 3.3: Linear v.s. Nonlinear deflection w: $T = 2\pi$, $\alpha = 1200$

Remark The "difference" at the endpoints of the deflection curves (as seen in Figure 3.3) is due to zero boundary values not being present in numerical computations.

Again, the part of the graph where the most significant difference can be observed is enlarged and the result is shown in Figure 3.4. From this figure one can see that the difference between the numerical approximation for 32 elements and the exact solution of the linear problem is less than 0.2×10^{-4}. (Take note of the scale on the vertical axis in Figure 3.4.)

If one assumes that the linear model is valid, then it is clear from the experiment that the numerical approximations for the nonlinear model converge. On the other hand, if one assumes that the non-linear model is valid because it has less assumptions and is derived rigorously, then the results show that the linear model gives a good approximation for small disturbances.

© University of Pretoria

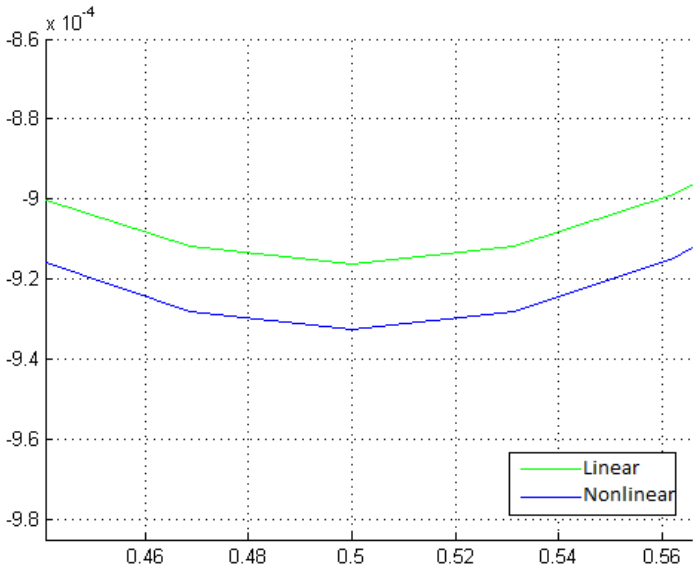

Figure 3.4: Linear v.s. Nonlinear deflection w (Enlarged)

3.3.2 Forced vibration

Consider a Cantilever beam with $\alpha = 1200$, set in motion by the load $P_2 = c\sin(\omega t)x$ with $\omega = 1$ and $c = 0.1$ while $P_1 = 0$. The initial conditions $u(x,0)$, $w(x,0)$, $\phi(x,0)$ and their time derivatives are all zero.

Experiment 2: Convergence for a Cantilever beam with load

Since the load is large it causes very large oscillations. The results are not realistic from a modelling perspective but the objective was to study convergence for large solutions. The results displayed are for $T = 2\pi$. (The final time T is chosen such that it is the period of the load.)

Approximations were obtained for 8, 16, 32 and 64 elements. The results for the deflection of the beam and the angle of rotation can be seen in Figure 3.5 and Figure 3.6 respectively.

© University of Pretoria

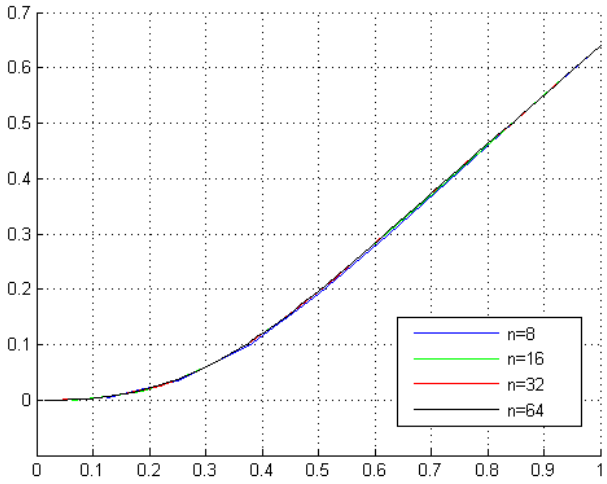

Figure 3.5: Forced vibration: Deflection w for $T = 2\pi$, $\alpha = 1200$

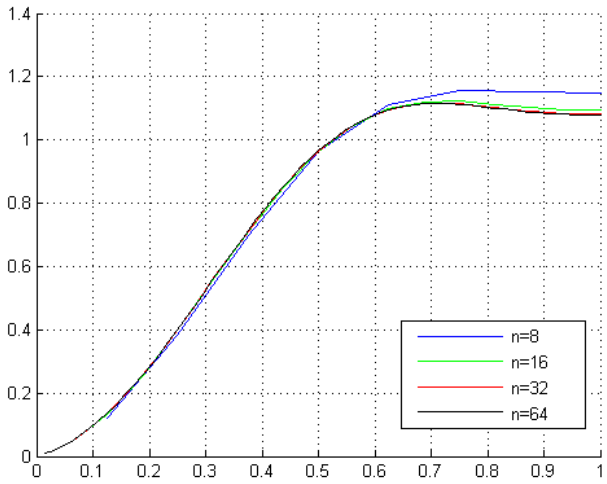

Figure 3.6: Forced vibration: Angle of rotation ϕ for $T = 2\pi$, $\alpha = 1200$

To better see the results, a part of Figure 3.5 was enlarged, this can be seen in Figure 3.7. Similarly, the part of Figure 3.6 where the largest differences were observed (i.e. $0.84 < x < 0.94$) was also enlarged and the results are shown in Figure 3.8. (Note the scale on the axes.)

© University of Pretoria

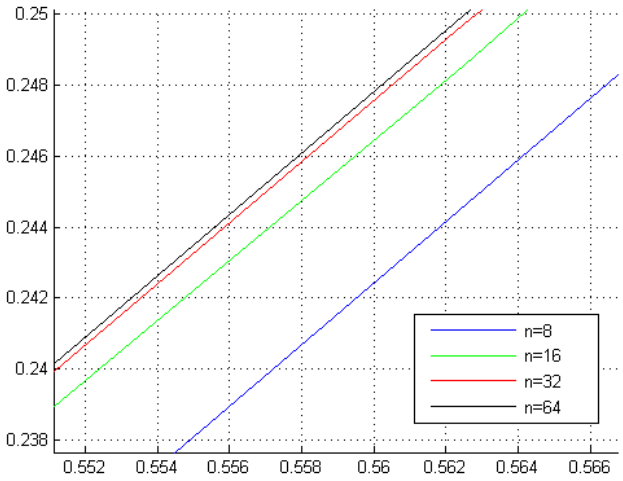

Figure 3.7: Forced vibration: Deflection w (Enlarged)

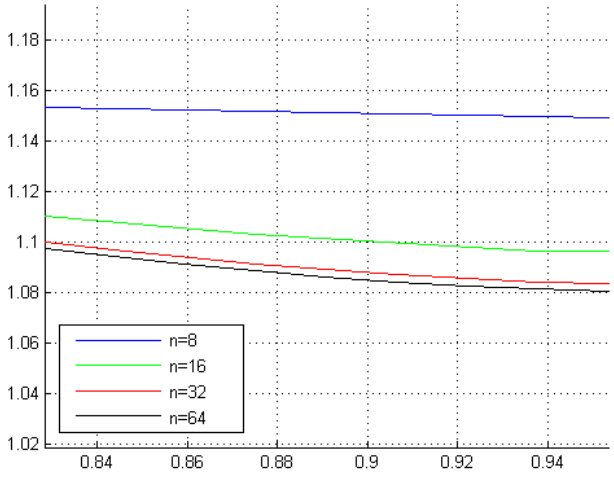

Figure 3.8: Forced vibration: Angle of rotation ϕ (Enlarged)

A notable improvement is observed when using 16 elements instead of 8. Thereafter the results changes slightly. The difference between the results using 32 elements and 64 elements is more or less 0.003 at both the left and right end-points of the subinterval. This gives an error of less than 0.3%.

Consider the same experiment but with a final time $T = 11\pi$. The following

© University of Pretoria

results were obtained.

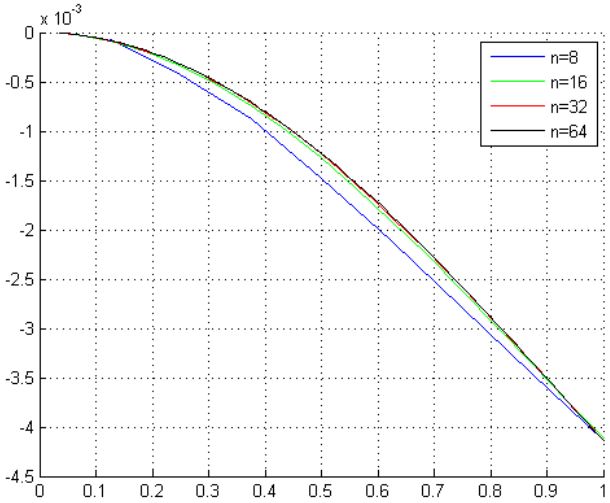

Figure 3.9: Forced vibration: Deflection w for $T = 11\pi$

A part of Figure 3.9 is enlarged in Figure 3.10 for closer inspection.

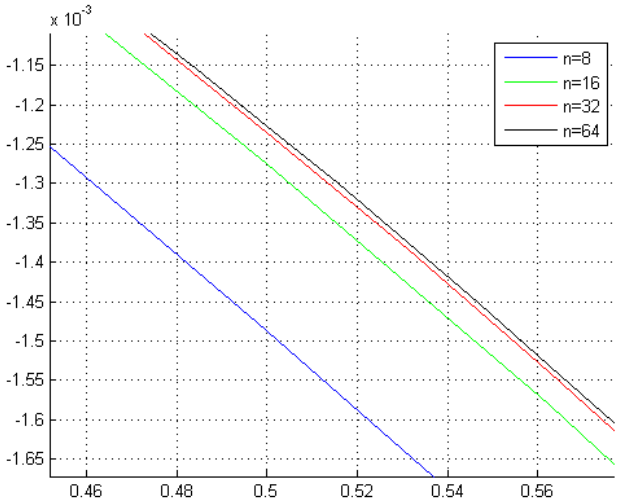

Figure 3.10: Forced vibration: Deflection w for $T = 11\pi$ (Enlarged)

Considering the scale on the vertical axis it is clear that the approximations obtained using 8 and 64 elements respectively, are surprisingly close

© University of Pretoria

to one another. Doing similar calculations as in the previous subsection, it was found that the ratios of differences are less than 1/2. Repeating this experiment for the different values of ω, c and final times T produces similar results.

Considering the outcome of the preliminary experiment it is reasonable to assume that the approximations converge. More comprehensive experiments are part of future work.

3.4 Applicability of the Local Linear Timoshenko model

In this section the aim is to show that there exists situations where the LLT model is applicable but the linear model not. To establish this we first determine when solutions for these models differ significantly. However, it is required that the beam strains remain acceptable, i.e. the strains $\theta - \phi$, $\partial_x s - 1$ and $\partial_x \phi$ are required to be small as discussed in Section 2.4.2 and briefly in the previous section. (Recall that $\partial_x \phi$ may be an order larger than other strains, depending on the value of α.)

Two experiments are considered in this section. In Subsection 3.4.1 the LLT model for a pinned-pinned beam is compared with the exact solution of the linear model and in Subsection 3.4.2 the forced vibration of a cantilever beam is simulated and the oscillations of nonlinear and linear models are compared.

All experiments are carried out with a sufficient number of elements and time steps to ensure four significant digits can be guaranteed. The results are displayed visually for convenience.

3.4.1 Comparison to classical linear Timoshenko model

In Experiment 1 "periodic-like" motion was observed. The "period" of the nonlinear problem cannot be determined exactly, but the oscillations closely resemble periodic motion. Obviously, oscillation of the beam does not imply that that the solution is periodic.

Experiment 3: Free vibration of a pinned-pinned beam

© University of Pretoria

In this experiment a pinned-pinned beam with non-zero initial displacement is considered. The situation is the same as for Experiment 1, but now we choose $\alpha = 4800$ (hence the beam is more flexible) and the initial deflection is a scalar multiple of the deflection from Experiment 1.

Although there is some duplication between this subsection and Subsection 3.3.1 the aim is different and experiments are performed with larger values of c. From the previous experiment it is clear that for $c = 0.001$ and smaller the nonlinear model behaves like the linear model. Again, there is no forcing on the beam, i.e. $P_1 = P_2 = 0$. As in Subsection 3.3.1 the first mode is used as an exact solution. Since α is different the mode will be different with $\lambda = 0.0804$, $A = (\pi^2 - \lambda)/\pi$ and $\omega = \sqrt{\lambda}$. The dimensionless period is $2\pi/\omega = 22.16$ correct to four significant digits. Recall that the initial condition is given by

$$\begin{aligned} w(x,0) &= c\sin(\pi x), \\ \phi(x,0) &= cA\cos(\pi x), \\ u(x,0) &= 0. \end{aligned}$$

A larger value of c, $c = 0.01$, is now considered to obtain larger oscillations.

The initial strains are calculated as follows:

$$\begin{aligned} \max|\phi'| &= |-cA\pi| < c(\pi^2 - \lambda) < \pi^2 \times 10^{-2}, \\ \max|w' - \phi| &= |(\pi - A)c| < \frac{c\lambda}{\pi} < \frac{0.0804}{\pi} \times 10^{-2} < 3 \times 10^{-4}, \\ \max|s' - 1| &= |\sqrt{1 + (\pi c)^2} - 1| < \frac{1}{2}\pi^2 \times 10^{-4}. \end{aligned}$$

Although the maximum of $w(x,0)$ is ten times the value in Experiment 1, the strains are still acceptable. (See the discussion in Subsection 2.4.2 and note that in this experiment $\alpha = 4800$.)

The expectation is that the nonlinear model will differ significantly from the exact solution of the linear model. Different final times were considered but specifically, the results close to the period of the exact solution are displayed.

The deflection curves w are shown in Figures 3.11 and 3.12 for final times $T = 21$ and $T = 22$ respectively, using 32 elements. In Figure 3.11 it is clear that the deflection for the nonlinear case is approximately the same as the initial deflection but this is not the case for the linear problem. The deflection curve for the linear problem "reaches" this "position" at time $T = 22$ (see Figure 3.12). This is in agreement with the fact that the period is 22.16.

© University of Pretoria

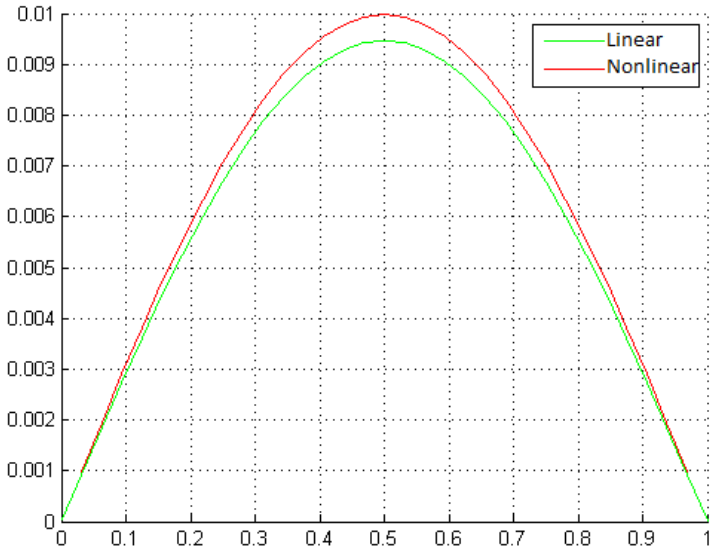

Figure 3.11: Deflection w at $T = 21$ with $\alpha = 4800$

In Figure 3.12 it can also be seen that the deflection curve for the nonlinear beam is "moving down" already.

For more information, consider Figure 3.13. Here a final time of $T = 25$ is used and the difference between the deflection curves is significant. It is also clear that the nonlinear beam is "moving down fast" while the linear beam has "hardly started". Considering Figure 3.13 together with Figures 3.11 and 3.12 it is clear that the solution of the nonlinear model is approximately periodic and has a significantly shorter "period" than the solution of the linear model.

For $c = 0.01$ the nonlinear model behaves similar to the linear model, but significant differences can be observed. Simulations were also done with $c = 0.005$ and similar results were obtained except at larger end times such as $T = 43$ and $T = 45$.

Values for c as large as 0.1 were used and solutions for the nonlinear model differed to the extent that they could not be compared to solutions of the linear model. Unfortunately, large deflections resulted in large strains and hence the nonlinear model was not valid. Since the beam is fixed at both ends, it must stretch, leading to these unacceptable strains. Consequently, a cantilever beam is considered in the next experiment.

© University of Pretoria

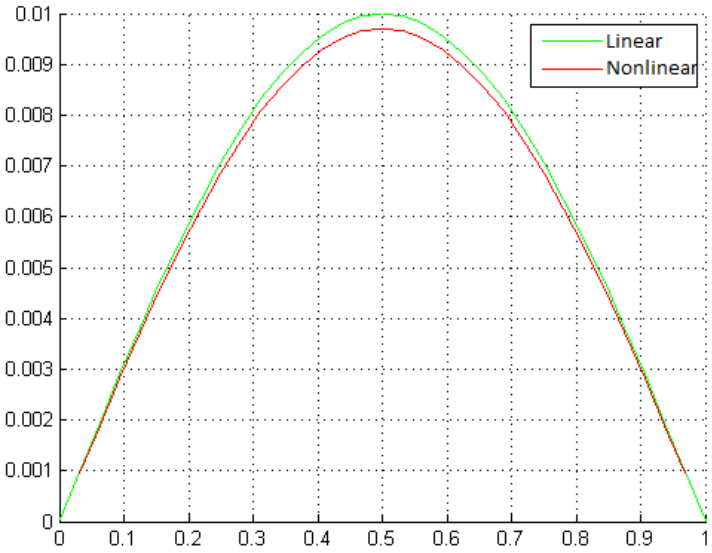

Figure 3.12: Deflection w at $T = 22$ with $\alpha = 4800$

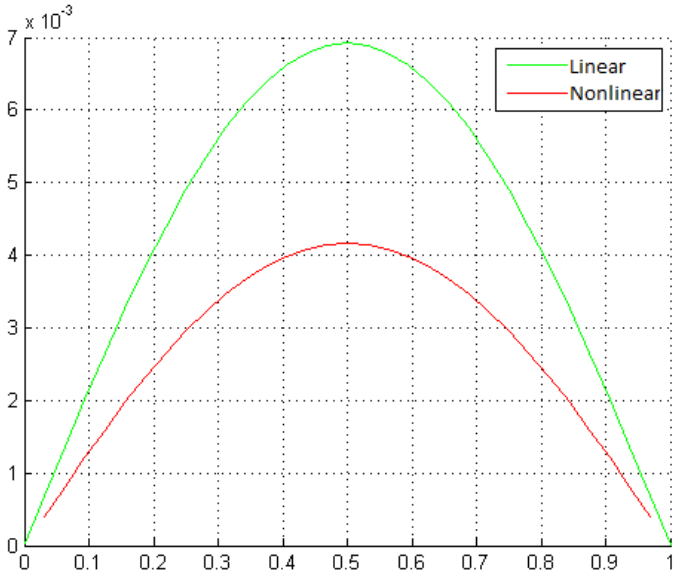

Figure 3.13: Deflection w at $T = 25$ with $\alpha = 4800$

© University of Pretoria

3.4.2 Nonlinear oscillations of the Local Linear Timoshenko beam model

In this subsection forced vibration of a cantilever beam is considered. Recall that the aim is to find a situation where the LLT model differs significantly from the linear model, while the rod strains are sufficiently small to ensure that the model is locally linear.

Experiment 4: Forced vibration of a cantilever beam

In this experiment the models for a cantilever beam with $\alpha = 4800$, set in motion by a periodic load, are compared. The load is concentrated toward the endpoint of the beam. To be precise

$$\begin{aligned} P_1 &= 0, \\ P_2 &= c\sin(\omega t)q(x), \end{aligned}$$

where $c = 0.001$, $\omega = 1$ and

$$q(x) = \begin{cases} x - 0.9 & \text{for } x > 0.9 \\ 0 & \text{for } x \leq 0.9. \end{cases}$$

To interpret the results, note that the fundamental period for the beam is approximately 20π while the period of P_2 is much smaller (2π).

Solutions were approximated on the time interval $[0, 12\pi]$ using $n = 32$ elements. The beam is initially at rest with $\omega = \phi = 0$. As before, a sufficient number of time steps are used to guarantee four significant digits to be reliable. The results are shown in Figure 3.14.

It is clear that the linear and nonlinear model behave differently and yield significantly different solutions. (Note that the scale on the vertical axis varies between 10^{-4} and 10^{-5}.)

The shape of the deflection curve for the nonlinear problem changes dramatically in each of the intervals $[8\pi, 9\pi]$ and $[9\pi, 10\pi]$.

As mentioned before, it is necessary to monitor the strains for the nonlinear beam to confirm that they remain small. Since the largest changes in the deflection were observed for $8\pi < t < 10\pi$, the strains were calculated at time $t = 9\pi$. The following results were obtained:

$$|\theta - \phi| < 9.278 \times 10^{-6}, \quad |\partial_x \phi| < 1.1 \times 10^{-3} \quad \text{and} \quad |\partial_x s - 1| < 10^{-6}.$$

© University of Pretoria

Considering the results above, it is reasonable to assume that the strains remain small during the motion.

Remark For the numerical approximation of the solution of the linear beam model the Mixed Finite Element Method (MFEM) was used.

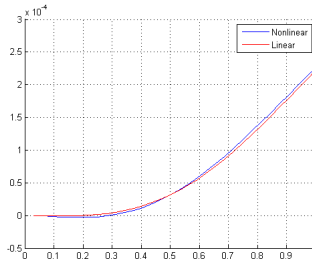

(a) $T = 4\pi$

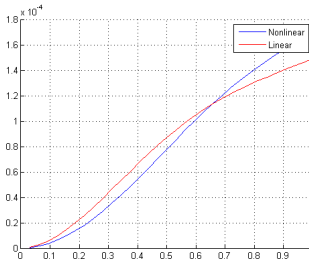

(b) $T = 5\pi$

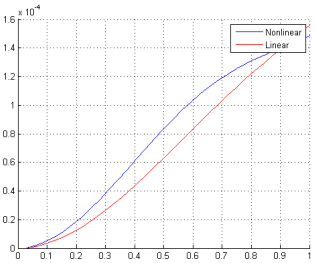

(c) $T = 6\pi$

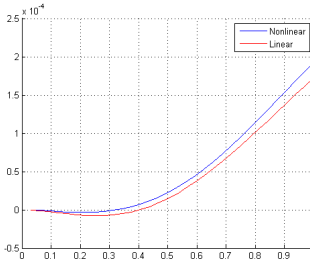

(d) $T = 7\pi$

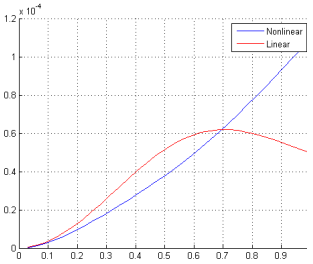

(e) $T = 8\pi$

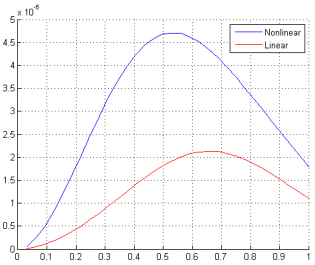

(f) $T = 9\pi$

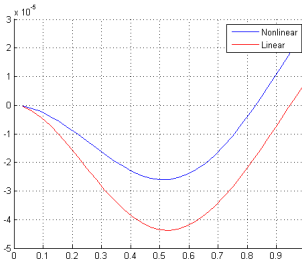

(g) $T = 10\pi$

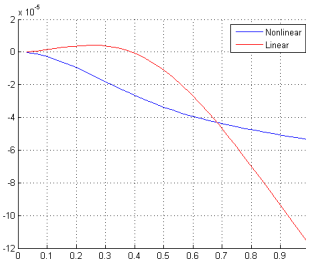

(h) $T = 11\pi$

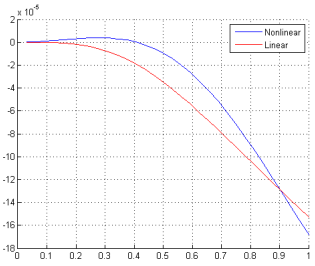

(i) $T = 12\pi$

Figure 3.14: Forced vibration for $T = 2\pi$ to $T = 12\pi$ with $\alpha = 4800$

© University of Pretoria

3.4.3 Conclusion

Bear in mind that the numerical experiments in this section are of an exploratory nature. Nevertheless, the results are interesting and induce a degree of confidence in the LLT model. We also believe that there are situations where the LLT model is a very good choice - when the strains are small enough so that the assumptions hold, but the range of the motion and rotation does not allow for the classical Timoshenko model to be used. More experiments are needed and some future work is discussed in Section 7.3.

© University of Pretoria

Chapter 4

Wind and earthquake induced oscillations of vertical structures

4.1 Introduction

The effect of wind and earthquake induced oscillations on high-rise structures such as buildings, masts and chimneys is of considerable interest to structural engineers. Obviously, the relevant structure should be able to withstand these oscillations. In [RM05] the authors draw attention to the following, not so obvious, considerations. First of all there is a large investment in non-structural components which may be damaged. Also, "...localized damage in certain non-structural systems can affect the functionality of large portions of the building." "Recent earthquakes have shown that damage in non-structural components and in building contents can have large economic consequences as well as safety and egress concerns." In many cases there are serious consequences even when buildings suffer no structural damage. See also [Mir99], [WFH01], [MT05] and the references provided in these articles.

It is mentioned in [RM05] that research and recovered data is used to determine the safety specifications and recommendations of buildings. The authors provide a brief account of how ongoing research influences these specifications and recommendations.

Clearly, reliable mathematical models are needed to determine the effect of

© University of Pretoria

oscillations on buildings. In [RM05] the authors state that: "Modelling of the building is by far the most time-consuming task associated with obtaining its dynamic characteristics." Damage to non-structural components is caused by acceleration demands on these components. To estimate acceleration demands simplified beam models have been used for a long time; many references are given in the articles mentioned above. Simplified models can also be used to design damping mechanisms.

In this chapter the focus is on high-rise buildings subjected to earthquake induced oscillations. However, the models of such structures and the mathematical analysis thereof are also relevant for wind induced oscillations.

In [WFH01] the Euler-Bernoulli beam is used to model a high-rise building with a tuned mass damper. The effect of gravity is included as well as a non-linear term for compression. The model is used to simulate the motion of the building. In a subsequent article, [WL07], they proceeded to use this model to find a method to control the vibration.

In this Chapter the adapted Timoshenko beam model for a high-rise structure is presented (as derived in Chapter 2). A motivation for the use of the Timoshenko model as well as a comparison to other models was done in Chapter 1. As further justification for the use of the Timoshenko model consider the tube model of Takabatake. In the 1996 article by Takabatake [Tak96] he investigated a model for high-rise structures. A doubly symmetric tube structure is considered, in which a frame-tube structure is replaced with an equivalent rod (or beam) which includes the effects of bending, transverse shear deformation and shear-lag.

In [Mir99], [RM05] and [MT05] shear is introduced into the model. The authors present a twin-beam model: a shear beam connected to a flexural beam. The acceleration demands are estimated using the first six modes of vibration.

As a consequence of these works, we consider the twin-beam model since it provides another way to introduce shear. Modal analysis is done on this model. Furthermore the natural frequencies of the Timoshenko model are compared to those of the twin-beam model. We also explain why the parameters given in [RM05] (see the application in Subsection 4.3.1) are not enough for the purpose of comparing models.

The variational form and finite element semi-discrete approximation for the models are discussed. Finally, results for the simulation of the transient

© University of Pretoria

response of a building to an earthquake are presented in Section 4.5.

4.2 Two beam models for high-rise structures

In this section we consider the application of the adapted Timoshenko model to vertical structures and introduce the twin-beam model. A given vertical structure is modelled as a beam with vertical axis when at rest. The "beam" is clamped at ground level.

4.2.1 Adapted Timoshenko model

Recall that in Chapter 2 a model (Model 1, Section 2.6) was derived from the planar motion of a one-dimensional continuum, using the constitutive equations of the Timoshenko theory. It is presented here for convenience:

$$\partial_t^2 u = \partial_x S + P, \tag{4.2.1}$$
$$\partial_t^2 w = \partial_x V + Q, \tag{4.2.2}$$
$$\frac{1}{\alpha}\,\partial_t^2 \phi = (1+\partial_x u)V + \partial_x M - S\partial_x w, \tag{4.2.3}$$
$$M = \frac{1}{\beta}\,\partial_x \phi, \tag{4.2.4}$$
$$V = \partial_x w - \phi, \tag{4.2.5}$$
$$S = \frac{1}{\gamma}\partial_x u \tag{4.2.6}$$

Longitudinal vibration and gravity

In (4.2.1) and (4.2.2) u and w denote the vertical (axial) and horizontal (transverse) displacements respectively. Equation (4.2.1) makes provision for longitudinal vibration. The force density due to gravitation is denoted by P. In (4.2.3) the term $S\partial_x w$ is due to longitudinal vibration and gravity.

In this chapter only the transverse vibration is considered as in [RM05]. Then $S = \mu(x-1)$ in dimensionless form with the dimensionless constant $\mu = \dfrac{\rho g \ell}{G\kappa^2}$. (This force density is not considered in [RM05] but in [WFH01].)

Simplifying assumption

© University of Pretoria

Consider the Adapted Timoshenko model (Model 2) in Subsection 2.6.2. The term $(1+\partial_x u)V$ in Equation (4.2.3) may be approximated by V since $\partial_x uV = \gamma SV = \gamma\mu(x-1)V$ and μ is small. Using this approximation the equations of motion now read

$$\partial_t^2 w = \partial_x V + Q, \tag{4.2.7}$$

$$\frac{1}{\alpha}\,\partial_t^2\phi = V + \partial_x M - S\partial_x w. \tag{4.2.8}$$

Assuming a linear model with small dimensionless displacements one may use the superposition principle and decompose the oscillations as in [RM05] into East-West and North-South oscillations.

Boundary conditions

At the top (regardless of earthquake or wind induced oscillations) and for **all the models**

$$M(1,t) = 0 \quad \text{and} \quad V(1,t) = 0. \tag{4.2.9}$$

Earthquake induced oscillations

The force density $Q = 0$ since the motion is due to forcing by the earthquake. At ground level $x = 0$, the boundary conditions are

$$w(0,t) = w_E(t), \quad \phi(0,t) = 0. \tag{4.2.10}$$

In the relevant literature an earthquake is considered to be the superposition of a number of harmonic functions, i.e. $w_E(t) = \sum c_k \sin(p_k t)$. To simplify the analysis, one component at a time is often used.

In the case where longitudinal vibration is considered the boundary condition is $u(0,t) = u_E(t) \neq 0$. The assumption $u_E(t) = 0$ is made in [MT05] and [RM05], where the authors draw attention to the fact that damage to non-structural components is caused primarily by lateral displacements.

Equivalent problem

The boundary conditions must be homogeneous for modal analysis. The earthquake model problem is equivalent to an artificial "wind problem" for a cantilever beam. The boundary condition $w(0,t) = w_E(t)$ can be homogenized: Let $\tilde{w}(x,t) = w(x,t) - w_E(t)y(x)$ and $\tilde{V} = \partial_x\tilde{w} - \phi$. Equations (4.2.7)

© University of Pretoria

and (4.2.8) are transformed as follows

$$\partial_t^2 \tilde{w} = \partial_x \tilde{V} - w_E(t) - \ddot{w}_E(t) y(x), \tag{4.2.11}$$

$$\frac{\gamma}{\beta} \partial_t^2 \phi = \tilde{V} + w_E(t) y'(x) + \partial_x M - \partial_x w S, \tag{4.2.12}$$

where the function y satisfies $y(0) = 1$ and $y'(1) = 0$. (An example is $y(x) = 1 + x - \frac{1}{2}x^2$.) Consider the boundary conditions for $\tilde{w}$. Since $y(0) = 1$,

$$\tilde{w}(0,t) = w_E(t) - w_E(t) y(0) = 0.$$

At the top

$$\tilde{V}(1,t) = V(1,t) - w_E(t) y'(1) = V(1,t) = 0.$$

The other boundary conditions remain unchanged, i.e.

$$M(1,t) = 0 \quad \text{and} \quad \phi(0,t) = 0.$$

Remarks The function y may be replaced by another function that satisfies the same boundary conditions. However, this should not be a cause for concern since $y(x)w_E(t)$ must be added to obtain the final solution.

We now have a model problem for a cantilever beam where the forces at ground level are replaced by a distributed load. This equivalent problem provides justification for modal analysis of a cantilever beam. In [RM05] the authors do not explain this procedure, see the next subsection.

Existence

The general existence theory in [VS19] cannot be applied to the model problem for earthquake induced oscillations due to the nonhomogeneous boundary condition $w(0,t) = w_E(t)$. However, the theory can be applied to the equivalent problem (as was done in [VS19]).

4.2.2 Twin-beam model of Miranda and Taghavi

A twin-beam model for a building is used in [RM05]. It is the partial differential equation [RM05, Equation (5)]. It can be derived from a model in [Mir99] for a building in equilibrium subjected to a distributed load. A shear beam is combined with an Euler-Bernoulli (flexural) beam. The idea

© University of Pretoria

is discussed in more detail in [Mir99]. It is a simplification of the interaction of shear walls and frames. (Credit is given to [KS64] and [HS73].)

The derivation of the partial differential equation for vibration is not shown in [RM05] or the preceding article [MT05]. For completeness we present a derivation using the equations in [RM05, Section 2]. Note that a single beam is partitioned into two beams. The partial differential equation for the Euler-Bernoulli beam is

$$d_E \partial_t^2 w = -\frac{1}{\beta_E} \partial_x^4 w + F,$$

where $d_E = \frac{\rho_E A_E}{\rho A}$. The subscripts E denote parameters for the flexural beam. For shear, use Equation (5) with $V = \sigma \partial_x w$:

$$d_S \partial_t^2 w = \sigma \partial_x^2 w - F,$$

where $d_S = \frac{\rho_s A_S}{\rho A}$ and $\sigma = \frac{G_S A_S}{G A \kappa^2}$. The subscript S denotes parameters for the shear beam. The force density F represents the interaction between the beams. Adding the two partial differential equations yields

$$(d_S + d_E)\partial_t^2 w = \sigma \partial_x^2 w - \frac{1}{\beta_E} \partial_x^4 w, \tag{4.2.13}$$

which is equivalent to [RM05, Equation (5)]. Note that gravity is neglected in this model.

In [RM05, Equation (6)] a parameter α_0, referred to as the lateral stiffness ratio, is introduced. It is clear that α_0^2 is the product of β_E and σ. To avoid confusion we will use α_M for α_0^2, hence

$$\alpha_M = \beta_E \sigma. \tag{4.2.14}$$

Boundary conditions for an earthquake are discussed in the previous subsection. At ground level

$$w(0,t) = w_E(t) \text{ and } \partial_x w(0,t) = 0.$$

The boundary conditions at the top are the same as for the Timoshenko model, i.e. (4.2.9). For this model it translates to

$$\partial_x^2 w(1,t) = 0 \quad \text{and} \quad \partial_x w(1,t) - \frac{1}{\alpha_M} \partial_x^3 w(1,t) = 0. \tag{4.2.15}$$

The boundary conditions can be verified using the variational form, see Section 4.4.

Remark The boundary conditions for the partial differential equation are not discussed in [RM05] and it is necessary to read [MT05].

© University of Pretoria

Equivalent problem

The equivalent model is again a cantilever beam with artificial load. The procedure below is implicit in the analysis done in [MT05].

Let $\tilde{w}(x,t) = w(x,t) - w_E(t)$. The new partial differential equation is of the form

$$\frac{d}{\sigma}\partial_t^2\tilde{w} = \partial_x^2\tilde{w} - \frac{1}{\alpha_M}\partial_x^4\tilde{w} - \frac{d}{\sigma}\ddot{w}_E(t), \tag{4.2.16}$$

with $d = d_S + d_E$. The boundary conditions remain the same except that now $\tilde{w}(0,t) = 0$.

Modal analysis of the model is done in Section 4.3.

4.2.3 Damping

In this subsection our concern is modelling of the structure. With the exception of [MT05], none of the relevant studies indicate how damping is modelled. Terms reflecting damping are not in the partial differential equations or the boundary conditions. Yet damping is considered in the modal analysis. To avoid confusion, note that we are not referring to active or passive damping devices such as the "Tuned mass damper" in [WFH01].

In [MT05] a viscous damping term is in the partial differential equation, which results in constant modal damping ratios. The authors acknowledge that "... better estimates can be obtained by using different modal damping for each mode."

The importance of damping in the structure is stressed in [TMF+11]. The damping is due to hard rubber dampers inserted in the frame. No mathematical model is provided.

Recall that our concern is to determine reliable yet simplified models for structures. To design damping devices, one must first know the dynamic properties of the structure. The challenge is to model internal friction in building material (material damping). In the Timoshenko model damping in (4.2.7) shear or (4.2.8) flexure or both are possible. For the Rayleigh and Euler-Bernoulli models damping due to bending can be built into the partial differential equation. The Twin-beam model (Equation (4.2.13)) can accommodate damping due to shear as well as bending.

© University of Pretoria

Since it is difficult to determine the parameters, even without damping, we consider it beyond the scope of this chapter to model damping.

4.2.4 Wind-induced oscillations

Modelling the effect of wind is discussed in [FL10] and [HV07]. The load caused by vortex shedding leads to the oscillation of the structure. In recent years, more and more super tall constructions have been built and these are also affected by the wind. In [WFH01] the authors refer to earlier studies where it is recommended that " ... for increasing the levels of structural safety, integrity and occupant comfort, it is necessary to reduce the levels of earthquake- or wind-induced displacements and accelerations in tall buildings."

From a mathematical perspective, a problem modelling wind-induced oscillations are not any different from a so called artificial wind problem, referred to in Subsection 4.2.1.

For wind induced oscillations $Q \neq 0$ in Equation (4.2.2), and is a force density due to the wind. At ground level the boundary conditions are

$$u(0,t) = w(0,t) = \phi(0,t) = 0.$$

In [FL10] a forcing function simulating the wind is applied only to a part of the beam, e.g. between $x = 0.4$ and $x = 0.5$. To be precise, the wind is modelled by $q(x,t) = g(x)f(t)$ where

$$g(x) = \begin{cases} 1 & \text{if} \quad 0.4 \leq x \leq 0.5, \\ 0 & \text{otherwise} \end{cases}$$

and $f(t) = A \sin \omega t$.

4.3 Modal analysis and parameters

In this section we consider the modal analysis of the Timoshenko and Twin-beam models. Modal analysis to compare standard beam models is done in Subsection 1.2.3 and is also done in [RM05]. Since the model in [RM05] does not include a gravitational force term we will also omit it in the eigenvalue problem for the Timoshenko model.

© University of Pretoria

The derivation of natural frequencies and modes are done in [MT05] and only results presented in [RM05]. Also, boundary conditions for the eigenvalue problem is provided in [MT05] but not in [RM05].

4.3.1 Natural frequencies of the Twin-beam model

Separation of variables for equation (4.2.16) leads to the eigenvalue problem

$$u^{(4)} - \alpha_M u'' - \lambda \alpha_M u = 0 \tag{4.3.1}$$

with

$$\begin{aligned} u(0) = u'(0) &= 0, \\ \frac{1}{\alpha_M} u'''(1) - u'(1) &= 0, \\ u''(1) &= 0. \end{aligned}$$

The solutions of $dT'' + \sigma\lambda T = 0$ yield the natural angular frequencies.

The general solution of the differential equation (4.3.1) is given by

$$u(x) = A\sinh\mu x + B\cosh\mu x + C\sin\omega x + D\cos\omega x, \tag{4.3.2}$$

where

$$\mu^2 = \frac{\alpha_M}{2}\left(1 + \sqrt{1 + \frac{4\lambda}{\alpha_M}}\right) \quad \text{and} \quad \omega^2 = \frac{\alpha_M}{2}\left(-1 + \sqrt{1 + \frac{4\lambda}{\alpha_M}}\right). \tag{4.3.3}$$

Using the boundary conditions we obtain

$$C = -\frac{\mu}{\omega}A, \quad -D = B = \frac{-\mu^2\sinh\mu - \mu\omega\sin\omega}{\mu^2\cosh\mu + \omega^2\cos\omega},$$

by choosing $A = 1$. It follows from Equation (4.3.3) that

$$\mu^2 - \omega^2 = \alpha_M, \tag{4.3.4}$$

an identity also used in [RM05].

From the boundary conditions and (4.3.4) we also obtain the following frequency equation

$$\left(2 + \frac{\alpha_M^2}{\mu^2\omega^2}\right)\cosh\mu\cos\omega + \frac{\alpha_M}{\mu\omega}\sinh\mu\sin\omega + 2 = 0. \tag{4.3.5}$$

© University of Pretoria

Combining (4.3.3) and (4.3.5) in an elementary numerical procedure yields the eigenvalues. The natural angular frequency corresponding to λ_i is $\sqrt{\frac{\lambda_i \sigma}{d}}$.

Application

It is problematic to compare the Twin-beam model with the other models. As mentioned, only the parameter $\alpha_M = \sigma\beta_E$ is given in [RM05]. To compare them we need β_E and σ separately. Assumptions would have to be made to attempt a comparison.

The first assumption is that $G = G_E = G_S$. Since β is defined as $\frac{AG\kappa^2\ell^2}{EI}$, we obtain $\frac{\beta}{\beta_E} = \frac{AI_E}{A_E I}$. Now, if we assume that the area moment of inertia is $I = kA^2$, then $\frac{\beta}{\beta_E} = \frac{A_E}{A}$ and therefore $\beta_E = \beta\frac{A}{A_E}$. Substituting this into α_M,

$$\alpha_M = \beta\frac{A}{A_E}\sigma = \beta\frac{A}{A_E}\left(\frac{G_S A_S}{GA\kappa^2}\right) = \beta\frac{A_S}{A_E\kappa^2}. \tag{4.3.6}$$

This gives us a relation between α_M used in [RM05] and β for the one beam model.

If we assume that $\rho_S = \rho_E$, we have $d = 1$. Also, as a result of the assumptions $\sigma = \frac{A_S}{A\kappa^2}$. (The parameter κ^2 varies between 3/5 and 5/6.) Using all these assumptions the partial differential equation (4.2.16) becomes

$$\frac{1}{\sigma}\partial_t^2\tilde{w} = \partial_x^2\tilde{w} - \frac{1}{\alpha_M}\partial_x^4\tilde{w} - \frac{1}{\sigma}\ddot{w}_E(t).$$

The possibility that there is excess mass that does not contribute to structural stiffness must be considered. In that case the coefficient for the acceleration term in (4.2.16) will not be $\frac{d}{\sigma}$.

4.3.2 Stiffness parameters

The choice of parameters and determination thereof is problematic. In [RM05] we see that three parameters, the fundamental period ($\tau = \tau_1$), the damping ratio (ξ) and stiffness ratio (α_M), are used. As mentioned before, $\alpha_M = \beta_E\sigma$ is known but as can be seen from the previous section, we need to know both β_E and σ.

The value for β_E should be related to the dimensions of the frame of the building: $\left(\frac{\text{height}}{\text{width}}\right)^2$ should be in line with the value of β_E. Note that

© University of Pretoria

reference to steel frames and shear walls is made in [RM05] and [MT05] to motivate their mathematical model.

If sufficient information is not available, the only option is to determine the parameters using the data on accelerations and displacements. This approach has the drawback that the parameters are dependent on the mathematical model used which we are trying to evaluate indepently and compare to our model (both cases for which we need accurate and reliable data).

4.3.3 Natural frequencies and the fundamental period

Calculation of the natural angular frequencies of the two models is discussed in Subsections 1.2.3 and 4.3.1 respectively. Due to the assumption in Subsection 4.2.2, the natural angular frequencies for the Twin-beam model is $\sqrt{\lambda_i \sigma}$. For a selected Timoshenko beam $\beta = \beta_T$ is known. To compare, choose a ratio $r = \frac{A_S}{A}$, and calculate $\beta_E = \frac{\beta}{1-r}$, $\sigma = \frac{r}{\kappa^2}$ and $\alpha_M = \frac{r}{r-1}\frac{\beta}{\kappa^2}$.

To determine if a model is realistic, one may calculate the fundamental period and compare it to the measured value. We calculated the fundamental periods for the two buildings in Table 4.1 below and converted it from dimensionless time to real time. Recall that $t_0 = \ell\sqrt{\dfrac{\rho}{G\kappa^2}}$ and if ρ and G for a steel frame with length $200m$ is used, we have $t_0 = 0.079$. The calculated periods were way off the mark for both models; the Timoshenko model being closer for $r \leq 1/2$. (The fundamental period varied between 0.30 and 0.34 seconds for the Twin-beam model.) Clearly a 5% damping ratio will not fix the problem. A possible explanation for the huge difference is additional mass not contributing to stiffness.

Remark The parameter ρ in [RM05] and [MT05] denotes mass per unit length. This parameter is not dimensionless and no information is given on the magnitude or influence of the parameter. Note that it is not relevant when the ratios of frequencies are used as in [RM05].

4.3.4 Comparison of two buildings

Using data from [RM05] we do a comparison of two Los Angeles buildings, referred to as LA-52 and LA-54 in [RM05], both hit by Northridge earthquake and both $\pm 30km$ from the epicentre of the earthquake. It is interesting to

© University of Pretoria

note the huge difference in the values for α_M. But the dimensions of the buildings are comparable: the height is the same (around 200m) and the floor dimensions of LA-52 is $48m \times 48m$ and that of LA-54 is $60m \times 37m$.

Below is a summary of the relevant information given in [RM05] regarding the buildings and their response to the Northridge earthquake.

	LA-52		LA-54	
	NS	EW	NS	EW
Stiffness parameter α_M	60.8	43.6	756	912
Fundamental period (s)	5.8	6	6.2	5.2
Peak ground acceleration (cm/s^2)	165	109	165	98
Peak roof acceleration (cm/s^2)	389	220	177	139

Table 4.1: Information on LA-52 and LA-54

Even though the beam stiffness parameters for LA-52 are much smaller than those for LA-54 (indicating that LA-52 is a more rigid beam) we see that LA-52 had much greater peak roof accelerations. Also note that the fundamental periods for East-West motion differ by less than 20%, but α_M is 20 times greater for LA-54. We opine that these "discrepancies" could possibly be explained if β_E and σ are known, instead of only $\alpha_M = \beta_E\sigma$.

4.3.5 Remarks on modal analysis

There are limits to the value of modal analysis. In [RM05] only the ratios of the first 6 modes to the fundamental mode is given (we obtained the same ratios). The authors in [RM05] mention the fact that for a specific building the fourth mode is close to the predominant period of ground motion (recall that an earthquake is given by a combination of harmonic functions). Since the number of modes involved is not obvious in general, simulation of the transient response is necessary (see Section 4.5).

In Section 4.2 one boundary condition of the earthquake model was homogenized using a function y. In a remark it was mentioned that this function is not uniquely determined. (Another function satisfying the boundary conditions is for example $\tilde{y}(x) = -x^3 + 3x + 1$.) Note that the participation factor (defined in [Mir99]) changes when the function used is altered.

© University of Pretoria

4.4 Semi-discrete finite element approximation

In this section we derive a system of ordinary differential equations for the adapted Timoshenko model to be used for simulation.

It is well known that shear locking is a problem. To get past this there are two options: Polynomials of higher degree can be used as basis functions (e.g. Hermite cubics) or the Mixed Finite Element Method can be used. For more information on simulation with Hermite cubics, see [VVR10] and for information regarding the Mixed Finite Element Method, see [Sem94] or [HKO11]. In this section we use the Mixed Finite Element Method (MFEM) with piecewise linear basis functions.

Similar to (2.7.7) and (2.7.8), we start with the variational equations of motion

$$\begin{aligned}\int_0^1 \partial_t^2 w(\cdot,t)v = &-\int_0^1 V(\cdot,t)v' + \int_0^1 Q(\cdot,t)v \\ &+ V(1,t)v(1) - V(0,t)v(0), \qquad (4.4.1)\\ \int_0^1 \frac{1}{\alpha}\,\partial_t^2\phi(\cdot,t)\psi = &+\int_0^1 V(\cdot,t)\psi - \int_0^1 M(\cdot,t)\psi' - \int_0^1 S\partial_x w\psi \\ &+ M(1,t)\psi(1) - M(0,t)\psi(0). \qquad (4.4.2)\end{aligned}$$

Denote the space of test functions $T[0,1] = \{v \in C^1[0,1] \mid v(0) = 0\}$, use the boundary conditions in Equation (4.2.9) and substitute M and S to obtain the following variational equations of motion

$$\int_0^1 \partial_t^2 w(\cdot,t)v = -\int_0^1 V(\cdot,t)v' + \int_0^1 Q(\cdot,t)v \qquad (4.4.3)$$

and

$$\int_0^1 \frac{1}{\alpha}\,\partial_t^2\phi(\cdot,t)\psi = -\frac{1}{\beta}\int_0^1 \partial_x\phi(\cdot,t)\psi' + \int_0^1 V(\cdot,t)\psi - \int_0^1 \mu(x-1)\partial_x w\psi, \qquad (4.4.4)$$

for all v and $\psi \in T[0,1]$.

Note that w is not a test function in the case of the earthquake problem; it must satisfy the prescribed boundary conditions at $x = 0$: $w(0,t) = w_E(t)$.

© University of Pretoria

Since we make use of MFEM the constitutive equation for V is not substituted. Multiply Equation (4.2.4) by an arbitrary function ξ in $C^1[0,1]$ and integrate to obtain

$$\int_0^1 V\xi \;=\; \int_0^1 \partial_x w\xi - \int_0^1 \phi\xi. \tag{4.4.5}$$

Model problem in variational form Find the functions w, ϕ and V such that $w(\cdot,t), V(\cdot,t) \in C^1[0,1]$ and $\phi(\cdot,t) \in T[0,1]$ for all $t>0$, $w(0,t) = w_E(t)$ and Equations (4.4.3), (4.4.4) and (4.4.5) hold for all v, $\psi \in T[0,1]$ and $\xi \in C^1[0,1]$ respectively.

The initial conditions are $w(\cdot,0) = w_0$ and $\phi(\cdot,0) = \phi_0$.

To obtain the Galerkin approximation of the problem we refer the reader to Subsections 3.2.2 and 3.2.3. The M, K and L matrices are defined in (3.2.19). An additional matrix is needed for this problem and is defined as follows:

$$N_{ij} = \mu((1-x_i)\delta_j', \delta_i), \tag{4.4.6}$$

where δ_i are the C_0 piecewise linear basis functions.

System of ODE's for Timoshenko model

$$\begin{aligned} M\ddot{\bar{w}} &= L\bar{V} \\ \frac{1}{\alpha}M\ddot{\bar{\phi}} &= M\bar{V} - \frac{1}{\beta}K\bar{\phi} + N\bar{w} \\ M\bar{V} &= L^T\bar{w} - M\bar{\phi}. \end{aligned}$$

Similarly, a system of ODE's for the Twin-beam model can be derived.

System of ODE's for Twin-beam model

$$\frac{d}{\sigma}M\ddot{\bar{w}} = -K_1\bar{w} - \frac{1}{\alpha_M}K_2\bar{w},$$

where $K_1 = K$ is the stiffness matrix and K_2 the bending matrix, see [SF73] or [LVV05] for more details. Note that the matrices are not square due to the fact that w is not a test function.

© University of Pretoria

4.5 Finite element simulations

As mentioned, modal analysis is in our view not sufficient and simulations of the actual motion should also be used to determine accelerations at different points of the structure. As mentioned before, the Timoshenko and Twin-beam models do not compare well, for reasons mentioned. Nevertheless, simulations for the Timoshenko model are illuminating.

In this section we simulate the transient response of a structure modelled as a Timoshenko beam. Simulation will also be used to demonstrate the significance of a given parameter. Finally we compare the motion of the top of the structure (free end of the structure) for two different values of the parameter β.

In these simulations we consider the boundary conditions for the earthquake as given in Equation (4.2.10), not the equivalent problem. We chose $w(0,t) = w_E(t) = D\sin(Pt)$ with D and P constants, which are the amplitude and frequency of the ground motion respectively. Note that displacement and time are in dimensionless units. In the experiments enough elements and time steps were used to guarantee the results for at least 3 significant digits.

Motion of the structure

We first demonstrate the transient response of a vertical structure due to an earthquake using the Timoshenko model. We show a full period of the ground disturbance ($\tau_g = 8$) with $\beta = 500$ in Figure 4.1. Note that this period is in dimensionless time.

© University of Pretoria

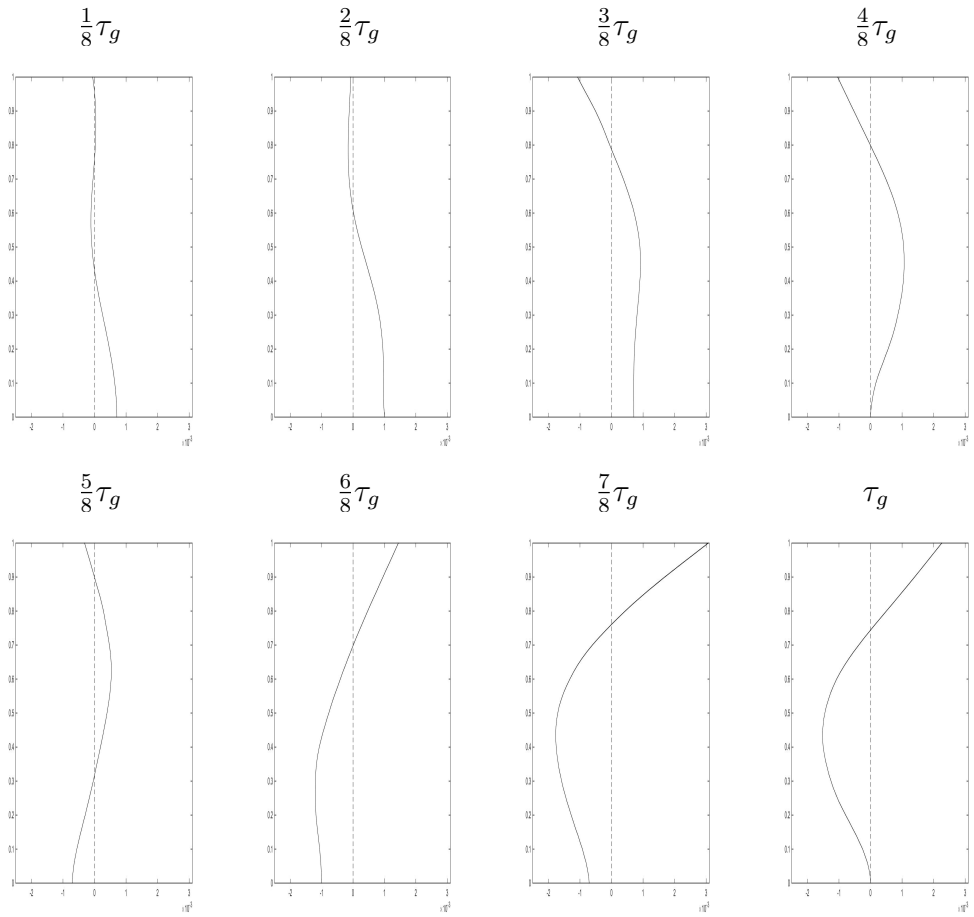

Figure 4.1: Transient response for Timoshenko model

Note the "whiplash" effect of the top of the building between $\frac{5}{8}\tau_g$ and $\frac{7}{8}\tau_g$.

Influence of the parameter β

To illustrate the influence of this parameter we chose the values $\beta = 50$ (rather thick) and $\beta = 800$ (slender). We show the movement for $\beta = 50$ (dashed) and $\beta = 800$ (solid) for the Timoshenko model in Figure 4.2.

© University of Pretoria

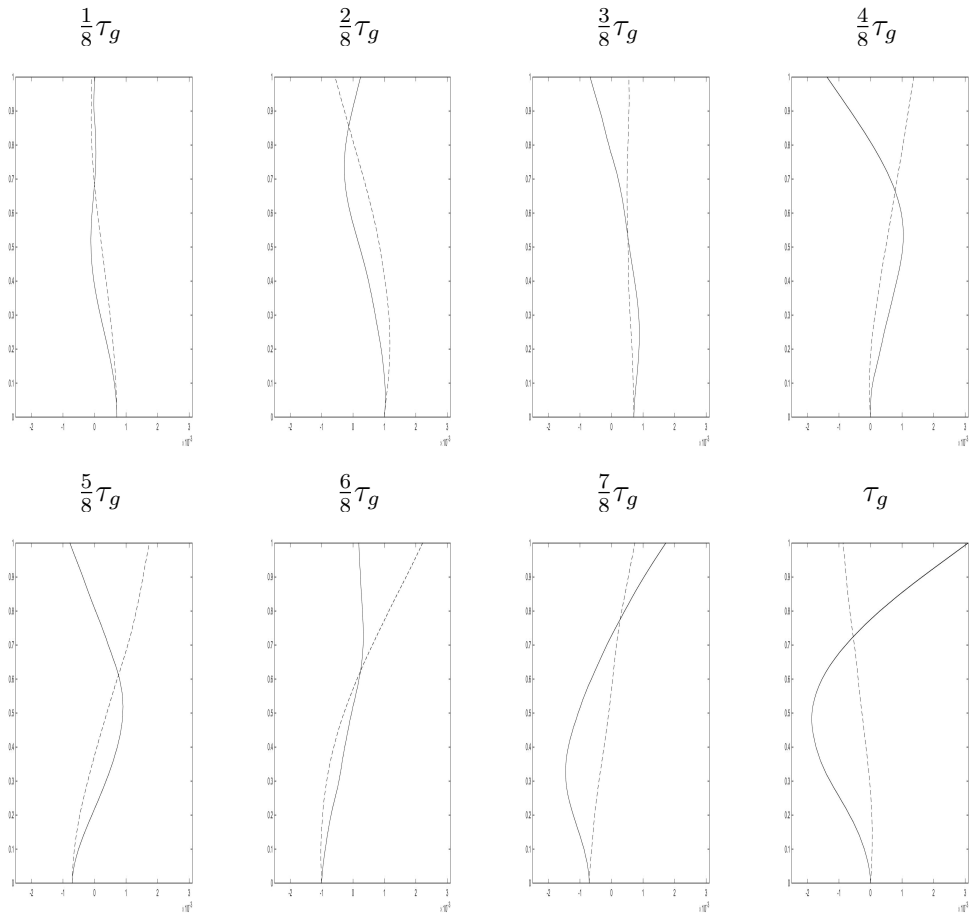

Figure 4.2: Illustration of the influence of the parameter β ($\beta = 50$ *(dashed) and* $\beta = 800$ *(solid)*).

Note that the structure is less slender when $\beta = 50$ and therefore the displacement of the top of the structure is smaller than for $\beta = 800$. Also note the significant difference in the middle of the structure.

Motion of the free end of the structure

Since the fundamental periods are different for the Timoshenko and Twin-beam model, there is no purpose in comparing the motion of the top for the two models. From the observations in Figures 4.1 and 4.2 it may be worthwhile however to study the motion of the top of the structure for the different values of the parameter β.

© University of Pretoria

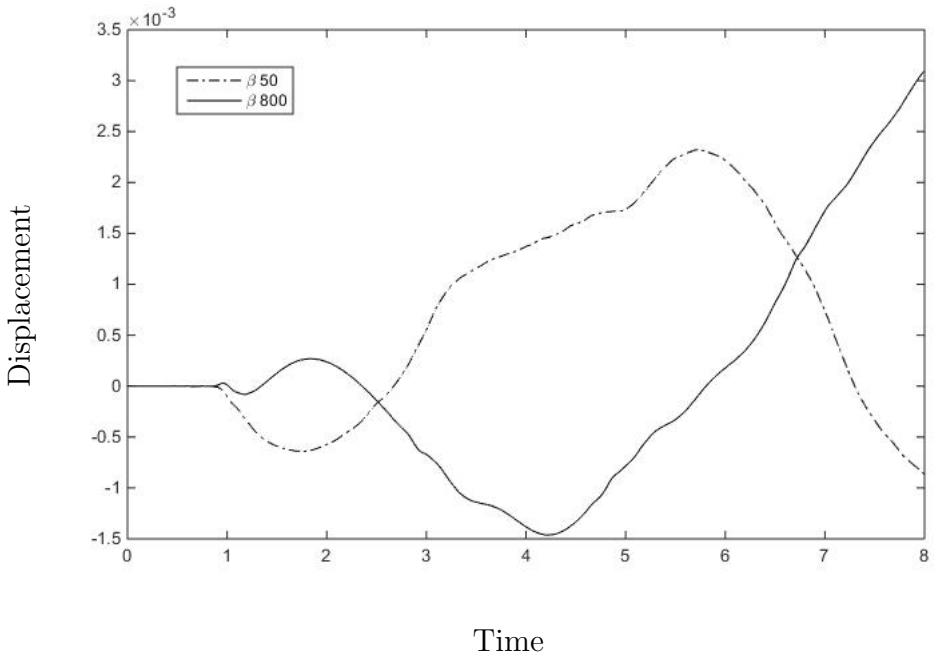

Figure 4.3: Motion of the top of a building for Timoshenko model

From Figure 4.3 we see that it takes 1 dimensionless time unit for the top of the structure to start moving, regardless of the value of β. It can also be observed from the figure that there are significant (possibly severe) accelerations for both cases at that instant as well as at other times (for example at about $t = 1.8$ and $t = 5.7$ for $\beta = 50$).

4.6 Conclusion

It is clear from the literature that beam models are a serious consideration for the modelling of buildings. It may sound strange to some to model a building as a beam, but consider the variation of possible cross-sections for a beam in [Cow66]. In this chapter we created a theoretical framework for the comparison of beam models for a building, either by modal analysis or by finite element simulation.

The main conclusion is that the Timoshenko model can provide meaningful insights to the effect of oscillations on high rise buildings. We not only presented such a model for earthquake induced oscillations, but provided an al-

© University of Pretoria

ternative formulation for modal analysis of a cantilever beam. To supplement this, results from finite element simulations are provided. It is unfortunate that a proper comparison could not be made to data for real buildings due to a lack of information in the articles considered. A preliminary study of the articles [Mir99], [WFH01], [JLK04], [MT05], [RM05] and [TMF+11] lead to the erroneous conclusion that such a comparison should be possible.

For buildings a realistic value of β is not that large, and for these values of β the Rayleigh (or Euler-Bernoulli) model does not compare well to the Timoshenko model. We consider reference to moment-resisting steel frames significant. Especially the "framed tube" in LA-54 ([RM05, Subsection 3.1.6]).

If parts of the building can be modelled as different beams, the Twin-beam model is realistic. The authors in [RM05] compared acceleration results. The computed results compare well to recorded accelerations, but the three parameters were determined from the recorded motion using the same mathematical model.

© University of Pretoria

Chapter 5

Multiple beam model

5.1 Introduction

From the results in the previous chapter as well as the literature it is clear that beam models are considered seriously for when it comes to the modelling of buildings. One such article is [WFH01] in which the authors study the dynamic behaviour of a building. In the article a building is modelled as a beam with several lumped masses. The author used Hamiltons principle to derive the partial differential equation for the Euler Bernoulli theory and used the Finite Element Method to analyse the dynamic behaviour.

In this chapter the possibility of a multiple beam model for a building is investigated. An alternative model to [WFH01] is considered, which is more realistic in several ways. First of all an Euler Bernoulli or Rayleigh model should not be used for a building; a Timoshenko model should be used instead (see motivation given in Chapters 1, 2 and 3). Secondly, rather than one beam, a number of beams in series linked by rigid bodies (or concentrated masses) to represent floors are used. Figure 5.1 illustrates the setup.

To develop an algorithm, obtain data and implement the algorithm will most likely be a project in its own right. The objective in this thesis is to determine the feasibility of doing so.

© University of Pretoria

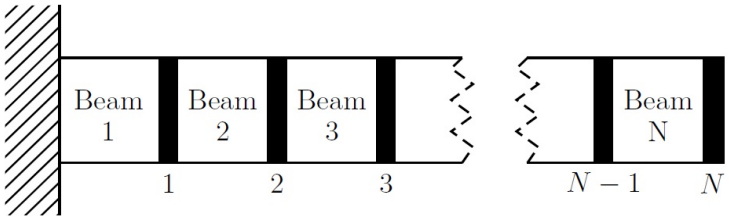

Figure 5.1: Illustration of linked beams

5.2 Model problem

In this section a model consisting of a number of serially connected beams connected by thin plates is derived. The adapted Timoshenko model from Chapters 2 and 4 is used for the beams.

Each dimensionless beam has the interval $[0, 1]$ as reference configuration.

Recall the equations of motion and constitutive equations:

$$\partial_t^2 w = \partial_x V + q, \tag{5.2.1}$$

$$\frac{1}{\alpha}\partial_t^2 \phi = V + \partial_x \mathbf{m} - S\partial_x w, \tag{5.2.2}$$

$$\mathbf{m} = \frac{1}{\beta}\partial_x \phi, \tag{5.2.3}$$

$$V = \partial_x w - \phi, \tag{5.2.4}$$

where S denotes the axial force.

Remark The normal notation for moment (M) was changed to $\mathbf{m}$ as above in order to avoid confusion in Section 5.4.3.

Boundary conditions and interface conditions

For the first beam (at ground level) the boundary conditions are

$$w_1(0, t) = w_E(t) \text{ and } \phi_1(0, t) = 0, \tag{5.2.5}$$

where $w_E(t)$ is a function modelling the movement at ground level due to an earthquake.

For the last beam (at the top of the building)

$$V_N(1, t) = \mathbf{m}_N(1, t) = 0. \tag{5.2.6}$$

© University of Pretoria

The other boundary conditions for the beams are referred to as interface conditions. Note that the displacement at the bottom of each beam (except the first) must be the same as the displacement at the top of the previous beam i.e. $w_k(1,t) = w_{k+1}(0,t)$. The same is true for the angles.

For the body (the floor) between beam k and $k+1$ we have the interface conditions

$$\mu_k \partial_t^2 w_k(1,t) = V_{k+1}(0,t) - V_k(1,t) \tag{5.2.7}$$
$$I_k \partial_t^2 \phi_k(1,t) = \mathbf{m}_{k+1}(0,t) - \mathbf{m}_k(1,t), \tag{5.2.8}$$

where μ_k is the mass of the floor and I_k is the moment of inertia.

We assume that the building is at rest before the earthquake hits. The initial conditions are therefore $w_k(\cdot,0) = \phi_k(\cdot,0) = \partial_t w_k(\cdot,0) = \partial_t \phi_k(\cdot,0) = 0$. The initial conditions for $\mathbf{m}_k$ and V_k are determined by (5.2.3) and (5.2.4) respectively.

Dimensionless form

First, Equations (5.2.7) and (5.2.8) should also be rewritten in dimensionless form using the same scaling as before. The dimensionless mass and moment of inertia are

$$\mu_k^* = \frac{\mu_k}{\rho A \ell} \quad \text{and} \quad I_k^* = \frac{I_k}{\rho A \ell^3}.$$

The interface conditions remain (5.2.7) and (5.2.8) but now all the physical quantities are dimensionless.

The multiple beam system above is referred to as **Problem MT-beam**.

5.3 Variational form

Due to the appearance of the shear force and bending moment in the interface conditions it is preferable to use a variant of the Mixed Finite Element Method (MFEM) (see Section 4.4). (It is well known that the MFEM is more accurate than the standard method, see [Arn81] and [Sem94].)

To derive the variational form, the same procedure is followed as in Section 2.7. Multiplying Equations (5.2.1) and (5.2.2) with arbitrary functions

© University of Pretoria

v and ψ in $C^1[0,1]$ respectively, integrating and using integration by parts yields

$$\begin{aligned}\int_0^1 \partial_t^2 w(\cdot,t)v &= -\int_0^1 V(\cdot,t)v' + [V(x,t)v(x)]_0^1 \\ &\quad + \int_0^1 q(\cdot,t)v, \qquad (5.3.1)\\ \int_0^1 \frac{1}{\alpha}\partial_t^2\phi(\cdot,t)\psi &= \int_0^1 V(\cdot,t)\psi - \int_0^1 \mathbf{m}(\cdot,t)\psi' \\ &\quad + [\mathbf{m}(x,t)\psi(x)]_0^1 - \int_0^1 S\partial_x w\psi. \qquad (5.3.2)\end{aligned}$$

The constitutive equations are not substituted into the equations of motion. Multiplying Equations (5.2.3) and (5.2.4) with arbitrary functions ζ and ξ in $C^1[0,1]$ and integrating we obtain

$$\begin{aligned}\int_0^1 \mathbf{m}(\cdot,t)\zeta &= \int_0^1 \frac{1}{\beta}\partial_x\phi(\cdot,t)\zeta, \qquad (5.3.3)\\ \int_0^1 V(\cdot,t)\xi &= \int_0^1 \partial_x w(\cdot,t)\xi - \int_0^1 \phi(\cdot,t)\xi. \qquad (5.3.4)\end{aligned}$$

Depending on the beam under consideration, the boundary terms in (5.3.1) and (5.3.2) are handled differently. Therefore the test functions are not the same for all beams.

The variational forms of the first and last beam will be slightly different. For the first beam w is not a test function since $w_1(0,t) = w_E(t) \neq 0$. For the first beam the test functions are chosen as $v_1(0) = \psi_1(0) = 0$, so a term will fall away in each of the first two equations. For the other beams there are no restrictions and for the last beam we enforce $V_N(1,t) = \mathbf{m}_N(1,t) = 0$ which are natural boundary conditions.

Test functions Denote the space of test functions by $T[0,1] = \{f \in C^1[0,1] \mid f(0) = 0\}$.

Consider the variational form for the k_{th} beam where $k > 1$. The problem is to find functions $(w_k, \phi_k, \mathbf{m}_k, V_k)$ such that $w_k(\cdot,t)$, $\phi_k(\cdot,t)$, $V_k(\cdot,t)$ and

© University of Pretoria

$\mathbf{m}_k(\cdot,t)$ are in $C^1[0,1]$ and

$$\begin{aligned}\int_0^1 \partial_t^2 w_k(\cdot,t)v_k &= -\int_0^1 V_k(\cdot,t)v_k' + V_k(1,t)v_k(1) - V_k(0,t)v_k(0) \\ &\quad + \int_0^1 q(\cdot,t)v_k, \qquad (5.3.5)\\ \int_0^1 \frac{1}{\alpha}\,\partial_t^2\phi_k(\cdot,t)\psi_k &= \int_0^1 V_k(\cdot,t)\psi_k - \int_0^1 \mathbf{m}_k(\cdot,t)\psi_k' + \mathbf{m}_k(1,t)\psi_k(1) \\ &\quad -\mathbf{m}_k(0,t)\psi_k(0) - \int_0^1 S_k\partial_x w_k(\cdot,t)\psi_k \qquad (5.3.6)\end{aligned}$$

for all v_k and ψ_k in $C^1[0,1]$ and with axial force

$$S_k = \mu_k(1-x) + \mu_k(N-k). \qquad (5.3.7)$$

In addition, for $k = 1$ to N,

$$\begin{aligned}\int_0^1 \mathbf{m}_k(\cdot,t)\zeta_k &= \int_0^1 \frac{1}{\beta}\partial_x\phi_k(\cdot,t)\zeta_k, \qquad (5.3.8)\\ \int_0^1 V_k(\cdot,t)\xi_k &= \int_0^1 \big(\partial_x w_k(\cdot,t) - \phi_k(\cdot,t)\big)\xi_k \qquad (5.3.9)\end{aligned}$$

for each $(\zeta_k,\xi_k) \in C^1[0,1]\times C^1[0,1]$. Note that for the last beam, $V_N(1,t) = \mathbf{m}_N(1,t) = 0$.

Now, consider the first beam, i.e. $k = 1$: $w(\cdot,t) \in C^1[0,1]$, $\phi(\cdot,t) \in T[0,1]$ and $w_1(0,t) = w_E(t)$

$$\int_0^1 \partial_t^2 w_1(\cdot,t)v_1 = -\int_0^1 V_1(\cdot,t)v_1' + V_1(1,t)v_1(1) + \int_0^1 q(\cdot,t)v_1, \qquad (5.3.10)$$

$$\begin{aligned}\int_0^1 \frac{1}{\alpha}\,\partial_t^2\phi_1(\cdot,t)\psi_1 &= \int_0^1 V_1(\cdot,t)\psi_1 - \int_0^1 \mathbf{m}_1(\cdot,t)\psi_1' \\ &\quad + \mathbf{m}_1(1,t)\psi_1(1) - \int_0^1 S_1\partial_x w_1(\cdot,t)\psi_1. \qquad (5.3.11)\end{aligned}$$

In the equations above $v_1 \in T[0,1]$ and $\psi_1 \in T[0,1]$ are arbitrary.

Test space $\mathbf{T_N}$ We define the test space for the beam as follows:
v is in T_N if v_1 is in $T[0,1]$, v_k is in $C^1[0,1]$ for $k > 1$ and $v_k(1) = v_{k+1}(0)$.

From Equations (5.2.7) and (5.2.8) the following constraints for the interface between beam k and $k+1$ are obtained

$$\begin{aligned}V_{k+1}(0,t)v_k(1) - V_k(1,t)v_k(1) &= \mu_k\partial_t^2 w_k(1,t)v_k(1) \qquad (5.3.12)\\ \mathbf{m}_{k+1}(0,t)\psi_k(1) - \mathbf{m}_k(1,t)\psi_k(1) &= I_k\partial_t^2\phi_k(1,t)\psi_k(1). \qquad (5.3.13)\end{aligned}$$

© University of Pretoria

These interface conditions hold for $k = 1, \cdots, N-1$.

To obtain the variational form one must add all the equations. Summing Equations (5.3.5) and (5.3.6) over k and using (5.3.12) and (5.3.13) yields

$$\sum_{k=1}^{N} \int_0^1 \partial_t^2 w_k(\cdot,t) v_k = -\sum_{k=1}^{N} \int_0^1 V_k(\cdot,t) v_k' - \sum_{k=1}^{N-1} \mu_k \partial_t^2 w_k(1,t) v_k(1) + \sum_{k=1}^{N} \int_0^1 q(\cdot,t) v_k, \tag{5.3.14}$$

$$\sum_{k=1}^{N} \int_0^1 \frac{1}{\alpha} \partial_t^2 \phi_k(\cdot,t) \psi_k = \sum_{k=1}^{N} \int_0^1 V_k(\cdot,t) \psi_k - \sum_{k=1}^{N} \int_0^1 \mathbf{m}_k(\cdot,t) \psi_k' - \sum_{k=1}^{N-1} I_k \partial_t^2 \phi_k(1,t) \psi_k(1) - \sum_{k=1}^{N} \int_0^1 S_k \partial_x w_k(\cdot,t) \psi_k, \tag{5.3.15}$$

for $v, \psi \in T_N$.

The variational form of the problem can now be formulated.

Problem MT-beam-V

Find functions w, ϕ, $\mathbf{m}$ and V such that $w(\cdot,t)$, $\phi(\cdot,t) \in T_N$ and $\mathbf{m}_k$, $V_k \in C^1[0,1]$ for all $t > 0$ and the following hold: Equations (5.3.14) and (5.3.15), together with the constitutive equations given in Equations (5.3.8) and (5.3.9) for all v, $\psi \in T_N$ and ζ_k, $\xi_k \in C^1[0,1]$, with the boundary conditions $w_0(0,t) = w_E(t)$, $\phi(0,t) = 0$.

The variational form for the problem can be used for the theory, e.g. existence of a solution.

5.4 Semi-discrete approximation

5.4.1 Variational form in a finite dimensional subspace

Recall that we use a variant of the Mixed Finite Element Method in this chapter (see Section 5.3). In this case piecewise linear basis functions can be used. However, if the standard Finite Element Method is used, Equations (5.3.8) and (5.3.9) are substituted into Equations (5.3.14) and (5.3.15) and cubic basis functions are then required because of the derivatives.

© University of Pretoria

The variational form of the problem is for the whole system of N beams. To obtain the approximate solutions the variational forms of the beams are treated separately.

Due to the complexity of the multiple beam model and interface conditions the Galerkin approximation is explained in detail in this subsection.

The following notation is used for the finite dimensional subspaces:

S^h is the space of piecewise polynomial functions in $C^1[0,1]$;

S_0^h is the space of piecewise polynomial functions in $T[0,1]$, i.e. $f(0)=0$;

S_T^h is a finite dimensional subspace of T_N;

S_N^h is the cartesian product of N subspaces: $S_N^h = S^h \times \cdots \times S^h$.

Let w^h, ϕ^h, $\mathbf{m}^h$ and V^h be approximations of w, ϕ, $\mathbf{m}$ and V respectively, in the finite dimensional subspace.

Consider the equations of motion for the k_{th} beam (excluding $k=1$) in the finite dimensional subspace S^h.

$$\begin{aligned}\int_0^1 \partial_t^2 w_k^h(\cdot,t)v_k &= -\int_0^1 V_k^h(\cdot,t)v_k' + V_k^h(1,t)v_k(1) - V_k^h(0,t)v_k(0) \\ &\quad + \int_0^1 q(\cdot,t)v_k, \qquad (5.4.1)\\ \int_0^1 \frac{1}{\alpha}\,\partial_t^2 \phi_k^h(\cdot,t)\psi_k &= \int_0^1 V_k^h(\cdot,t)\psi_k - \int_0^1 \mathbf{m}_k^h(\cdot,t)\psi_k' + \mathbf{m}_k^h(1,t)\psi_k(1) \\ &\quad -\mathbf{m}_k^h(0,t)\psi_k(0) - \int_0^1 S_k \partial_x w_k^h(\cdot,t)\psi_k \qquad (5.4.2)\end{aligned}$$

for all v_k and ψ_k in S^h. Recall that for $k=1$, $v_1(0)=\psi_1(0)=0$. The following constitutive equations must also hold for every k:

$$\begin{aligned}\int_0^1 \mathbf{m}_k^h(\cdot,t)\zeta_k &= \int_0^1 \frac{1}{\beta}\partial_x \phi_k^h(\cdot,t)\zeta_k, \qquad (5.4.3)\\ \int_0^1 V_k^h(\cdot,t)\xi_k &= \int_0^1 \big(\partial_x w_k^h(\cdot,t) - \phi_k^h(\cdot,t)\big)\xi_k \qquad (5.4.4)\end{aligned}$$

for each $(\zeta_k, \xi_k) \in S^h \times S^h$.

© University of Pretoria

The constraints, interface conditions and boundary conditions can all be written in terms of functions in the finite dimensional subspaces.

For each pair of consecutive beams the following **constraints** must hold:

$$\begin{aligned} w_k^h(1,t) &= w_{k+1}^h(0,t), \\ \phi_k^h(1,t) &= \phi_{k+1}^h(0,t). \end{aligned}$$

From Equations (5.3.12) and (5.3.13) the **interface conditions** become

$$V_{k+1}^h(0,t)v_k(1) - V_k^h(1,t)v_k(1) = \mu_k \partial_t^2 w_k^h(1,t)v_k(1), \tag{5.4.5}$$

$$\mathbf{m}_{k+1}^h(0,t)\psi_k(1) - \mathbf{m}_k^h(1,t)\psi_k(1) = I_k \partial_t^2 \phi_k^h(1,t)\psi_k(1), \tag{5.4.6}$$

for all v_k^h and ψ_k^h in S^h and the **boundary conditions** are given by

$$\begin{aligned} w_1^h(0,t) &= w_E(t), \\ \phi_1^h(0,t) &= 0. \end{aligned}$$

As mentioned before, the boundary conditions at $k = N$ are natural boundary conditions and are not enforced.

As in Section 5.3 it is necessary to sum over Equations (5.4.1) and (5.4.2) from $k = 1$ to N. This yields the problem given below.

Problem MT-beam-V^h

Find functions $(w^h, \phi^h, \mathbf{m}^h, V^h)$ such that $w^h(\cdot,t) \in S_N^h$, $\phi^h(\cdot,t) \in S_T^h$ and $V^h(\cdot,t)$ and $\mathbf{m}^h(\cdot,t)$ are in S_N^h and

$$\begin{aligned} \sum_{k=1}^{N} \int_0^1 \partial_t^2 w_k^h v_k + \sum_{k=1}^{N-1} \mu_k \partial_t^2 w_k^h(1,t)v_k(1) &= -\sum_{k=1}^{N} \int_0^1 V_k^h v_k' \\ &\quad + \sum_{k=1}^{N} \int_0^1 q v_k, \end{aligned} \tag{5.4.7}$$

$$\begin{aligned} \frac{1}{\alpha} \sum_{k=1}^{N} \int_0^1 \partial_t^2 \phi_k^h \psi_k + \sum_{k=1}^{N-1} I_k \partial_t^2 \phi_k^h(1,t)\psi_k(1) &= \sum_{k=1}^{N} \int_0^1 V_k^h \psi_k \\ &\quad - \sum_{k=1}^{N} \int_0^1 \mathbf{m}_k^h \psi_k' - \sum_{k=1}^{N} \int_0^1 S_k \partial_x w_k^h \psi_k, \end{aligned} \tag{5.4.8}$$

with $v,\ \psi \in S_T^h$. The constitutive equations (5.4.3) and (5.4.4), interface conditions and boundary conditions must also hold for every k.

© University of Pretoria

5.4.2 Basis functions

Another advantage of MFEM as used in this chapter is the following. The shear force and bending moment values are immediately available and since the problem under consideration is already complex, the use of C_0 piecewise linear basis functions is a considerable advantage.

Consider one beam: The interval $[0,1]$ is divided into n elements of equal length and the nodes are numbered from 0 to n. Let S^h be the span of the continuous piecewise linear basis functions δ_i, for $i = 0, 1, ..., n$ and S_0^h the span of the same basis functions but without δ_0.

It is convenient and much simpler to inspect the beams separately. In order to decouple the beams the following substitutions are made. For any beam k, replace v_k by δ_i where $i = 1, \cdots, n-1$ (avoiding the interfaces and boundary points) and $v_j = 0$ for $j \neq k$. It is also valid to replace v_k by δ_n provided that v_{k+1} is replaced by δ_0. For $k = 1$, δ_0 is not a test function and therefore not used. These substitutions are valid since the equations must hold for all functions in the space.

By making these substitutions the multiple beam model is decoupled and the beams can be considered separately. Consider an arbitrary beam k with $w^h,\ \phi^h \in S^h$, then

$$\int_0^1 \partial_t^2 w_k^h(\cdot,t)\delta_i = -\int_0^1 V_k^h(\cdot,t)\delta_i' + \int_0^1 q(\cdot,t)\delta_i, \quad i = 1, \cdots, n-1, \tag{5.4.9}$$

$$\int_0^1 \frac{1}{\alpha}\,\partial_t^2 \phi_k^h(\cdot,t)\delta_i = \int_0^1 V_k^h(\cdot,t)\delta_i - \int_0^1 \mathbf{m}_k^h(\cdot,t)\delta_i' - \int_0^1 S_k \partial_x w_k^h(\cdot,t)\delta_i, \quad i = 1, \cdots, n-1. \tag{5.4.10}$$

The interface conditions are given by

$$V_{k+1}^h(0,t)\delta_n - V_k^h(1,t)\delta_n = \mu_k \partial_t^2 w_k^h(1,t)\delta_n, \tag{5.4.11}$$

$$\mathbf{m}_{k+1}^h(0,t)\delta_n - \mathbf{m}_k^h(1,t)\delta_n = I_k \partial_t^2 \phi_k^h(1,t)\delta_n. \tag{5.4.12}$$

Note that $\delta_i(1)$ is zero everywhere except when $i = n$.

The constitutive equations are given by

$$\int_0^1 \mathbf{m}_k^h(\cdot,t)\delta_i = \int_0^1 \frac{1}{\beta}\partial_x \phi_k^h(\cdot,t)\delta_i, \tag{5.4.13}$$

$$\int_0^1 V_k^h(\cdot,t)\delta_i = \int_0^1 \big(\partial_x w_k^h(\cdot,t) - \phi_k^h(\cdot,t)\big)\delta_i, \tag{5.4.14}$$

© University of Pretoria

for $i = 0, \cdots, n$.

In the case where $k = 1$, the equations remain the same except that $\phi_1 \in S_0^h$.

In order to write the problem as an ordinary differential equation, the relevant matrices must be derived. Before this can be done, write w^h, ϕ^h, $\mathbf{m}^h$ and V^h in terms of the basis functions:

$$w_k^h(x,t) = \sum_{j=0}^{n} w_{kj}(t)\delta_j(x), \text{ for all } k,$$

$$\phi_k^h(x,t) = \sum_{j=0}^{n} \phi_{kj}(t)\delta_j(x) \text{ for } k > 1 \text{ and } \phi_1^h(x,t) = \sum_{j=1}^{n} \phi_{1j}(t)\delta_j(x),$$

$$\mathbf{m}_k^h(x,t) = \sum_{j=0}^{n} \mathbf{m}_{kj}(t)\delta_j(x) \text{ for all } k,$$

$$V_k^h(x,t) = \sum_{j=0}^{n} V_{kj}(t)\delta_j(x) \text{ for all } k,$$

where n is the number of subintervals on $[0,1]$.

Notation

At this point it is convenient to introduce notation to distinguish between time and spatial derivatives. Dots will now be used to denote time derivatives while primes will be used to denote spatial derivatives.

The subscript notation previously used to indicate the k_{th} beam will be suppressed from this point onward, i.e. w_{kj} will be replaced by w_j. The subscript notation will only be used in special cases where it is necessary to indicate a specific beam.

Equations (5.4.9) and (5.4.10) are now written in terms of the basis functions.

$$\sum_{j=0}^{n} \ddot{w}_j \int_0^1 \delta_j\delta_i = -\sum_{j=0}^{n} V_j \int_0^1 \delta_j\delta_i' + \int_0^1 q\delta_i, \quad i = 1, \cdots, n-1, \tag{5.4.15}$$

$$\frac{1}{\alpha}\sum_{j=0}^{n} \ddot{\phi}_j \int_0^1 \delta_j\delta_i = \sum_{j=0}^{n} V_j \int_0^1 \delta_j\delta_i - \sum_{j=0}^{n} \mathbf{m}_j \int_0^1 \delta_j\delta_i' - \sum_{j=0}^{n} w_j \int_0^1 S_k\delta_j'\delta_i,$$
$$i = 1, \cdots, n-1. \tag{5.4.16}$$

© University of Pretoria

Note that these equations hold for beam N with $i = 1, \cdots, n$.

Now examine the interface from beam k to $k+1$. Recall that if $v_k(1) \neq 0$, then $v_{k+1}(0)$ is not allowed to be 0, i.e. if v_k is replaced by δ_n, v_{k+1} must be replaced by δ_0. When using the constraints it is necessary to indicate the relevant beam, therefore the subscript notation is used.

Consider beam $k+1$ for $i = 0$, and beam k for $i = n$. It is necessary to add these two equations in order for the interface conditions to hold. The following is obtained:

$$\begin{aligned}\sum_{j=0}^{n} \ddot{w}_{j,k} \int_0^1 \delta_j \delta_n + \sum_{j=0}^{n} \ddot{w}_{j,k+1} \int_0^1 \delta_j \delta_0 + \mu_k \ddot{w}_{n,k} \delta_n = -\sum_{j=0}^{n} V_{j,k} \int_0^1 \delta_j \delta_n' \\ - \sum_{j=0}^{n} V_{j,k+1} \int_0^1 \delta_j \delta_0' + \int_0^1 q\delta_0 + \int_0^1 q\delta_n, \qquad (5.4.17)\end{aligned}$$

$$\begin{aligned}\frac{1}{\alpha} \sum_{j=0}^{n} \ddot{\phi}_{j,k} \int_0^1 \delta_j \delta_n + \frac{1}{\alpha} \sum_{j=0}^{n} \ddot{\phi}_{j,k+1} \int_0^1 \delta_j \delta_0 + I_k \ddot{\phi}_{n,k} \delta_n = \sum_{j=0}^{n} V_{j,k} \int_0^1 \delta_j \delta_n \\ + \sum_{j=0}^{n} V_{j,k+1} \int_0^1 \delta_j \delta_0 - \sum_{j=0}^{n} \mathbf{m}_{j,k} \int_0^1 \delta_j \delta_n' - \sum_{j=0}^{n} \mathbf{m}_{j,k+1} \int_0^1 \delta_j \delta_0' \\ - \sum_{j=0}^{n} w_{j,k} \int_0^1 S_k \delta_j' \delta_n - \sum_{j=0}^{n} w_{j,k+1} \int_0^1 S_{k+1} \delta_j' \delta_0. \qquad (5.4.18)\end{aligned}$$

Recall that $\delta_i(1) = 0$ for all $i \neq n$.

Boundary conditions

$$\phi_1^h(0) = 0 \text{ and } w_1^h(0) = w_E(t).$$

For the last beam recall that the boundary conditions are natural boundary conditions.

Now consider the constitutive equations. Following the same procedure as before, the test functions ζ_k and ξ_k are replaced by the basis function δ_i.

$$\int_0^1 \mathbf{m}_j^h(\cdot, t)\delta_i = \int_0^1 \frac{1}{\beta} \partial_x \phi_j^h(\cdot, t)\delta_i, \quad i = 0, 1, \cdots, n, \qquad (5.4.19)$$

$$\int_0^1 V_j^h(\cdot, t)\delta_i = \int_0^1 \big(\partial_x w_j^h(\cdot, t) - \phi_j^h(\cdot, t)\big)\delta_i, \quad i = 0, 1, \cdots, n. \qquad (5.4.20)$$

© University of Pretoria

Rewrite $\mathbf{m}_k$ and V_k in terms of the basis functions, then constitutive equations are written as:

$$\int_0^1 \sum_{j=0}^{n} \mathbf{m}_j \delta_j \delta_i = \int_0^1 \sum_{j=0}^{n} \frac{1}{\beta} \phi_j \delta_j' \delta_i, \quad i = 0, 1, \cdots, n, \tag{5.4.21}$$

$$\int_0^1 \sum_{j=0}^{n} V_j \delta_j \delta_i = \int_0^1 \sum_{j=0}^{n} \big(w_j \delta_j' - \phi_j \delta_j\big) \delta_i, \quad i = 0, 1, \cdots, n. \tag{5.4.22}$$

Note that if $k = 1$, the terms on the right hand side will only hold for $j = 1, \cdots, n$.

5.4.3 Matrices and systems of ordinary differential equations

The aim is to write Problem MT-beam-V^h as a system of ordinary differential equations. Using Equations (5.4.15), (5.4.16), (5.4.21) and (5.4.22) the matrices are set up for the problem. Recall that piecewise linear basis functions are used.

Notation The following notation will be used in this subsection:

$X_{i,j}$ denotes the components of the matrix X; $(f, g) = \int_0^1 fg$.

The M, K and L matrices are defined in Section 4.4 in Equation (3.2.19). The R matrix is defined as

$$R_{i,j} = (S\delta_j', \delta_i),$$

with S denoting the axial force.

Let A be a matrix representing M, K, L or R. Follow the notation as introduced in (3.2.20) in Section 3.2.3, i.e.

A is a complete matrix, i.e. no rows or columns are deleted.

A_0 has its first row and column deleted.

A_r has its first row deleted.

A_c has its first column deleted.

© University of Pretoria

More notation is needed and introduced here:

A_{rr} has its first and last rows deleted.

A^c_{rr} has its first and last rows deleted as well as the first column.

Let $\bar{w}_r$ indicate that the first entry of $\bar{w}$ has been deleted.

Definition $\bar{q}_I$ and q_i

Define $\bar{q}_I$ as the interpolant of $q(x_i)$. Define the load at a point as follows: $q_i = \int_0^1 q\delta_i$ for $i = 0, \cdots, n$.

Ordinary differential equations

Firstly, the equations for w are considered and written as ordinary differential equations. We use Equation (5.4.15) (for $1 < k < N$ and avoiding the interfaces) and follow standard procedure to find

$$M_{rr}\ddot{\bar{w}} = -L_{rr}\bar{V} + M_{rr}\bar{q}_I. \tag{5.4.23}$$

The ordinary differential equation for the first beam is

$$M^c_{rr}\ddot{\bar{w}}_r = -L_{rr}\bar{V} + M_{rr}\bar{q}_I, \tag{5.4.24}$$

and for the last beam

$$M_r\ddot{\bar{w}} = -L_r\bar{V} + M_r\bar{q}_I. \tag{5.4.25}$$

Equation (5.4.17) (for the interface) is written as

$$\begin{aligned}&(M_{0,0} + M_{n,n} + \mu_k)\ddot{w}_{n,k} + M_{0,1}\ddot{w}_{1,k+1} + M_{n,n-1}\ddot{w}_{n-1,k} = -L_{0,0}V_{0,k+1}\\ &-L_{0,1}V_{1,k+1} - L_{n,n-1}V_{n-1,k} - L_{n,n+1}V_{n+1,k} + q_n + q_0.\end{aligned} \tag{5.4.26}$$

Recall that $w_{n,k} = w_{0,k+1}$.

Write the equations for ϕ as ordinary differential equations. Use Equation (5.4.16) (for $1 < k < N$ and avoiding the interfaces) to obtain

$$\frac{1}{\alpha}M_{rr}\ddot{\bar{\phi}} = M_{rr}\bar{V} - L_{rr}\bar{\mathbf{m}} - R_{rr}\bar{w}. \tag{5.4.27}$$

The first and last beams are given by

$$\frac{1}{\alpha}M^c_{rr}\ddot{\bar{\phi}}_r = M_{rr}\bar{V} - L_{rr}\bar{\mathbf{m}} - R^c_{rr}\bar{w}_r \tag{5.4.28}$$

© University of Pretoria

and

$$\frac{1}{\alpha}M_r\ddot{\bar{\phi}} = M_r\bar{V} - L_r\bar{\mathbf{m}} - R_r\bar{w} \tag{5.4.29}$$

respectively. By making use of the fact that $w_{n,k} = w_{0,k+1}$ and $\phi_{n,k} = \phi_{0,k+1}$, Equation (5.4.18) (for the interface) is written as

$$\begin{aligned}\frac{1}{\alpha}(M_{0,0} + M_{n,n} + I_k)\ \ddot{\phi}_{n,k} + \frac{1}{\alpha}(M_{0,1}\ \ddot{\phi}_{1,k+1} + M_{n,n-1}\ddot{\phi}_{n-1,k}) = \\ M_{0,0}V_{0,k+1} + M_{0,1}V_{1,k+1} + M_{n,n-1}V_{n-1,k} + M_{n,n}V_{n,k} - L_{0,0}\mathbf{m}_{0,k+1} \\ - L_{0,1}\mathbf{m}_{1,k+1} - L_{n,n-1}\mathbf{m}_{n-1,k} - L_{n,n}\mathbf{m}_{n,k} - R_{0,1}w_{1,k+1} \\ - R_{n,n-1}w_{n-1,k} - (R_{0,0} + R_{n,n})w_{n,k}.\end{aligned} \tag{5.4.30}$$

The constitutive equations (5.4.21) and (5.4.22) are written as

$$M\mathbf{m} = \frac{1}{\beta}L\phi, \tag{5.4.31}$$

$$MV = L^T w - M\phi. \tag{5.4.32}$$

Note that for $k > 1$ no rows or columns are deleted from these matrices. If $k = 1$ the constitutive equations become

$$M\mathbf{m} = \frac{1}{\beta}L^c\phi, \tag{5.4.33}$$

$$MV = (L^T)^c w - M^c\phi. \tag{5.4.34}$$

Problem MT-beam ODE

The system of ordinary differential equations for the model is given by Equations (5.4.23) to (5.4.25) for w and (5.4.27) to (5.4.29) for ϕ, Equations (5.4.26) and (5.4.30) for the interfaces of w and ϕ respectively as well as the constitutive equations given in (5.4.31) to (5.4.34).

5.5 Conclusion

The aim of this chapter was to see if it is theoretically possible to implement a multiple beam model for a slender structure such as a high-rise building. To correctly apply the interface conditions in the variational form proved to be a challenge. In order to deal with the additional terms due to the

© University of Pretoria

interface conditions a variant of the Mixed Finite Element Method was used where neither of the constitutive equations are substituted into the equations of motion. Finally, a system of ordinary differential equations was derived and Problem MT-beam ODE was presented. It is clear that it is feasible to use this model for this application.

The simulation of this problem will be a part of future research. Possible obstacles to consider include obtaining realistic data for, amongst others, the mass of the floors, the dimensions of the buildings and the various other parameters involved.

© University of Pretoria

Chapter 6

Cantilever Timoshenko beam and tip body with elastic behaviour at the interfaces

6.1 Introduction

As mentioned in Chapter 1, beam models have a lot of applications, for example it can be part of an elastic multi-structure (as in [LZ14]) or a model for a slender vertical structure (as in [LVV05]). It can also be used to manipulate an object (as in [LM88]), i.e. the beam has a body attached to it.

Although important, [LM88] is but one of many publications on structures containing tip bodies. In these publications, analysis of vibration modes, stabilization and optimal control of the vibration are topics considered, see e.g. [Gro10] for references up to 2008. Successful manipulation of objects by robotic arms depends on damping of unwanted vibration and natural damping in a beam is often insufficient. The possibility of using a tip body in order to stabilize a system is considered in [AS02] and [RA15].

Recall that the Timoshenko model is more realistic than the Euler-Bernoulli model, see Section 1.2.1. According to [Gro10] hybrid models for a Timoshenko beam has attracted more attention since the late eighties, but it appears as if a Timoshenko beam model with tip body where rotary inertia is taken into account, was not considered before 2004.

© University of Pretoria

In the article [ZVV04] the Finite Element Method is used to compute natural frequencies and modes of vibration for a Timoshenko beam with tip body. Rotary inertia of the tip body is taken into account. The stabilization of such a Timoshenko beam is considered in [Gro10] and [RA15]. (The model problem in these articles is the same as in [ZVV04].) In [RA15] the authors mention that the position of the center of mass of the tip body need not be at the endpoint of the beam but then neglect a resulting additional term in their linear approximation. They proceed to prove an existence result and a stability result for the linear case.

With few exceptions the publications mentioned above were concerned with the stabilization of different configurations rather than modelling the configuration.

In this chapter our main concern is to develop a realistic way of modelling the interface between the endpoint of the beam and the attached body. The study is motivated by a comparison of the two articles [AS02] and [ZVV04]. In the first an Euler-Bernoulli beam with a damping tip body is considered and in the second a Timoshenko beam with a tip body and boundary damping is investigated. The model in [AS02] is more realistic than models in preceding articles due to the fact that the distance between the endpoint of the beam and the position of the center of mass of the tip body is taken into account. The Timoshenko theory provides a better model for the beam but there is a complication at the interface with the tip body. In [AS02] the angle of rotation of the tip body is assumed to be the same as that for the endpoint of the beam, which appears to be realistic. However, making this assumption for a Timoshenko beam leads to an inadmissable interface condition. The interface condition in [ZVV04] is admissible in the variational form but appears less realistic than the alternative.

In [BCLS08] and [LZ14] Euler-Bernoulli beams were connected to "legs" using the same geometry as in [AS02]. In [Gro10] and [RA15] the connection between the Timoshenko beam and tip body is the same as in [ZVV04]. This is also the case in [FES17] where a rigid body is fitted between two Timoshenko beams.

We propose that both models discussed above, can be questioned and that an elastic interface must be considered. Exactly how to model this is explained in Subsection 6.2.3. It is important to note that the main issue here is the interface conditions when fixing a body to the beam, not damping.

After the derivation of the equations of motion for the tip body, we present

© University of Pretoria

the interface conditions in [AS02], [ZVV04] and our proposed alternative, highlighting the different assumptions. A comparison can thus be made. At the so called clamped end we model an elastic interface that resists rotation.

Concerning an analysis of the new hybrid model, we prove existence and uniqueness of a solution for the initial boundary value problem. We derive the variational form to obtain the weak variational form for existence theory. The variational form is also used to prove dissipation of energy and to formulate the Galerkin approximation which in turn yields the system of ordinary differential equations for the dynamic simulation.

Using an abstract general result for convergence of the Galerkin approximation [BSV17], we derive error estimates for the finite element approximation.

To complement the theory, we present results of numerical experiments. Various values of the elastic constants for interfaces were considered.

6.2 The model problems

6.2.1 Equations of motion

Firstly, the Timoshenko beam model (see Section 1.2) with the addition of possible damping terms is presented. The equations of motion and constitutive equations (in dimensionless form) are given by:

$$\partial_t^2 w = \partial_x V - c_1 \partial_t w + q, \tag{6.2.1}$$

$$\frac{1}{\alpha}\partial_t^2 \phi = V + \partial_x M, \tag{6.2.2}$$

$$M = \frac{1}{\beta}\partial_x \phi + c_2 \partial_t \partial_x \phi, \tag{6.2.3}$$

$$V = \partial_x w - \phi, \tag{6.2.4}$$

where c_1 and c_2 denote dimensionless damping parameters.

The term containing c_1 models viscous damping. Material damping (also strain rate or Kelvin-Voigt damping) is modelled in Equation (6.2.3) by the term containing c_2. For the Euler-Bernoulli model it becomes $c_2 \partial_t \partial_x^2 w$, see Equation (6.2.6) below as well as [Inm94]. In this chapter however, our main concern is a realistic way to model the interface between the endpoint of the beam and the attached body.

© University of Pretoria

For the dimensionless scaling see Subsection 1.2.1. For convenience the original notation was retained in Equations (6.2.1) - (6.2.4). Damping coefficients c_v (for viscous damping) and c_{sr} (for strain rate damping) can be recovered as $c_v = AG\kappa^2 t_0 \ell^{-2} c_1$ and $c_{sr} = AG\kappa^2 \ell^2 t_0 c_2$.

Elimination of the shear force V from (6.2.1) and (6.2.2) and replacement of ϕ by $\partial_x w$, lead to the Rayleigh model

$$\partial_t^2 w - \frac{1}{\alpha}\partial_t^2 \partial_x^2 w = -\partial_x^2 M - c_1 \partial_t w + q \tag{6.2.5}$$

with constitutive equation

$$M = \frac{1}{\beta}\partial_x^2 w + c_2 \partial_t \partial_x^2 w. \tag{6.2.6}$$

The constitutive equation (6.2.4) is now redundant. The Euler-Bernoulli model (used in [AS02]) can be obtained by discarding the rotary inertia term $-\frac{1}{\alpha}\partial_t^2 \partial_x^2 w$ (which is considered to be insignificant in the Euler-Bernoulli theory) in Equation (6.2.5).

6.2.2 Boundary and interface conditions

In order to formulate the boundary and interface conditions, it is necessary to examine the dynamics of the tip body. The interface conditions considered in the two articles that motivated this study are also explained in this subsection.

Dynamics of the tip body

The interface conditions are determined by the interaction between the beam and the rigid body illustrated in Figure 6.1. The angle of the tip body relative to the beam is exaggerated in Figure 6.2 for clarity. Although the dynamics are elementary, it is necessary to consider the equations of motion for the rigid body carefully when deriving these conditions. The position of the center of mass C of the tip body relative to the endpoint of the beam (see Figure 6.1) is

$$d\cos\theta(t)\ \mathbf{i} + d\sin\theta(t)\ \mathbf{j},$$

© University of Pretoria

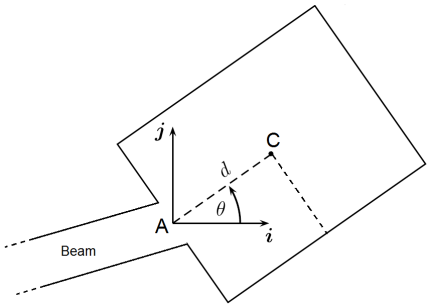

Figure 6.1: Tip body

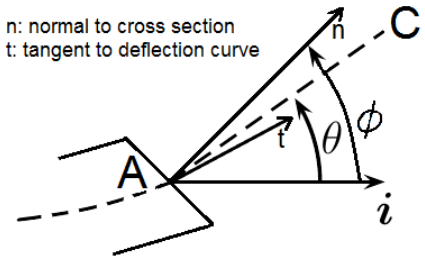

Figure 6.2: Relevant angles

where **i** is in the direction of the axis of the undeformed beam. Clearly, the velocity $\mathbf{v}_C$ and acceleration $\mathbf{a}_C$ of the center of mass are given by

$$\begin{aligned}\mathbf{v}_C &= \partial_t w(\ell,t)\ \mathbf{j} - d\dot{\theta}(t)\sin\theta(t)\ \mathbf{i} + d\dot{\theta}(t)\cos\theta(t)\ \mathbf{j},\\ \mathbf{a}_C &= \partial_t^2 w(\ell,t)\ \mathbf{j} - d\ddot{\theta}(t)\sin\theta(t)\ \mathbf{i} + d\ddot{\theta}(t)\cos\theta(t)\ \mathbf{j} - d\dot{\theta}^2(t)\cos\theta(t)\ \mathbf{i}\\ &\quad - d\dot{\theta}^2(t)\sin\theta(t)\ \mathbf{j}.\end{aligned}$$

For the linear approximation it is assumed that the term $-d\dot{\theta}^2(t)\sin\theta(t)\ \mathbf{j}$ in the acceleration may be neglected and $\cos\theta(t) \approx 1$. (Apart from $\theta(t)$ small, the frequency of oscillations should be moderate.) Using these approximations, we have the following expressions for the transverse components of the velocity and acceleration:

$$\partial_t w(\ell,t) + d\dot{\theta}(t) \quad \text{and} \quad \partial_t^2 w(\ell,t) + d\ddot{\theta}(t).$$

Using Newton's second law for the motion of the center of mass we have

$$m\partial_t^2 w(\ell,t) + md\ \ddot{\theta}(t) = F_B(t) - k_1\partial_t w(\ell,t) - k_1 d\dot{\theta}(t), \tag{6.2.7}$$

where m is the mass of the tip body and F_B is the force on the body. The last two terms are effectively the damping suggested in [AS02]. Taking moments about the center of mass we have

$$J\ddot{\theta}(t) = M_B(t) - dF_B(t) - dk_2\dot{\theta}(t), \tag{6.2.8}$$

where F_B is the force on the tip body, M_B is the couple on the rigid body and J is the moment of inertia about the center of mass. Here, the last term with damping parameter k_2 is a damping term proposed by [AS02].

We have reached a point where the differences between [AS02], [ZVV04] and the present work can be explained.

© University of Pretoria

The model problem in [AS02]

The authors in [AS02] used the Euler-Bernoulli theory (as mentioned) with Kelvin-Voigt damping. For the interface conditions they assume that the angle of deflection curve at the endpoint is equal to $\theta(t)$. As a consequence $\theta(t) \approx \partial_x w(\ell, t)$ in the linear approximation and hence $\dot{\theta}(t) \approx \partial_t \partial_x w(\ell, t)$ and $\ddot{\theta}(t) \approx \partial_t^2 \partial_x w(\ell, t)$. Using these approximations, the transverse components of the velocity and acceleration become

$$\partial_t w(\ell, t) + d\partial_t \partial_x w(\ell, t) \quad \text{and} \quad \partial_t^2 w(\ell, t) + d\partial_t^2 \partial_x w(\ell, t).$$

The term $d\partial_t \partial_x w(\ell, t)$ in the transverse component of the velocity is also neglected in [AS02]. Doing the necessary substitutions, one obtains the interface conditions in [AS02]:

$$\begin{aligned} m\partial_t^2 w(\ell, t) + md\, \partial_t^2 \partial_x w(\ell, t) + k_1 \partial_t w(\ell, t) &= -V(\ell, t), \\ J\partial_t^2 \partial_x w(\ell, t) + dk_2 \partial_t \partial_x w(\ell, t) &= -M(\ell, t) + dV(\ell, t). \end{aligned}$$

Standard boundary conditions are used at the clamped end.

The model problem in [ZVV04]

In [ZVV04] the distance between the endpoint of the Timoshenko beam and the center of mass is neglected, i.e. $d = 0$. For the interface it is assumed that $\theta(t) = \phi(\ell, t)$. As mentioned, boundary damping (or control) is considered in [ZVV04]. The authors proposed the following interface conditions:

$$\begin{aligned} m\partial_t^2 w(\ell, t) &= -V(\ell, t) - k_1 \partial_t w(\ell, t), \\ J\partial_t^2 \phi(\ell, t) &= -M(\ell, t) - k_2 \partial_t \phi(\ell, t), \end{aligned}$$

The left endpoint of the beam is clamped and the boundary conditions are the usual; $w(0, t) = \phi(0, t) = 0$.

6.2.3 Proposed new model

Alternative boundary conditions for the clamped end

Suppose for example that a beam is clamped at the end $x = 0$. The usual boundary conditions are $\partial_x w = 0$ for the Euler-Bernoulli beam and $\phi = 0$ for

© University of Pretoria

the Timoshenko beam. Note that ϕ is the angle of rotation of the normal of the cross section, measured from the direction of $\mathbf{i}$. Since $\phi = 0$, $\partial_x w \neq 0$ for the Timoshenko beam or we are lead to the absurd conclusion that $V = 0$ at the clamped end. This anomaly was pointed out in [Van01] and [Bha09].

However, considering the variational form, we see that both boundary conditions are mathematically convenient. Consider the Timoshenko model for example. Multiplying Equation (6.2.2) by a test function ψ and employing integration by parts yields

$$\int_0^\ell \frac{1}{\alpha}\partial_t^2\phi\psi \quad = \quad \int_0^\ell V\psi + \int_0^\ell M\psi' + M(\ell,t)\psi(\ell) - M(0,t)\psi(0).$$

Relevant to the discussion are the terms $M(\ell,t)\psi(\ell)$ and $-M(0,t)\psi(0)$. Since $M \neq 0$ at a clamped end, the variational formulation requires that $\psi = 0$. By a similar argument, $\partial_x w = 0$ for the Euler-Bernoulli model.

In [Van01] the author suggested as an alternative the condition $M(0,t) = \mu\phi(0,t)$, with the dimensionless elastic constant $\mu > 1$. The idea is that the deviation from the standard condition ($\phi = 0$) is resisted elastically. No definite conclusion was reached regarding the value of μ but it should be large to ensure that $\phi(0,t)$ is small. For the mathematical model in this chapter, the boundary conditions at the clamped end are

$$w(0,t) = 0, \tag{6.2.9}$$
$$M(0,t) = \mu\phi(0,t) \tag{6.2.10}$$

with $\mu > 0$. It follows from the scaling for moments that the real elastic coefficient is $AG\kappa^2\ell\mu$.

Interface conditions between the beam and tip body

In this chapter we question the interface conditions in both [AS02] and [ZVV04] and model an elastic interface. The assumption $\theta(t) = \partial_x w(\ell,t)$ in [AS02] appears to be a natural choice but there must be some deformation in either the end of the beam or the "rigid" body. We claim that the gradient of the deflection curve at ℓ will differ from $\theta(t)$. Likewise we also propose that $\theta(t) \neq \phi(\ell,t)$ due to warping of the cross-section. (Warping of a cross section is well known, see e.g. [LVV09] where this effect can be seen in Figure 5. A two-dimensional beam model is also compared to a Timoshenko beam.)

© University of Pretoria

First, Equations (6.2.7) and (6.2.8) should also be rewritten in dimensionless form using the same scaling as before. The dimensionless constants are

$$m^* = \frac{m}{\rho A \ell}, \quad J^* = \frac{JGk}{\ell \rho EI}, \quad k_1^* = \frac{k_1 \ell}{AGkT}, \quad k_2^* = \frac{k_2 \ell}{EIT}$$
$$M_B^* = \frac{M_B}{AG\kappa^2 \ell} \quad \text{and} \quad F_B^* = \frac{F_B}{AG\kappa^2}.$$

Rewriting the interface conditions in dimensionless form, returning to the original notation and substituting $M_B(t) = -M(1,t)$ and $F_B(t) = -V(1,t)$, we have

$$m\partial_t^2 w(1,t) + md\ddot{\theta}(t) + k_1 \partial_t w(1,t) + k_1 d\dot{\theta}(t) = -V(1,t) \tag{6.2.11}$$

and

$$J\ddot{\theta}(t) + dk_2\dot{\theta}(t) = -M(1,t) + dV(1,t). \tag{6.2.12}$$

For this study we model the interaction by

$$M(1,t) = \gamma(\theta(t) - \phi(1,t)), \tag{6.2.13}$$

where the dimensionless parameter γ is positive, reasoning that the deviation of $\theta - \phi$ from zero is resisted elastically. As above, the elastic coefficient is $AG\kappa^2 \ell \gamma$.

Results of numerical experiments are provided in Section 6.9. Various values for μ and γ were considered.

Mathematical model

The model consists of the equations of motion

$$\partial_t^2 w = \partial_x V - c_1 \partial_t w + q, \tag{6.2.14}$$
$$\frac{1}{\alpha}\partial_t^2 \phi = V + \partial_x M; \tag{6.2.15}$$

and the constitutive equations

$$M = \frac{1}{\beta}\partial_x \phi + c_2 \partial_t \partial_x \phi, \tag{6.2.16}$$
$$V = \partial_x w - \phi; \tag{6.2.17}$$

© University of Pretoria

with boundary conditions

$$w(0,t) = 0, \tag{6.2.18}$$
$$M(0,t) = \mu\phi(0,t); \tag{6.2.19}$$

and the interface conditions

$$m\partial_t^2 w(1,t) + md\ddot{\theta}(t) + k_1\partial_t w(1,t) + k_1 d\dot{\theta}(t) = -V(1,t) \tag{6.2.20}$$
$$J\ddot{\theta}(t) + dk_2\dot{\theta}(t) = -M(1,t) + dV(1,t). \tag{6.2.21}$$

The initial conditions are $w(\cdot,0) = w_0$, $\phi(\cdot,0) = \phi_0$, $\theta(0) = \theta_0$, $\partial_t w(\cdot,0) = w_d$, $\partial_t\phi(\cdot,0) = \phi_d$ and $\dot{\theta}(0) = \theta_d$.

6.3 Variational form

As usual we start by multiplying Equations (6.2.1) and (6.2.2) by arbitrary functions v and ψ respectively, then integrating both sides and using integration by parts to obtain

$$\begin{aligned}\int_0^1 \partial_t^2 w(\cdot,t)v = &-\int_0^1 V(\cdot,t)v' - c_1\int_0^1 \partial_t w(\cdot,t)v + \int_0^1 q(\cdot,t)v \\ &+ V(1,t)v(1) - V(0,t)v(0),\end{aligned} \tag{6.3.1}$$

$$\begin{aligned}\int_0^1 \frac{1}{\alpha}\partial_t^2\phi(\cdot,t)\psi = &-\int_0^1 M(\cdot,t)\psi' + \int_0^1 V(\cdot,t)\psi \\ &+ M(1,t)\psi(1) - M(0,t)\psi(0).\end{aligned} \tag{6.3.2}$$

To eliminate $V(1,t)$ in Equation (6.2.12), we multiply Equation (6.2.11) by d and add the resulting equation to Equation (6.2.12). Then, we substitute Equation (6.2.13) to obtain

$$\begin{aligned}&J\ddot{\theta}(t) + dk_2\dot{\theta}(t) + dm\partial_t^2 w(1,t) + md^2\ddot{\theta}(t) + dk_1\partial_t w(1,t) + k_1 d^2\dot{\theta}(t) \\ &= -\gamma\big(\theta(t) - \phi(1,t)\big).\end{aligned} \tag{6.3.3}$$

Denote the space of test functions by $T[0,1] = \{v \in C^1[0,1] \mid v(0) = 0\}$. Using the boundary and interface conditions (6.2.10), (6.2.11), (6.2.13) and

© University of Pretoria

(6.3.3), Equations (6.3.1) and (6.3.2) become

$$\int_0^1 \partial_t^2 w(\cdot,t)v = -\int_0^1 V(\cdot,t)v' - c_1\int_0^1 \partial_t w(\cdot,t)v + \int_0^1 q(\cdot,t)v - \Big(m\partial_t^2 w(1,t) + md\ddot{\theta}(t) + k_1\partial_t w(1,t) + k_1 d\dot{\theta}(t)\Big)\, v(1) \tag{6.3.4}$$

and

$$\int_0^1 \frac{1}{\alpha}\,\partial_t^2\phi(\cdot,t)\psi = -\int_0^1 M(\cdot,t)\psi' + \int_0^1 V(\cdot,t)\psi + \gamma\big(\theta(t)-\phi(1,t)\big)\psi(1) - \mu\phi(0,t)\psi(0), \tag{6.3.5}$$

for all $v \in T[0,1]$ and $\psi \in C^1[0,1]$.

The model problem is now written in variational form.

Problem TT-beam-V

Find the functions w, ϕ and θ such that $w(\cdot,t) \in T[0,1]$, $\phi(\cdot,t) \in C^1[0,1]$ and $\theta(t) \in \mathbb{R}$ for all $t > 0$ and the following equations hold for all $v \in T[0,1]$ and $\psi \in C^1[0,1]$:

$$\int_0^1 \partial_t^2 w(\cdot,t)v = \int_0^1 (-\partial_x w(\cdot,t) + \phi(\cdot,t))v' - c_1\int_0^1 \partial_t w(\cdot,t)v + \int_0^1 q(\cdot,t)v - \Big(m\partial_t^2 w(1,t) + md\ddot{\theta}(t) + k_1\partial_t w(1,t) + k_1 d\dot{\theta}(t)\Big)\, v(1), \tag{6.3.6}$$

$$\int_0^1 \frac{1}{\alpha}\,\partial_t^2\phi(\cdot,t)\psi = -\int_0^1 \frac{1}{\beta}\partial_x\phi(\cdot,t)\psi' - c_2\int_0^1 \partial_t\partial_x\phi(\cdot,t)\psi' + \int_0^1 \partial_x w(\cdot,t)\psi - \int_0^1 \phi(\cdot,t)\psi + \gamma\big(\theta(t)-\phi(1,t)\big)\psi(1) - \mu\phi(0,t)\psi(0), \tag{6.3.7}$$

$$(J+md^2)\ddot{\theta}(t) + (k_1d^2 + dk_2)\dot{\theta}(t) + dm\partial_t^2 w(1,t) + dk_1\partial_t w(1,t) = -\gamma\big(\theta(t)-\phi(1,t)\big). \tag{6.3.8}$$

It is instructive to consider the decay of energy for the model in the absence of forcing. The kinetic energy is given by

$$T(t) = \frac{1}{2}\left[\int_0^1 \big(\partial_t w(\cdot,t)\big)^2 + \int_0^1 \frac{1}{\alpha}\big(\partial_t\phi(\cdot,t)\big)^2 + m\Big(\partial_t w(1,t) + d\dot{\theta}(t)\Big)^2 + J\Big(\dot{\theta}(t)\Big)^2\right]$$

© University of Pretoria

and the elastic potential energy by

$$V(t) = \frac{1}{2}\left[\int_0^1 \frac{1}{\beta}\big(\partial_x\phi(\cdot,t)\big)^2 + \int_0^1 \big(\partial_x w(\cdot,t) - \phi(\cdot,t)\big)^2 + \mu\big(\phi(0,t)\big)^2 + \gamma\big(\theta(t) - \phi(1,t)\big)^2\right].$$

If $E(t) = T(t) + V(t)$, then it follows from the time derivatives of $T(t)$ and $V(t)$ and Equations (6.3.6), (6.3.7) and (6.3.8) that

$$\dot{E}(t) = -c_1\int_0^1 \big(\partial_t w(\cdot,t)\big)^2 - c_2\int_0^1 \big(\partial_t\partial_x\phi(\cdot,t)\big)^2 - k_1\big[\partial_t w(1,t) + d\dot{\theta}(t)\big]^2 - k_2 d\left[\dot{\theta}(t)\right]^2.$$

Since all the parameters are positive it follows that $\dot{E}(t) \leq 0$ for a solution of the model problem. This result should be expected from Physics (and is therefore reassuring).

Equations (6.3.6), (6.3.7) and (6.3.8) are used for the application of the Finite Element Method. For the theory we need a single variational equation. First, we multiply Equation (6.3.8) by an arbitrary real number z and then add the three equations to obtain

$$\begin{aligned}
&\int_0^1 \partial_t^2 w(\cdot,t)v + \int_0^1 \frac{1}{\alpha}\,\partial_t^2\phi(\cdot,t)\psi \\
&+ \Big(m\partial_t^2 w(1,t) + md\ddot{\theta}(t) + k_1\partial_t w(1,t) + k_1 d\dot{\theta}(t)\Big)\,v(1) \\
&+ \Big(J\ddot{\theta}(t) + dk_2\dot{\theta}(t) + dm\partial_t^2 w(1,t) + md^2\ddot{\theta}(t) + dk_1\partial_t w(1,t) + k_1 d^2\dot{\theta}(t)\Big)\,z \\
&= -\int_0^1 \frac{1}{\beta}\,\partial_x\phi(\cdot,t)\psi' - c_2\int_0^1 \partial_t\partial_x\phi(\cdot,t)\psi' - \int_0^1 \big(\partial_x w(\cdot,t) - \phi(\cdot,t)\big)(v' - \psi) \\
&\quad - c_1\int_0^1 \partial_t w(\cdot,t)v + \int_0^1 q(\cdot,t)v - \gamma\big(\theta(t) - \phi(1,t)\big)(z - \psi(1)) - \mu\phi(0)\psi(0).
\end{aligned} \tag{6.3.9}$$

The problem is to find a function $\langle w,\phi,\theta\rangle$ such that for all $t > 0$, $w(\cdot,t) \in T[0,1]$, $\phi(\cdot,t) \in C^1[0,1]$, $\theta(t) \in \mathbb{R}$ and (6.3.9) holds for all (v,ψ,z) in $T[0,1]\times C^1[0,1]\times\mathbb{R}$. The initial conditions are $w(\cdot,0) = w_0$, $\phi(\cdot,0) = \phi_0$, $\theta(0) = \theta_0$, $\partial_t w(\cdot,0) = w_d$, $\partial_t\phi(\cdot,0) = \phi_d$ and $\dot{\theta}(0) = \theta_d$.

© University of Pretoria

6.4 Weak variational form

Let $H^1(0,1)$ denote the Sobolev space with weak first order derivatives in $\mathcal{L}^2(0,1)$. The inner product for $H^1(0,1)$ is denoted by $(f,g)_1$ and the corresponding norm by $||f||_1$. Let $V(0,1)$ be the closure of $T[0,1]$ in $H^1(0,1)$.

Instead of considering functions w and ϕ defined on $[0,1]\times[0,T_1]$, consider functions $u_i : [0,T_1] \to H^1(0,1)$, $i = 1,2$. (If the problem has a classical solution, then $u_1(t)(x) = w(x,t)$ and $u_2(t)(x) = \phi(x,t)$).

We need to define a value $f(p)$ of a function $f \in H^1(0,1)$. The trace operator may be used, see [OR76], but the one-dimensional case is quite simple. An elementary inequality is required. If $f \in C^1[0,1]$ and f has a zero in $[0,1]$, it is easy to prove that $|f(x)| \leq \|f'\|$ for each $x \in [0,1]$. If f does not have a zero, then

$$|f(x)| \leq 2\|f\|_1 \quad \text{for each} \quad x \in [0,1]. \tag{6.4.1}$$

By taking limits, it follows that these inequalities hold for any $f \in H^1(0,1)$. Now, for any point p a linear functional γ_p is defined on $C[0,1]$ by $\gamma_p(f) = f(p)$. The inequality above implies that it is bounded on $C^1[0,1]$ with respect to the norm of $H^1(0,1)$ and hence it can be extended to $H^1(0,1)$. We will write $f(p)$ for $\gamma_p(f)$.

In this section and the next, Poincaré type inequalities will be used frequently. First, for $f \in C^1[0,1]$ and any points p and q in $[0,1]$

$$|f(p)| \leq \|f'\| + |f(q)|. \tag{6.4.2}$$

By taking limits, it follows that (6.4.2) holds for any $f \in H^1(0,1)$.

To write the model problem in weak variational form, we need the following product spaces and use the notation in Table 6.1 such that:

$$\begin{aligned} X &= \mathcal{L}^2(0,1)\times\mathcal{L}^2(0,1)\times\mathbb{R}^2, \\ H^1 &= H^1(0,1)\times H^1(0,1)\times\mathbb{R}^2, \\ V_P &= V(0,1)\times H^1(0,1)\times\mathbb{R}^2, \\ V &= \{u = \langle u_1,u_2,u_3,u_4\rangle \in V_P \mid u_4 = u_1(1)\}. \end{aligned}$$

© University of Pretoria

Table 6.1: Notation for inner products and norms

Space	Inner product	Norm
$\mathcal{L}^2(0,1)$	$(\cdot,\cdot)$	$\|\cdot\|$
X	$(x,y)_X = (x_1,y_1) + (x_2,y_2) + x_3y_3 + x_4y_4$	$\|\cdot\|_X$
H^1	$(x,y)_{H^1} = (x_1,y_1)_1 + (x_2,y_2)_1 + x_3y_3 + x_4y_4$	$\|\cdot\|_{H^1}$

Now, for the weak variational form, we define the following bilinear forms on the product spaces. For f and g in X and u and v in H^1,

$$\begin{aligned}
c(f,g) =& \int_0^1 f_1g_1 + \int_0^1 \frac{1}{\alpha}\, f_2g_2 + mf_4g_4 + md\big(f_3g_4 + f_4g_3\big) \\
&+ (J + md^2)u_3v_3, \\
b(u,v) =& \int_0^1 \frac{1}{\beta}\, u_2'v_2' + \int_0^1 (u_1' - u_2)(v_1' - v_2) + \gamma(u_3 - u_2(1))(v_3 - v_2(1)) \\
&+ \mu u_2(0)v_2(0), \\
a(u,v) =& k_1u_1(1)v_1(1) + k_1d\big(u_3v_1(1) + u_1(1)v_3\big) + (k_1d^2 + dk_2)u_3v_3 \\
&+ c_1\int_0^1 u_1v_1 + c_2\int_0^1 u_2'v_2',
\end{aligned}$$

where the derivatives are weak derivatives.

Using the bilinear forms, Equation (6.3.9) can be written as

$$c(\partial_t^2 u(\cdot,t), v) + a(\partial_t u(\cdot,t), v) + b(u(\cdot,t), v) = \int_0^1 q(\cdot,t)v_1,$$

where $u = \langle w, \phi, \theta, w(1)\rangle$.

In the rest of this section we derive the properties of the bilinear forms. First note that the bilinear forms a, b and c are symmetric. For the weak variational form, we need to show that the bilinear forms c and b are inner products for X and V respectively.

Proposition 6.4.1. *The bilinear form c is an inner product for the space X.*

Proof. Since c is a symmetric bilinear form, it is an inner product if $c(u,u) =$

© University of Pretoria

0 implies $u = 0$. Now,

$$\begin{aligned} c(u,u) &= \int_0^1 u_1^2 + \frac{1}{\alpha}\int_0^1 u_2^2 + m(u_4 + du_3)^2 + Ju_3^2 \\ &\geq K_c\left(\|u_1\|^2 + \|u_2\|^2 + u_3^2\right) \qquad (\text{since } m > 0) \end{aligned} \tag{6.4.3}$$

where $K_c = \min\{1, \frac{1}{\alpha}, J\}$. Consequently, u_1, u_2, u_3 and $u_4 + du_3$ are zero if $c(u,u) = 0$. It follows that $u_4 = 0$ and we are done. □

Definition Inertia space W
We refer to the vector space X equipped with the inner product c as the space W. The norm $\|\cdot\|_W$ is defined by $\|u\|_W = \sqrt{c(u,u)}$.

The next result is crucial. Due to (6.4.2) the result is easy to derive when $w(0,t) = \phi(0,t) = 0$. In the literature on Timoshenko theory which we engage with, w and ϕ had zeros at one or both endpoints. In our case we do not have a zero for the function ϕ, which complicates the proof.

Remark In some proofs it is convenient to denote $u \in X$ by $\langle w, \phi, \theta, r\rangle$ instead of $\langle u_1, u_2, u_3, u_4\rangle$.

Proposition 6.4.2. *There exists a constant K_b such that $b(u,u) \geq K_b\|u\|_X^2$ for each $u \in V$.*

Proof. Assume that the result is not true. Then there exists a sequence $(u_n) =$
$(\langle w_n, \phi_n, \theta_n, w_n(1)\rangle)$ such that

$$\|w_n\|^2 + \|\phi_n\|^2 + \theta_n^2 + (w_n(1))^2 = 1, \text{while} \tag{6.4.4}$$

$$\frac{1}{\beta}\|\phi_n'\| + \|w_n' - \phi_n\|^2 + \gamma(\theta_n - \phi_n(1))^2 + \mu\phi_n(0)^2 \to 0. \tag{6.4.5}$$

From (6.4.5), $\|\phi_n'\| \to 0$, $\|w_n' - \phi_n\| \to 0$ and $\phi_n(0) \to 0$. It follows from (6.4.2) that $|\phi_n(1)| \leq \|\phi_n'\| + |\phi_n(0)|$, hence $\phi_n(1) \to 0$. We also have that $(\theta_n - \phi_n(1)) \to 0$ and therefore $\theta_n \to 0$.

For n sufficiently large,

$$\|w_n\| \leq \|w_n' - \phi_n\| + \|\phi_n\| < \frac{1}{4} + \|\phi_n\|,$$
$$|w_n(1)| \leq \|w_n' - \phi_n\| + \|\phi_n\| < \frac{1}{4} + \|\phi_n\|$$

© University of Pretoria

and $|\theta_n| < \frac{1}{4}$. This implies that $2(\frac{1}{16} + \frac{1}{2}\|\phi_n\| + \|\phi_n\|^2) + \|\phi_n\|^2 + \frac{1}{16} > 1$, and hence $\|\phi_n\| > \frac{1}{2}$.

Since $\|\phi_n'\| \to 0$ and $\phi_n(0) \to 0$, it follows from (6.4.2) that

$$|\phi_n(x)| \leq \|\phi_n'\| + |\phi_n(0)| < \tfrac{1}{4} \text{ for each } x \in [0,1]$$

for n sufficiently large. Consequently $\|\phi_n\|^2 = \int_0^1 \phi_n^2 \leq \frac{1}{16}$ which contradicts the previous inequality. □

Corollary 6.4.1. *The bilinear form b is an inner product for the space V.*

Definition Energy space V
We refer to the space V equipped with the inner product b as the energy space. The norm $\|\cdot\|_V$ is defined by $\|u\|_V = \sqrt{b(u,u)}$.

In the weak variational form of the model problem we consider a function u with domain an interval and range in X. The derivatives $u'(t)$ and $u''(t)$ are defined pointwise as limits. We write $u'(t) \in Z$ for some space Z if the limit is with respect to the norm of Z.

Model problem in weak variational form Let $\tilde{q}$ be the mapping $t \to q(\cdot, t)$ and $q_X = \langle \tilde{q}, 0, 0, 0\rangle$. Find u such that for each $t > 0$, $u(t) \in V$, $u'(t) \in V$, $u''(t) \in W$ and

$$c(u''(t), v) + a(u'(t), v) + b(u(t), v) = (q_X(t), v)_X \quad \text{for each} \quad v \in V,$$

while $u(0) = u_0 = \langle w_0, \phi_0, \theta_0, w_0(1)\rangle$ and $u'(0) = u_d = \langle w_d, \phi_d, \theta_d, w_d(1)\rangle$.

6.5 Equivalent norms and inequalities

The results in this section are necessary for existence theory and to derive error estimates for the finite element approximation.

Proposition 6.5.1. *The norms $\|\cdot\|_W$ and $\|\cdot\|_X$ are equivalent.*

Proof. First we prove that $\|u\|_X \leq K_1\|u\|_W$ for some $K_1 > 0$. From $|u_4| \leq |u_4 + du_3| + d|u_3|$ we have

$$u_4^2 \leq 2(u_4 + du_3)^2 + 2d^2u_3^2.$$

© University of Pretoria

Combining this inequality with (6.4.3) yields the desired inequality. Next, from the definition of $c(u, v)$,

$$c(u,u) \leq \int_0^1 u_1^2 + \frac{1}{\alpha}\int_0^1 u_2^2 + (J + md^2)u_3^2 + 2mu_4^2 + 2md^2u_3^2.$$

(We used the elementary inequality $|2ab| \leq a^2 + b^2$.) It follows that

$$\|u\|_W^2 \leq \|u_1\|^2 + \frac{1}{\alpha}\|u_2\|^2 + (J + 3md^2)u_3^2 + 2mu_4^2 \leq K_2\|u\|_X^2.$$

□

Corollary 6.5.1. *The space W is complete.*

Proposition 6.5.2. *There exists a constant C_b such that*

$$b(u,u) \quad \geq \quad C_b\|u\|_W^2 \quad \textit{for each } u \in V.$$

Proof. The result follows from Propositions 6.4.2 and 6.5.1. □

Proposition 6.5.3. *V is a dense subset of W.*

Proof. We have that $V(0,1)$ is dense in $\mathcal{L}^2(0,1)$, since $C_0^\infty(0,1)$ is dense in $\mathcal{L}^2(0,1)$ and $C_0^\infty(0,1) \subset V(0,1)$. For any $u = (w, \phi, \theta, r) \in X$ there exists a sequence $(y_n) = (w_n, \phi_n, \theta_n, w_n(1))$ in V, such that $\|w_n - w\|^2 + \|\phi_n - \phi\|^2 + (\theta_n - \theta)^2 \to 0$. But $w_n(1)$ need not converge to r.

It is not difficult to construct a sequence (η_n) in $H^1(0,1)$ with the following properties:

$$\eta_n(0) = 0, \ \eta_n(1) = 1 \ \text{ and } \ \|\eta_n\| \to 0.$$

Let $\tilde{w}_n = w_n + (r - w_n(1))\eta_n$, then $\tilde{w}_n(1) = w_n(1) + \eta_n(1)(r - w_n(1)) = r$. Also, define $\tilde{y}_n = (\tilde{w}_n, \phi_n, \theta_n, \tilde{w}_n(1))$, then $\|u - \tilde{y}_n\|_X^2 = \|w - \tilde{w}_n\|^2 + \|\phi - \phi_n\|^2 + (\theta - \theta_n)^2$. Now, $\|w - \tilde{w}_n\| \leq \|w - w_n\| + |r - w_n(1)|\|\eta_n\| \to 0$, and hence $\|u - \tilde{y}_n\|_X^2 \to 0$.

Therefore V is a dense subset of X. Using Proposition 6.5.1 the result follows. □

Proposition 6.5.4. *The norms $\|\cdot\|_V$ and $\|\cdot\|_{H^1}$ are equivalent on V.*

© University of Pretoria

Proof. First we prove that $b(u,u) \leq K\|u\|_{H^1}^2$. It is easy to see that

$$\int_0^1 \frac{1}{\beta}\big(\phi'\big)^2 + \int_0^1 \big(w' - \phi\big)^2 \leq K\|u\|_{H^1}^2.$$

Now, $(\theta - \phi(1))^2 \leq 2\theta^2 + 2\big(\phi(1)\big)^2 \leq 2\theta^2 + 8\|\phi\|_1^2$ by (6.4.1). Also, $|\phi(0)| \leq 2\|\phi\|_1$ by (6.4.1). The required inequality follows from the three inequalities above.

Next we prove that $b(u,u) \geq k\|u\|_{H^1}^2$. Clearly,

$$\|w'\|^2 \leq 2\|w' - \phi\|^2 + 2\|\phi\|^2.$$

Consequently, using $\|w\| \leq \|w'\|$ and $|w(1)| \leq \|w'\|$,

$$\begin{aligned}\|w\|_1^2 + \|\phi\|_1^2 + (w(1))^2 &\leq 3\|w'\|^2 + \|\phi'\|^2 + \|\phi\|^2 \\ &\leq 6\|w' - \phi\|^2 + \|\phi'\|^2 + 7\|\phi\|^2 \\ &\leq K_\beta b(u,u) + 7\|\phi\|^2.\end{aligned}$$

As a result

$$\begin{aligned}\|w\|_1^2 + \|\phi\|_1^2 + (w(1))^2 + \theta^2 &\leq K_\beta b(u,u) + 7\|\phi\|^2 + \theta^2 \\ &\leq K_\beta b(u,u) + 7\|u\|_X^2.\end{aligned}$$

The required inequality follows from Proposition 6.4.2. □

Corollary 6.5.2. *The space V is complete.*

Proposition 6.5.5. *There exists a constant K such that, for all u and v in V,*

$$|\,a(u,v)| \;\leq\; K\|u\|_V\|v\|_V.$$

Proof. Since a is symmetric and nonnegative, $|a(u,v)| \leq a(u,u)a(v,v)$. Now, using the definition of $\|\cdot\|_1$ and an elementary inequality,

$$\begin{aligned}a(u,u) &= k_1u_1(1)^2 + 2k_1du_1(1)u_3 + (k_1d^2 + dk_2)u_3^2 + c_1\int_0^1 u_1^2 + c_2\int_0^1 (u_2')^2 \\ &\leq 2k_1u_1(1)^2 + (2k_1d^2 + dk_2)u_3^2 + c_1\|u_1\|_1^2 + c_2\|u_2\|_1^2.\end{aligned}$$

By (6.4.1), it can be obtained that $u_1(1)^2 \leq 4\|u_1\|_1^2$. Therefore

$$|a(u,u)| \leq K\|u\|_{H^1}^2,$$

for some constant K. Since the norms $\|\cdot\|_V$ and $\|\cdot\|_{H^1}$ are equivalent, the result follows. □

© University of Pretoria

6.6 Existence

The weak variational form of the model problem in this section is a special case of the general linear vibration problem considered in [VV02] (given here for convenience): Find $u \in C^1([0,\infty), X)$ such that, for all $t > 0$, $u(t) \in V$, and $u''(t) \in W$, and

$$c(u''(t), v) + a(u'(t), v) + b(u(t), v) = (f(t), v)_X$$

for all $v \in V$, $u(0) = u_0$, $u'(0) = u_1$.

Assumptions E1 to E4 (necessary to obtain existence) as well as the existence result from the article [VV02] were presented in Subsection 1.3.3.

It is clear that Assumptions E1 to E4 are satisfied for our problem from Propositions 6.5.3, 6.5.2, 6.5.1 and 6.5.5 respectively. The existence of a unique solution for the weak variational form follows, provided that q_X is continuously differentiable w.r.t. the norm of X, which requires $\tilde{q}$ to be continuously differentiable with respect to the norm of $\mathcal{L}^2(0,1)$. If that condition is satisfied, Theorem 1.3.1 holds for the weak variational problem in Section 6.4.

Remark As stated in Chapter 1, other existence results are available in the literature, e.g. [Sho77]. The result from [VV02] is convenient for our problem, since it is given in terms of bilinear forms.

6.7 Semi-discrete finite element approximation

6.7.1 Semi-discrete problem

Suppose the space $S^h(0,1)$ is the span of piecewise Hermite cubic basis functions and $S_0^h(0,1)$ the subspace of $S^h(0,1)$ where the basis functions are zero at $x = 0$. Let V^h denote the subspace of V in $S_0^h(0,1) \times S^h(0,1) \times \mathbb{R}^2$.

Consider the Galerkin approximation of the weak variational form:
Find a function u_h such that for each $t > 0$, $u_h(t) \in V^h$ and

$$c(u_h''(t), v) + a(u_h'(t), v) + b(u_h(t), v) = (q_X, v)_X, \tag{6.7.1}$$

© University of Pretoria

for each $v \in V^h$, while $u_h(0) = u_0^h = \langle w_0^h, \phi_0^h, \theta_0, w_0^h(1)\rangle$ and $u_h'(0) = u_d^h = \langle w_d^h, \phi_d^h, \theta_d, w_d^h(1)\rangle$. We use the interpolants (defined below) for the initial conditions. Some authors use $\mathcal{L}^2$ projections for theoretical results instead of interpolants.

For the implementation we use a different form of the Galerkin approximation, we use Equations (6.3.6), (6.3.7) and (6.3.8). In the implementation we omit all the damping terms, except for the boundary damping, since our main concern is the influence of the tip body on the motion. The problem is to find $w^h(t) \in S_0^h(0,1)$, $\phi^h(t) \in S^h(0,1)$ and $\theta^h(t) \in \mathbb{R}$ for each $t > 0$ such that

$$\int_0^1 \partial_t^2 w^h(\cdot,t)v = -\int_0^1 \partial_x w^h(\cdot,t)v' + \int_0^1 \phi^h(\cdot,t)v' + \int_0^1 q(\cdot,t)v - \Big(m\partial_t^2 w^h(1,t) + md\ddot{\theta}^h(t) + k_1\partial_t w^h(1,t) + k_1 d\dot{\theta}^h(t)\Big)v(1) \tag{6.7.2}$$

$$\int_0^1 \frac{1}{\alpha}\partial_t^2\phi^h(\cdot,t)\psi = -\int_0^1 \frac{1}{\beta}\partial_x\phi^h(\cdot,t)\psi' + \int_0^1 \partial_x w^h(\cdot,t)\psi - \int_0^1 \phi^h(\cdot,t)\psi + \gamma\big(\theta^h(t) - \phi^h(1,t)\big)\psi(1) - \mu\phi^h(0,t)\psi(0) \tag{6.7.3}$$

$$(J + md^2)\ddot{\theta}^h(t) + (k_1 d^2 + dk_2)\dot{\theta}^h(t) + dm\partial_t^2 w^h(1,t) + dk_1\partial_t w^h(1,t) = -\gamma\big(\theta^h(t) - \phi^h(1,t)\big), \tag{6.7.4}$$

for all $v \in S_0^h(0,1)$ and $\psi \in S^h(0,1)$.

6.7.2 Convergence and error estimates

To prove convergence and obtain error estimates we use theory in [BSV17]. Our model problem is a special case of the general second order hyperbolic problem with general damping considered there. It is necessary to establish that the assumptions made in that article can be met. Assumptions E1 - E4 required for existence (see Section 1.3.2) are also required in [BSV17]. As mentioned in Section 6.6, these assumptions are all true for our model problem. They are not sufficient though.

Error estimates in the article were obtained by first considering a projection of the solution and then applying interpolation error estimates. In [BSV17] a generalized interpolation operator is defined. We need to use an interpolation

© University of Pretoria

operator that fits into the theory. We define the interpolation operator Π on the product space H^1 by

$$\Pi u = \langle \Pi_c\, u_1,\ \Pi_c\, u_2,\ u_3,\ u_4 \rangle \quad \text{for } u \in H^1,$$

where Π_c is the usual interpolation operator for piecewise Hermite cubic basis functions. Error estimates for Π_c are well known in the literature, and can be found in [OR76] for example.

Error estimates depend on the smoothness of the solution. To apply the results from [BSV17], the minimum requirements are that $u \in C^2((0,T);V)$ and that $u(t)$, $u'(t)$ and $u''(t)$ are in H^2.

Error estimate Let $u_0^h = \Pi u_0$ and $u_d^h = \Pi u_d$. Then, for any $t \in [0,T]$,

$$\|u(t) - u_h(t)\|_V + \|u'(t) - u_h'(t)\|_W \leq Ch,$$

where h is the maximum length of an interval.

If the solution is smooth, the error will be of order h^3.

Remark In theory, piecewise linear basis functions are suitable for the Timoshenko beam. However, due to the phenomenon of "locking", the rate of convergence in practice is not as predicted by the theory. For the Timoshenko beam locking can be avoided by using Hermite cubic basis functions according to [Bra01, p.302]. Our experiments confirmed this.

6.8 System of ordinary differential equations

As mentioned, we use piecewise Hermite cubic basis functions. To derive the differential equations for functions $\bar{w}$ (corresponding to w^h), $\bar{\phi}$ (corresponding to ϕ^h) and θ is standard procedure, [ZVV04]. Note that in this section we use dots for time derivatives and primes for spacial derivatives to avoid confusion.

The relevant matrices are defined in (3.2.19) in Section 3.2.3.

For $\bar{w}$ we obtain

$$M\ddot{\bar{w}} + K\bar{w} - L\bar{\phi} = -\big(m\ddot{w}_{n+1}(t) + k_1\dot{w}_{n+1}(t)\big)\delta_i(1) + M\bar{q}(t) + \tilde{F}_\theta, \quad (6.8.1)$$

where $q_i(t) = q(x_i,t)$ for $i = 1,2,...,n+1$ and $q_i(t) = q'(x_{i-n-1},t)$ for $i = n+2,...,2n+2$, and $\tilde{F}_\theta$ is a vector with a value only in the nth element, containing the θ terms.

© University of Pretoria

For $\bar{\phi}$ the system is

$$\frac{1}{\alpha}M\ddot{\bar{\phi}} + \frac{1}{\beta}K\bar{\phi} - L^T\bar{w} + M\bar{\phi} = \tilde{G}, \tag{6.8.2}$$

where the vector $\tilde{G}$ only has a value in the 1st and $(n+1)$th elements. The matrices in (6.8.2) are complete except for L^T where the first column is deleted.

Lastly, Equation (6.7.4) can be rewritten as follows

$$\begin{aligned}(J+md^2)\ddot{\theta}^h(t) + (dk_2 + d^2k_1)\dot{\theta}^h(t) + dm\ddot{w}_{n+1}(t) + dk_1\dot{w}_{n+1}(t)\\ = -\gamma\big(\theta^h(t) - \phi_{n+1}(t)\big).\end{aligned} \tag{6.8.3}$$

The system of ordinary differential equations is used to simulate the motion of the beam (see the next section). A finite difference scheme is applied to the system, using enough timesteps to ensure accuracy.

6.9 Numerical results and conclusion

One important objective was to obtain numerical results to show that the model provides realistic results. We are particularly interested in the influence of the tip body and the "additional" elasticity built into the endpoints of the beam. For this reason the damping parameters were kept small so that information is not damped out.

The main parameter we were interested in investigating for this study, was γ. It was found that different values of the parameter γ larger than 1 has no significant influence on the solution. Therefore we compared results for $\gamma = 0.1$ and $\gamma = 1$. Note that different values for μ were also considered. Similar to what was found for γ, different values of $\mu > 1$ had no significant influence. In the numerical experiments the damping parameters are zero, $\mu = 1$ and $\beta = 300$. All results obtained below are accurate to at least 5 significant digits.

With regards to the motion of the beam, it is at rest (horizontal) initially and then a periodic force is applied to it to set it into motion. The force used is of the form $q(x,t) = q_0 \sin(\frac{\pi}{4}t)g(x)$ with $g(x) = x(1-x)$. (The exact solution is sufficiently smooth to justify the use of cubics.) In Figure 6.3 we show the deflection of the beam at different dimensionless times for one period of the

© University of Pretoria

applied force with $q_0 = 0.1$ and $\gamma = 1$. (The function ϕ was also computed, but the shape of the solution curve given by the graph of w is of importance here.)

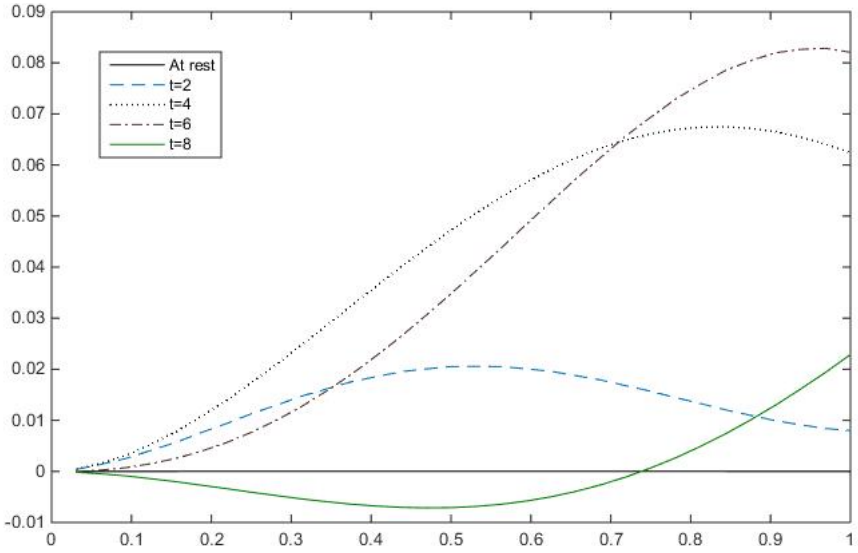

Figure 6.3: Motion of the beam $(w(\cdot, t))$ for $\gamma = 1$

As expected there is a lag at the endpoint of the beam due to the body attached there. At $t = 4$ the maximum displacement is at about $x = 0.8$, at $t = 6$ the maximum is closer to the endpoint. Of particular interest is the difference between θ and $\phi(1)$. In the tables below these values are compared for different times and for two different values of γ.

As can be seen from Table 2, for $\gamma = 1$ the values of θ and ϕ are close. For $\gamma = 0.1$ there is a notable difference.

Note that the additional elasticity in the interface creates an opportunity to evaluate the standard models by comparing it to the present model. If γ is large the interface condition in [ZVV04] and [RA15] could be used.

Conclusion

The new interface conditions required new theoretical results regarding existence and convergence of the finite element approximation. The general results in [VV02] and [BSV17] are convenient but the construction of Hilbert

© University of Pretoria

Table 6.2: Comparing θ and $\phi(1)$ for different values of γ

$\gamma = 0.1$		
t	θ	$\phi(1)$
2	-0,0032	-0,0107
4	-0,0231	-0,0196
6	-0,003	0,0224
8	0,0432	0,0455
10	0,0435	0,0296
12	0,0137	0,008
14	0,0126	0,028
16	0,0415	0,0396

$\gamma = 1$			
t	θ	$\phi(1)$	$\theta - \phi(1)$
2	-0,0037	-0,0045	0,0008
4	-0,0241	-0,0236	-0,0005
6	-8,85 $\times 10^{-4}$	0,0017	-0,0026
8	0,0456	0,0459	-0,0003
10	0,0464	0,0448	0,0016
12	0,0131	0,0126	0,0005
14	0,0131	0,0146	-0,0015
16	0,0411	0,0409	0,0002

spaces V, W and X needed to be done with care and the proofs of their properties are by no means trivial.

The numerical experiments had limited scope and were intended to complement the theory. The results obtained does however give us confidence in the model. Clearly, more experiments should be done but that would be a different investigation with different objectives. For example, numerical experiments to establish conditions where it is necessary to use the new model rather than the simpler models used previously.

Future work could also include stability analysis and implementation of the Mixed Finite Element Method.

© University of Pretoria

Chapter 7

Conclusion

7.1 Overview

Linear beam models

The research started with a review of classical beam models. The Timoshenko model was presented in dimensionless form and it was shown that the Rayleigh, Euler-Bernoulli, and Shear models can be derived from it by making additional assumptions. These models can be compared using natural frequencies. References regarding such comparisons were provided, except where the Timoshenko and Shear models were compared. The comparison between the Timoshenko and Shear models was done and included in the thesis.

Local Linear Timoshenko beam model

An important part of the thesis is the derivation of a nonlinear model which we call the Local Linear Timoshenko model (or LLT model). First the equations of motion are derived for a one-dimensional solid (called a rod). The result is well-known but the method in this thesis is different. From this model the equations of motion for planar motion are derived. Together with Timoshenko's constitutive equations for shear and bending and a constitutive equation for extension, the LLT model is obtained.

Note that the constitutive equations mentioned above are modelling assumptions and cannot be derived. (This fact was mentioned before.) However, in Section 2.9 an attempt was made to provide some justification for these as-

© University of Pretoria

sumed constitutive equations and it is instructive to observe the connection between the assumed constitutive equations and three-dimensional elasticity. It also transpires that warping of a cross-section is essential to satisfy the three-dimensional problem.

An important contribution related to the LLT model is the connection to existing linear and nonlinear models. It promotes insight into the LLT model itself as well as existing models.

First, a beam pivoted around one endpoint was considered. A trial solution where the beam rotated with constant angular velocity satisfied all eleven equations of the LLT model. As expected, the beam stretched but no other deformation occurred. Making simplifying assumptions, possible Kirchoff (nonlinear Euler-Bernoulli) models were derived from the LLT model.These models do not appear promising due to a complication with the shear force V which arises.

By making the appropriate assumptions for small vibrations, interesting linear and nonlinear models were derived from the LLT model. Short derivations for models in previous publications by other authors were obtained. Also, an adapted version of the linear Timoshenko model which allows for longitudinal vibration, was derived. A special case of this model is a model for transverse vibration of a Timoshenko beam with an axial force. It is of interest that the equations are derived from the LLT model instead of merely through inserting the axial force in the linear Timoshenko model.

Recall that for linear vibration problems, the variational form is used for theoretical purposes as well as to implement a finite element approximation. As a consequence we explored this avenue and derived the variational equations of motion for the LLT model as well as the Adapted (linear) Timoshenko model. For the last mentioned model problem, existence of a weak solution was proved in a recent article.

Since the variational form of the LLT model is available, finite element approximations of problems can be formulated. Furthermore, an algorithm was developed for the LLT model which we consider a substantial contribution. Through experiments convergence was demonstrated and properties of solutions of the model problems examined. The solution of the nonlinear model was compared to the solution of the linear Timoshenko model. For small vibrations the LLT and linear models compared well. Model problems were formulated where the linear Timoshenko beam yielded solutions that gave poor approximations to the corresponding solutions of the LLT model. For

© University of Pretoria

these problems it was verified that the strains were sufficiently small to satisfy necessary conditions for the LLT model. Therefore the LLT model can be applied for cases where linear beam models are not realistic.

Vertical structure applications

From the literature it is clear that beam models are often considered to model vertical slender structures. Some authors even used Euler-Bernoulli beam models. Others, e.g. E Miranda, stressed the necessity to include shear in the mathematical model (mentioning shear walls). This idea resulted in the Twin-beam model in two articles by Miranda and Taghavi, and Reinoso and Miranda (both in 2005). Particular attention was paid to these articles in the thesis since they provide a convincing way to introduce shear. Also, a wealth of information on various aspects is provided in these articles, for example why the relatively simple model of a beam can be useful when complex models for buildings are possible.

It was interesting that, at the time of this study, the Timoshenko model was not considered in the literature we considered. (As far as could be established most of these articles were written by experts in the field.)

Two chapters were dedicated to high-rise buildings subjected to earthquake induced oscillations. In the first the Timoshenko beam model was adapted for a high-rise structure by including the force due to gravity.

The earthquake model problem was rewritten as an artificial "wind problem" for a cantilever beam. (Consequently the model and the mathematical analysis thereof are also relevant for wind induced oscillations.) This 'new' model was referred to as the Equivalent problem which has homogenous boundary conditions. Consequently, the Timoshenko model could be compared to the Twin-beam model since modal analysis became applicable.

In our view, modal analysis was not sufficient (since the number of modes involved is not obvious in general) and as a consequence simulations of the actual motion were also performed which could be used to determine accelerations at different points of the structure. The transient response of a high-rise structure due to earthquake induced oscillations was also simulated, using the Timoshenko model. These simulations were used to investigate the effect of the dimensionless parameter β which relates to the stiffness of the beam.

It was worth investigating whether a multiple beam model might not render more accurate results than a single beam model, especially when dealing

© University of Pretoria

with high-rise structures. In order to do so, we first aimed to determine the feasibility of such a model. The structure was modelled as a series of beams connected by rigid bodies to represent the floors. To correctly apply the interface conditions in the variational form proved to be a challenge. In order to deal with the additional terms due to the interface conditions a variant of the Mixed Finite Element Method was used where neither of the constitutive equations are substituted into the equations of motion. Finally, a system of ordinary differential equations was derived from which any finite difference numerical method will yield an algorithm.

Hybrid model with elastic interfaces

A new hybrid Timoshenko beam model with a tip body was introduced with improved boundary and interface conditions that include the effect of elasticity. The study was motivated by two approaches to the problem in the literature. The one approach is to use an Euler-Bernoulli beam and the other a Timoshenko beam, each with a different way of defining the normal vector at the end of the beam. Both these interface conditions can be questioned and a more realistic elastic interface was applied. In order to do this a dimensionless parameter was introduced to formulate an equation for the elasticity in the interface. At the so called clamped end an elastic interface was also introduced.

In order to apply the general theory to prove the existence of a solution for this model, certain estimates were needed. It proved to be a serious challenge, but these estimates were derived and the existence of a solution was proved. Error estimates for the convergence of the finite element approximation were also provided.

Finally, the model problem was presented as a system of ordinary differential equations and numerical results were obtained. The results show that the new model will approximate the "standard" Timoshenko hybrid model when the dimensionless parameters for elasticity tends to infinity. This creates the opportunity to evaluate the "standard rigid" boundary and interface conditions.

7.2 Results

In retrospect, the most important contribution in this thesis is the development of the Local Linear Timoshenko model and its applications. Built on a

© University of Pretoria

technical report ([VDB16]) a detailed derivation is presented. Using the well-known equations of motion for a one-dimensional solid (often called a rod), these equations are rigorously simplified for planar motion. To complete the model, the constitutive equations for shear and bending is adapted from the linear Timoshenko theory for a beam and a simple constitutive equation for extension is used.

It is important to bear in mind that the constitutive equations mentioned above, cannot be derived unless other assumptions are made. However, the connection between the assumed constitutive equations and three-dimensional elasticity was studied and it was shown that warping of a cross-section is inevitable.

A significant property of the model is that existing linear and nonlinear models can be derived from it. This promotes insight into the LLT model itself as well as existing models. In particular, by making the appropriate assumptions for small vibrations, a number of linear and nonlinear models published by other authors, were derived. Of importance for this thesis is that an adapted version of the linear Timoshenko model which allows for longitudinal vibration, was derived. A special case of this linear model is a model for transverse vibration of a Timoshenko beam with an axial force. This last mentioned model is referred to as the Adapted Timoshenko model in this thesis and is used for vertical structures modelled as beams.

For linear vibration problems, the variational form can be used for existence theory as well as finite element approximation. The variational equations of motion for the LLT model were easy to derive but the constitutive equations could not simply be substituted into them. In the thesis it is explained why the problem should be considered "well defined".

Using the variational form of the LLT model, finite element approximations of problems can be formulated. For the approximations a rigorously defined algorithm was developed which we consider a substantial contribution. Through experiments where the Finite Element Method grid was refined, convergence was demonstrated. We also demonstrated that for small vibrations, solutions of the LLT and linear models compared well. Finally, it was shown that the LLT model can be applied to cases where the solutions of linear beam models are not realistic.

A model for earthquake induced oscillations in vertical structures, based on the Timoshenko model, was derived. The model was transformed to that for a cantilever beam with homogeneous boundary conditions. This made it

© University of Pretoria

possible to compare beam models using modal analysis.

The adapted Timoshenko model was compared to the Twin-beam model of E Miranda (presented in two articles in 2005). The models compared poorly and both predicted the measured fundamental period completely wrong. This is due to the lack of reliable information on additional mass not contributing to stiffness.

To supplement the modal analysis, finite element simulations were done. From the results valuable information can be obtained such as acceleration demands at different levels of the structure.

As an alternative, a building was modelled as a series of beams connected by rigid bodies to represent floors. Correct modelling of interface conditions made it possible to derive the variational form for the model which is a significant contribution. An adapted mixed finite element approximation was thus possible and a system of ordinary differential equations derived which can be used for simulations.

New interface and boundary conditions for a hybrid Timoshenko beam model with a tip body were derived. This model is an improvement on previous versions since elasticity at the interfaces is taken into account. The derivation of the estimates required to apply the general theory for existence needed to be done with care and the proofs were by no means trivial. Numerical experiments on this model had limited scope and were intended to complement the theory. The results obtained do however give us confidence in the model. The new model can be used to evaluate cases where "rigid" boundary and interface conditions may not be realistic.

7.3 Ongoing and future research

It should be clear that the results in this thesis indicate that there are various possibilities for future research. It is equally clear that not all the possibilities can be considered – at least not in the immediate future.

A priority at present is work related to the Local Linear Timoshenko model. It was shown in Section 2.6 that some linear and nonlinear models for small deflections can be derived from the LLT model. This work is in progress and some of it is presented in Subsection 7.3.1 below.

© University of Pretoria

The results of the numerical experiments in Chapter 3 are promising and must therefore be followed up - see Subsection 7.3.2.

7.3.1 Adapted Timoshenko beam model

As mentioned, a couple of linear and nonlinear models for small deflections were derived from the LLT model. In Subsection 2.6.1 Model 1 was derived using the approximations $F_1 = S$ and $F_2 = V$. Another possibility is to assume that

$$F_1 = S, \tag{7.3.1}$$
$$F_2 = S\partial_x w + V. \tag{7.3.2}$$

To start, substitute (7.3.2) into the Equation of motion (2.4.9):

$$\begin{aligned} \frac{1}{\alpha}\partial_t^2\phi &= (1+\partial_x u)(S\partial_x w + V) - \partial_x w S + \partial_x M. \\ &= (1+\partial_x u)V + S\partial_x u\partial_x w + \partial_x M. \end{aligned}$$

Neglecting the term $S\partial_x u\partial_x w$, we obtain an alternative to Model 1 in Subsection 2.6.1. Instead of (2.6.7) and (2.6.8), we have

$$\begin{aligned} \partial_t^2 w &= \partial_x(S\partial_x w + V) + P_2, \\ \frac{1}{\alpha}\partial_t^2\phi &= (1+\partial_x u)V + \partial_x M. \end{aligned}$$

As explained in Subsection 2.6.1, the system decouples and the following system for transverse vibration is obtained.

Model 3 Equations of motion

$$\begin{aligned} \partial_t^2 w &= \partial_x(S\partial_x w) + \partial_x V + P_2, \\ \frac{1}{\alpha}\partial_t^2\phi &= (1+\partial_x u)V + \partial_x M \end{aligned}$$

with u and S known. The constitutive equations are the same as before:

$$\begin{aligned} M &= \frac{1}{\beta}\partial_x\phi, \\ V &= \partial_x w - \phi. \end{aligned}$$

The model above is then another linear adaptation of the Timoshenko theory. Using the approximation (2.6.5) and assuming that $\partial_x S = 0$, yields the system of equations (2.6.16) and (2.6.17) that is used in [SR79].

© University of Pretoria

The equations of motion in Models 2 and 3 appear quite different and this calls for an investigation. (Especially since the constitutive equations are the same.) For simplicity we use the approximation (2.6.5) and assume that $\partial_x S = 0$. The simplified models are displayed for completeness.

Model 2S Equations of motion

$$\begin{aligned} \partial_t^2 w &= \partial_x V, \\ \frac{1}{\alpha}\partial_t^2 \phi &= V - S\partial_x w + \partial_x M \end{aligned}$$

Model 3S Equations of motion

$$\begin{aligned} \partial_t^2 w &= \partial_x (S\partial_x w) + \partial_x V, \\ \frac{1}{\alpha}\partial_t^2 \phi &= V + \partial_x M \end{aligned}$$

To compare the models we consider the relevant eigenvalue problems (as in Subsection 1.2.3) for the pinned-pinned case. The boundary conditions are the same for both models:

$$w(0) = w(1) = \phi'(0) = \phi'(1) = 0.$$

Eigenvalue problems

Eigenvalues are calculated for different choices of the axial force S.

Model 2S

$$-w'' + \phi' = \lambda w, \tag{7.3.3}$$

$$-\frac{1}{\beta}\phi'' + Sw' - w' + \phi = \frac{\lambda}{\alpha}\phi. \tag{7.3.4}$$

Model 3S

$$-Sw'' - w'' + \phi' = \lambda w, \tag{7.3.5}$$

$$-\frac{1}{\beta}\phi'' - w' + \phi = \frac{\lambda}{\alpha}\phi. \tag{7.3.6}$$

Eigenvalues

The variational forms of the two eigenvalue problems can be obtained by following the same procedure as in Subsection 1.3.1 or 2.7.3. Using the variational

© University of Pretoria

forms, the following Galerkin approximations are obtained. As in Subsection 3.2.1, let S^h denote a finite dimensional subspace of $H^1(0,1) \cap C[0,1]$ and S_2^h a subspace of S^h where $f \in S_2^h$ implies $f(0) = f(1) = 0$.

Let w_h and ϕ_h be approximations for w and ϕ in the finite dimensional subspace.

Model 2S Galerkin

Find functions (w^h, ϕ^h) such that $w^h \in S_2^h$, $\phi_h \in S^h$ and

$$(w_h', v') - (\phi_h, v') = \lambda(w_h, v), \tag{7.3.7}$$

$$\frac{1}{\beta}(\phi_h', \psi') + S(w_h', \psi) - (w_h', \psi) + (\phi_h, \psi) = \frac{\lambda}{\alpha}(\phi_h, \psi), \tag{7.3.8}$$

for all $v \in S_2^h$, $\psi \in S^h$.

Model 3S Galerkin

Find functions (w^h, ϕ^h) such that $w^h \in S_2^h$, $\phi_h \in S^h$ and

$$S(w_h', v') + (w_h', v') - (\phi_h, v') = \lambda(w_h, v), \tag{7.3.9}$$

$$\frac{1}{\beta}(\phi_h', \psi') - (w_h', \psi) + (\phi_h, \psi) = \frac{\lambda}{\alpha}(\phi_h, \psi), \tag{7.3.10}$$

for all $v \in S_2^h$, $\psi \in S^h$.

It is now possible to write these problems as matrix eigenvalue problems and calculate the eigenvalues. Tables 7.1 and 7.2 display the values obtained for Models 2S and 3S respectively. The results were verified independently by K Hohls [Hoh19] in another project.

Table 7.1: Eigenvalues for Model 2: $\alpha = 1200$

Eigenvalue	$S = -10^{-2}$	$S = -10^{-3}$	$S = 0$	$S = 10^{-3}$	$S = 10^{-2}$
λ_1	0.2171	0.3024	0.3120	0.3214	0.4068
λ_2	4.135	4.442	4.476	4.510	4.817
λ_3	18.76	19.36	19.43	19.49	20.09
λ_4	50.46	51.37	51.47	51.57	52.47
λ_5	103.2	104.4	104.6	104.7	105.9

© University of Pretoria

Table 7.2: Eigenvalues for Model 3: $\alpha = 1200$

Eigenvalue	$S = -10^{-2}$	$S = -10^{-3}$	$S = 0$	$S = 10^{-3}$	$S = 10^{-2}$
λ_1	0.2140	0.3022	0.3120	0.3217	0.4099
λ_2	4.091	4.437	4.476	4.514	4.860
λ_3	18.58	19.34	19.43	19.51	20.28
λ_4	49.98	51.32	51.47	51.62	52.96
λ_5	102.24	104.3	104.6	104.8	106.9

Considering the difference between the problems, it is surprising to see that the eigenvalues are virtually the same. The small differences in the cases where $S = -10^{-2}$ and $S = -10^{-3}$ can be attributed to possible buckling of the beam should the compressive force S be increased. Similarly, when considering $S = 10^{-2}$ and $S = 10^{-3}$ the differences may be due to the beam stiffening because of the tensile force S stretching it.

Further analysis and experiments are part of ongoing and future research.

7.3.2 Finite element analysis of the Local Linear Timoshenko model

The results of the numerical experiments in Chapter 3 are satisfactory measured against the limited objectives, however the results are only valid if the model satisfies the assumptions made initially, throughout the time of motion. First we suspect that this depends on the configuration; whether the beam is fixed at one end or both. Secondly excitation of the beam by forcing may have an effect different from an initial disturbance. Thirdly, the frequency of forcing may also influence the validity of results.

Consequently, a comprehensive array of numerical experiments are to be conducted.

7.3.3 Other possibilities for future work

Regarding the oscillations of vertical structures, the articles [MT05] and [RM05] clearly show the value of simplified models and the need for reli-

© University of Pretoria

able parameter values. We conclude that there is scope for further research by engineers as well as applied mathematicians.

An interesting article [HH19] appeared late in 2019. It featured the Twin-beam model in [MT05] and [RM05] but with one boundary condition adapted to allow for "soil-structure interaction". Also notable, was that the authors cite two recent articles (2016 and 2017) where the Timoshenko beam theory was used for a building. Consequently, the work in this article should also be considered.

Regarding the multiple beam model for buildings, an algorithm should be developed from the system of ordinary differential equations in Section 5.3. From the general linear theory in [BV13], one can expect that approximations will converge, but experiments should be carried out. Thereafter, numerical experiments should be carried out using realistic data for buildings to verify the applicability of the model.

© University of Pretoria

UNIVERSITEIT VAN PRETORIA
UNIVERSITY OF PRETORIA
YUNIBESITHI YA PRETORIA

Bibliography

[Ada75] R A Adams. *Sobolev spaces*. Series 3. Academic Press, New York, San Francisco, London, 1975.

[Ant76] S S Antman. Ordinary differential eqautions of non-linear elasticity i: Foundations of the theories of non-linear elastic rods and shells. *Archive for Rational Mechanics and Analysis*, 61:307–351, 1976.

[Ant96] S S Antman. Dynamical problems for geometrically exact theories of nonlinearly viscoelastic rods. *Journal of Nonlinear Science*, 6:1–18, 1996.

[Arn81] D N Arnold. Discretization by Finite Elements of a Model Parameter Dependent Problem. *Numerische Mathematik*, 37:405–421, 1981.

[Aro01] A Arosio. A geometrical nonlinear correction to the Timoshenko beam equation. *Nonlinear Analysis*, 47:729–740, 2001.

[AS02] K T Andrews and M Shillor. Vibrations of a beam with a damping tip body. *Mathematical and Computer Modelling*, 35:1033–1042, 2002.

[ASD16] R Ansari, F Sadeghi, and M Darvizeh. Continuum study on the oscillatory characteristics of carbon nanocones inside single-walled carbon nanotubes. *Physica B: Condensed Matter*, 482:28–37, 2016.

[BCLS08] JA Burns, EM Cliff, Z Liu, and RD Spies. On coupled transversal and axial motions of two beams with a joint. *Journal of Mathematical Analysis and Applications*, 339:182–196, 2008.

© University of Pretoria

[Bha09] A Bhaskar. Elastic waves in Timoshenko beams: the'lost and found' of an eigenmode. *Proceedings of the Royal Society A*, 465:239–255, 2009.

[Bra01] D Braess. *Finite elements*. Cambridge university press, Cambridge, ii edition, 2001.

[BSV17] M Basson, B Stapelberg, and NFJ Van Rensburg. Error estimates for semi-discrete and fully discrete galerkin finite element approximations of the general linear second-order hyperbolic equation. *Numerical Functional Analysis and Optimization*, 38(4):466–485, 2017.

[BV13] M Basson and NFJ Van Rensburg. Galerkin finite element approximation of general linear second order hyperbolic equations. *Numerical Functional Analysis and Optimization*, 34(9):976–1000, 2013.

[CDKP87] G Chen, MC Delfour, AM Krall, and G Payre. Modeling, stabilization and control of serially connected beams. *SIAM Journal on Control and Optimization*, 25(3):526–546, 1987.

[Cow66] G R Cowper. The shear coefficient in Timoshenko's beam theory. *Journal of Applied Mechanics*, 33:335–340, 1966.

[FES17] S H Farghaly and T A El-Sayed. Exact free vibration analysis for mechanical system composed of timoshenko beams with intermediate eccentric rigid body on elastic supports: An experimental and analytical investigation. *Mechanical Systems and Signal Processing*, 82:376–393, 2017.

[FL10] A Flaga and T Lipecki. Code approaches to vortex shedding and own model. *Engineering structures*, 32:1530–1536, 2010.

[Fun65] Y C Fung. *Foundations of solid mechanics*. Prentice-Hall Inc, Englewood Cliffs, New Jersey, 1965.

[Gro10] M Grobbelaar-Van Dalsen. Uniform stability for the Timoshenko beam with tip load. *Journal of Mathematical Analysis and Applications*, 361:392–400, 2010.

[HBW99] S M Han, H Benaroya, and T Wei. Dynamics of transversely vibrating beams using four engineering theories. *Journal of Sound and Vibration*, 225(5):935–988, 1999.

© University of Pretoria

[HH19] I F Huergo and H Hernández. Coupled-tow-beam discrete model for dynamic analysis of tall buildings with tuned mass dampers including soil-structure interaction. *Struct Design Tall Spec Build*, **29**:e1683:199–221, 2019.

[HKO11] E Hernández, D Kalise, and E Otárola. A locking-free scheme for the LQR control of a Timoshenko beam. *Journal of Computational and Applied Mathematics*, 235(5):1383–1393, 2011.

[Hoh19] K A Hohls. Eigenvalue problems for bilinear forms in Hilbert spaces with applications to modal analysis, 2019.

[HS73] A C Heidebrecht and B Stafford Smith. Approximate analysis of tall wall-frame structures. *Journal of Structural Division ASCE*, 99(2):199–221, 1973.

[HV07] J W Hijmissen and W T Van Horssen. On aspects of damping for a vertical beam with a tuned mass damper at the top. *Nonlinear Dynamics*, 50:169–190, 2007.

[Inm94] D J Inman. *Engineering vibration*. Prentice-Hall Inc, Englewood Cliffs, New Jersey, 1994.

[JLK04] T S Jan, M W Liu, and Y C Kao. An upper-bound pushover analysis procedure for estimating the seismic demands of high-rise buildings. *Engineering structures*, 26:117–128, 2004.

[KS64] F R Khan and J A Sbarounis. Interaction of shear walls and frames. *Journal of Structural Division ASCE*, 90(3):285–335, 1964.

[LA12] H Lang and M Arnold. Numerical aspects in the dynamic simulation of geometrically exact rods. *Applied Numerical Mathematics*, 62(10):1411 – 1427, 2012. Selected Papers from NUMDIFF-12.

[LL91] J E Lagnese and G Leugering. Uniform stabilization of a nonliner beam by nonliner boundary feedback. *Journal of Differential Equations*, 91:355–388, 1991.

[LM72] J L Lions and E Magenes. *Nonhomogeneous Bounday Value Problems and Applications*, volume 1. Springer-Verlag, New York, 1972.

© University of Pretoria

[LM88] W Littman and L Markus. Exact boundary controllability of a hybrid system of elasticity. *Archive for Rational Mechechanics and Analysis*, 103(3):193–236, 1988.

[LVV05] A Labuschagne, N F J Van Rensburg, and A J Van der Merwe. Distributed parameter models for a vertical slender structure on a resilient seating. *Mathematical and Computer Modelling*, 41:1021–1033, 2005.

[LVV09] A Labuschagne, N F J Van Rensburg, and A J Van der Merwe. Comparison of linear beam theories. *Mathematical and Computer Modelling*, 49:20–30, 2009.

[LZ14] Z Lui and Q Zhang. Stabiliztion of a joint-leg-beam system with boundary damping. *Journal of Mathematical Analysis and Applications*, 420:1455–1467, 2014.

[Mir99] E Miranda. Approximate lateral deformation demands in multistory buildings subjected to earthquakes. *Journal of Structural Engineering*, 125(4):417–425, 1999.

[MT05] E Miranda and S Taghavi. Approximate floor acceleration demands in multistory buildings. I: Formulation. *Journal of Structural Engineering*, 131(2):203–211, 2005.

[OR76] J T Oden and J N Reddy. *An introduction to the mathematical theory of finite elements*. John Wiley & Sons, New York-London-Sydney-Toronto, 1976.

[RA15] J E M Rivera and A I Ávila. Rates of decay to non homogeneous Timoshenko model with tip body. *J. Differential Equations*, 258:3468–3490, 2015.

[RM05] E Reinoso and E Miranda. Estimation of floor acceleration demands in high-rise buildings during earthquakes. *Struct. Design Tall Spec. Build.*, 14:107–130, 2005.

[Sem94] B Semper. Semi-discrete and fully discrete Galerkin methods for the vibrating Timoshenko beam. *Comput. Methods Appl. Mech. Engrg*, 117:353–360, 1994.

[SF73] G Strang and G J Fix. *An Analysis of the Finite Element Method*. Prentice-Hall, New Jersey, 1973.

© University of Pretoria

[Sho77] R E Showalter. *Hilbert space methods for partial differential equations*. Pitman, London, 1977.

[SP06] N G Stephen and S Puchegger. On the validity range of Timoshenko beam theory. *J. Sound Vib.*, 297:1082–1087, 2006.

[SR79] M Sapir and L Reiss. Dynamic buckling of a nonlinear Timoshenko beam. *Siam J. Appl. Math.*, 37(2):290–301, 1979.

[SVQ86] J C Simo and L Vu-Quoc. On the dynamics of flexible beams under large overall motions - the plane case: Part i. *Journal of Applied Mechanics*, 53:849–854, 1986.

[SVQ87] J C Simo and L Vu-Quoc. The role of nonlinear theories in transient dynamic analysis of flexible structures. *Journal of Sound and Vibration*, 119:487–508, 1987.

[Tak96] H Takabatake. A simplified analysis of doubly symmetric tube structures by the finite difference method. *The structural design of tall buildings*, 5:111–128, 1996.

[Tim21] S P Timoshenko. Lxvi. On the correction for shear of the differential equation for transverse vibrations of prismatic bars. *Philosophical Magazine Series*, 6(41):744–746, 1921.

[Tim22] S P Timoshenko. On the transverse vibrations of bars of uniform cross-section. *Philosophical Magazine*, 43:125–131, 1922.

[Tim37] S Timoshenko. *Vibration problems in Engineering*. D van Nostrand Company, Inc., New-York, 2 edition, 1937.

[TMF+11] I Takewaki, S Murakami, K Fujita, S Yoshitomi, and M Tsuji. The 2011 off the Pacific soast of Tohoku earthquake and response of high-rise buildings under long-period ground motions. *Soil Dynamics and Earthquake Engineering*, 31:1511–1528, 2011.

[Van01] N F J Van Rensburg. Boundary condition for a clamped Timoshenko beam. Technical report UPWT 2001/09, University of Pretoria, Pretoria, 2001.

[Van15] N F J Van Rensburg. Locally linear Timoshenko beam model. Technical Report, UPWT 2015/23, University of Pretoria, Pretoria, 2015.

© University of Pretoria

[VDB16] N F J Van Rensburg, S Du Toit, and M Basson. Locally linear Timoshenko beam model. Technical Report, UPWT 2016/06, University of Pretoria, Pretoria, 2016.

[VS19] N F J Van Rensburg and B Stapelberg. Existence and uniqueness of solutions of a general linear second-order hyperbolic problem. *IMA Journal of Applied Mathematics*, 84(1):1–22, 09 2019.

[VV02] N F J Van Rensburg and A J Van der Merwe. Analysis of the solvability of linear vibration models. *Applicable Analysis*, 81(5):1143–1159, 2002.

[VV06] N F J Van Rensburg and A J Van der Merwe. Natural frequencies and modes of a Timoshenko beam. *Wave Motion*, 44:58–69, 2006.

[VVR10] N F J Van Rensburg, A J Van der Merwe, and A Roux. Waves in a vibrating solid with boundary damping. *Wave motion*, 47:663–675, 2010.

[WFH01] A P Wang, R F Fung, and S C Huang. Dynamic analysis of a tall building with a tuned-mass-damper device subjected to earthquake excitations. *Journal of Sound and Vibration*, 244(1):123–136, 2001.

[WL07] A P Wang and Y H Lin. Vibration control of a tall building subjected to earthquake excitation. *Journal of Sound and Vibration*, 299:757–773, 2007.

[ZVV04] L Zietsman, N F J Van Rensburg, and A J Van der Merwe. A Timoshenko beam with tip body and boundary damping. *Wave Motion*, 39(3):199–211, 2004.

© University of Pretoria

UNIVERSITEIT VAN PRETORIA
UNIVERSITY OF PRETORIA
YUNIBESITHI YA PRETORIA

Appendix A

Sobolev Spaces

The space $\mathcal{L}^2(\Omega)$

Consider an open subset Ω of $\mathbb{R}^n$. The space $\mathcal{L}^2(\Omega)$ consists of functions f such that f^2 is Lebesgue integrable on Ω. The first result is well known.

Theorem A.1. *The space $\mathcal{L}^2(\Omega)$ is a Hilbert space with* **inner product**

$$(f, g) = \int_\Omega fg = \int_\Omega fg \, d\mu$$

where μ is the n-dimensional Lebesgue measure.

Theorem A.2. *The space $\mathcal{L}^2(\Omega)$ is separable. (See [Ada75, Th 2.15, p 28]).*

Theorem A.3. *$C_0^\infty(\Omega)$ is dense in $\mathcal{L}^2(\Omega)$. (See [Ada75, Th 2.13, p 28]).*

Suppose Ω is a **bounded open** interval in $\mathbb{R}$ (bounded open subset of $\mathbb{R}^n$ when higher dimensions are required). The **Sobolev spaces** $H^m(\Omega)$ are subspaces of functions in $\mathcal{L}^2(\Omega)$ with weak derivatives up to order m in $\mathcal{L}^2(\Omega)$.

Definition

For f and g in $H^m(\Omega)$,

$$[f, g]_m = (f^{(m)}, g^{(m)}) \quad \text{for} \quad m = 0, 1, \ldots$$

For $m \geq 1$, the bilinear form $[\cdot, \cdot]_m$ has all the properties of an inner product except that there exist functions $f \neq 0$ such that $[f, f]_m = 0$.

© University of Pretoria

Definition

For f in $H^m(\Omega)$,

$$|f|_m = \sqrt{[f,f]_m} \quad \text{for} \quad m = 0,\, 1,\, \ldots$$

The function $|\cdot|_m$ is a semi-norm for $m \geq 1$.

Suppose Ω is a **bounded open convex** subset of $I\!R^2$. The **Sobolev spaces** $H^m(\Omega)$ are subspaces of functions in $\mathcal{L}^2(\Omega)$ with weak partial derivatives up to order m in $\mathcal{L}^2(\Omega)$.

Remark

It is not necessary to require that Ω be convex, but it is sufficient for our purpose. In the theory it is usually assumed that Ω is star shaped or has the cone property.

Definition

For f and g in $H^m(\Omega)$,

$$[f,g]_m = \sum_{i+j=m} (\partial_1^i \partial_2^j f, \partial_1^i \partial_2^j g) \quad \text{for} \quad m = 0,\, 1,\, \ldots$$

For $m \geq 1$ the bilinear form $[\cdot,\cdot]_m$ has all the properties of an inner product except that there exist functions $f \neq 0$ such that $[f,f]_m = 0$.

Definition

For f in $H^m(\Omega)$,

$$|f|_m = \sqrt{[f,f]_m} \quad \text{for} \quad m = 0,\, 1,\, \ldots$$

The function $|\cdot|_m$ is a semi-norm for $m \geq 1$.

The boundary

Recall that a curve is called **smooth** if its parametrization has a continuous derivative. The boundary of Ω is called **piecewise smooth** if it consists of a finite number of smooth curves.

For a vector valued function r such that $r_i \in C^1[a,b]$ for $i = 1,\, 2$, the range $\boldsymbol{C}$ of r defines a smooth curve in the plane.

© University of Pretoria

Suppose that $\boldsymbol{C}$ is a part of the boundary of Ω. A function f is Lebesgue integrable on $\boldsymbol{C}$ if $f \circ r \sqrt{(r_1')^2 + (r_2')^2}$ is Lebesgue integrable on the interval $[a, b]$.

A function f is in $\mathcal{L}^2(\boldsymbol{C})$ if f^2 is Lebesgue integrable over $\boldsymbol{C}$. The inner product for $\mathcal{L}^2(\boldsymbol{C})$ is defined by

$$(f, g)_{\boldsymbol{C}} = \int_{\boldsymbol{C}} fg \, ds = \int_a^b (f \circ r)\,(g \circ r)\,\sqrt{(r_1')^2 + (r_2')^2}\,.$$

When necessary, we use the **notation** $(f, g)_\Omega$ and $(f, g)_\Gamma$ to avoid confusion.

Vector valued functions

Definition

$u \in \mathcal{L}^2(\Omega)^2$ if $u_i \in \mathcal{L}^2(\Omega)$ for $i = 1, 2$.

$u \in \mathcal{L}^2(\Gamma)^2$ if $u_i \in \mathcal{L}^2(\Gamma)$ for $i = 1, 2$.

$u \in H^k\Omega)^2$ if $u_i \in H^k(\Omega)$ for $i = 1, 2$.

$[u, v]_{m,2} = [u_1, v_1]_m + [u_2, v_2]_m$ for $u \in \mathcal{L}^2(\Omega)^2$ and $v \in \mathcal{L}^2(\Omega)^2$.

$|u|_{m,2} = \sqrt{[u, u]_{m,2}}$ for $u \in \mathcal{L}^2(\Omega)^2$.

The function $|\cdot|_{m,2}$ is a semi-norm for $m \geq 1$.

When we need to distinguish between domains, we will use superscripts Ω and Γ in the cases of a double subscript, e.g. $\|\cdot\|^{\Omega}_{m,2}$ and $\|\cdot\|^{\Gamma}_{m,2}$.

Definitions

Suppose Ω is a **bounded open interval** or a **bounded open convex** subset of $\mathbb{R}^2$.

Notation

$H^0(\Omega) = \mathcal{L}^2(\Omega)$ and $H^0(\Omega)^2 = \mathcal{L}^2(\Omega)^2$.

Definition

The inner product for $H^m(\Omega)$ is defined by

$$(f, g)_m = \sum_{k=0}^{m} [f, g]_k \quad \text{for} \quad m = 0, 1, \ldots$$

© University of Pretoria

Definition

The norm for $H^m(\Omega)$ is defined by

$$\|f\|_m = \sqrt{(f,g)_m} \quad \text{for} \quad m = 0,\ 1,\ \ldots$$

Definition

The inner product for $H^m(\Omega)^2$ is defined by

$$(f,g)_{m,2} = \sum_{k=0}^{m} [f,g]_{k,2} \quad \text{for} \quad m = 0,\ 1,\ \ldots$$

Definition

The norm for $H^m(\Omega)^2$ is defined by

$$\|f\|_{m,2} = \sqrt{(f,g)_{m,2}} \quad \text{for} \quad m = 0,\ 1,\ \ldots$$

Theorem A.4. *The space $H^m(\Omega)$ is complete (See [Ada75, Th 3.2, p 45]).*

Theorem A.5. *$C^m(\bar{\Omega})$ is dense in $H^m(\Omega)$ with respect to the norm of $H^m(\Omega)$.*
(See [OR76, Th 2.10, p 53].)

Trace

Definition (Trace operator Γ)

For $u \in C(\bar{\Omega})$, the function Γu is the restriction of the function u to Γ.

Theorem A.6. *The trace operator Γ can be extended to a bounded linear operator mapping $H^1(\Omega)$ onto $L^2(\partial\Omega)$ and $\|\Gamma u\|_{\partial\Omega} \leq K\|u\|_1^{\Omega}$.*

Proof. This result is a special case of results in [OR76, p 141-142]. □

Definition

For $u \in H^1(\Omega)^2$, we define Γu by

$$\Gamma u = \langle \Gamma u_1, \Gamma u_2 \rangle.$$

© University of Pretoria